NRL/MR/6183--93-7335

Post-Flashover Fires in Shipboard Compartments Aboard ex-USS *Shadwell*: Phase IV—Impact of Navy Fire Insulation

A. F. Durkin and F. W. Williams
Navy Technology Center for Safety and Survivability, Chemistry Division

J. L. Scheffey, T. A. Toomey, and S. P. Hunt
Hughes Associates, Inc., Columbia, MD

R. L. Darwin
Naval Sea Systems Command, Washington, DC

June 9, 1993

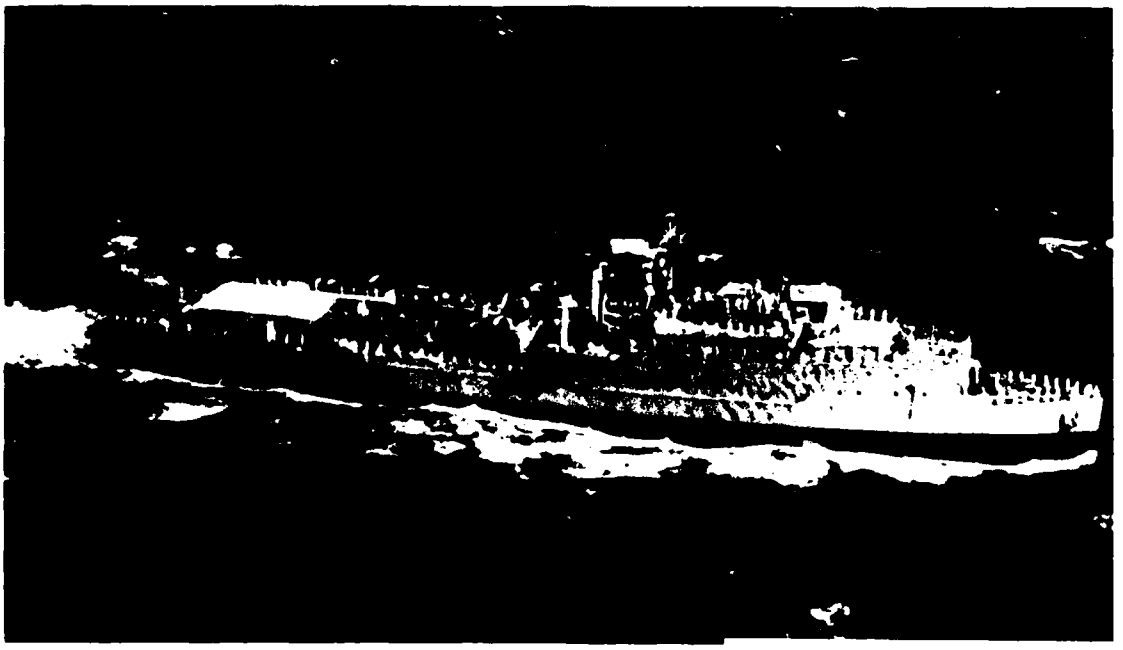

DISCLAIMER NOTICE

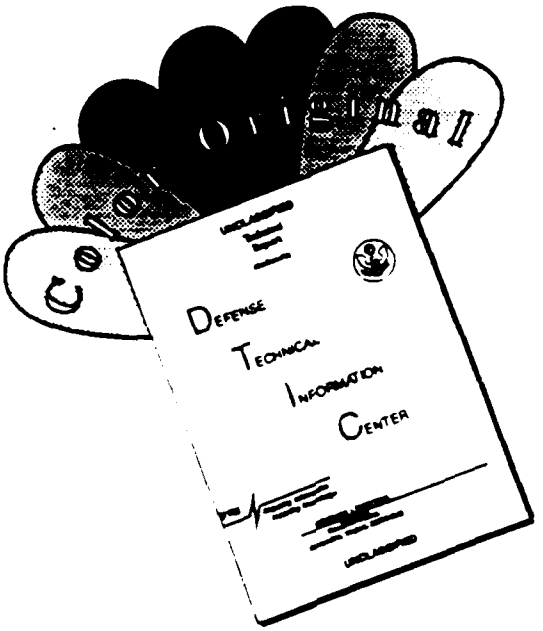

THIS DOCUMENT IS BEST QUALITY AVAILABLE. THE COPY FURNISHED TO DTIC CONTAINED A SIGNIFICANT NUMBER OF COLOR PAGES WHICH DO NOT REPRODUCE LEGIBLY ON BLACK AND WHITE MICROFICHE.

REPORT DOCUMENTATION PAGE

Form Approved
OMB No. 0704-0188

1. AGENCY USE ONLY (*Leave Blank*)	2. REPORT DATE	3. REPORT TYPE AND DATES COVERED
	1993	

4. TITLE AND SUBTITLE

Post-Flashover Fires in Shipboard Compartments Aboard ex-USS *Shadwell*: Phase IV—Impact of Navy Fire Insulation

5. FUNDING NUMBERS

P.E. 63514
Project S1565
61-0066-0-2

6. AUTHOR(S)

J.L. Scheffey,* T.A. Toomey,* S.P. Hunt,*, A.F. Durkin,
R.L. Darwin,** and F.W. Williams

7. PERFORMING ORGANIZATION NAME(S) AND ADDRESS(ES)

Naval Research Laboratory
Washington, DC 20375-5320

8. PERFORMING ORGANIZATION REPORT NUMBER

NRL/MR/6183--93-7335

9. SPONSORING/MONITORING AGENCY NAME(S) AND ADDRESS(ES)

Naval Sea Systems Command
Washington, DC 20362

10. SPONSORING/MONITORING AGENCY REPORT NUMBER

11. SUPPLEMENTARY NOTES

*Hughes Associates, Inc., Columbia, MD 21045
**Naval Sea Systems Command, Washington, DC 20362

12a. DISTRIBUTION/AVAILABILITY STATEMENT

Approved for public release; distribution unlimited.

12b. DISTRIBUTION CODE

13. ABSTRACT (*Maximum 200 words*)

As part of the Internal Ship Conflagration Control Project, a post-flashover fire was created in the port wing wall of the fire test ship, ex-USS SHADWELL. Prior tests indicated that standard Navy mineral wool degraded when exposed to post-flashover compartment temperatures. In this test series, the performance of standard Navy insulation with protective coatings and alternative materials were evaluated.

The results of earlier testing were confirmed. The mineral wool degrades when subjected to temperatures on the order of 1000°C. When attached to the overhead, the material lacks mechanical strength in a fire. The data suggest, however, that critical temperatures (232°C) on the unexposed side of the steel may be reached in about the same time even if 2.5-cm (1-in.) thick mineral wool stays in place. Protective coatings testing was ineffective in delaying heat transfer.

A candidate replacement material, Manville Structo-gard, showed improved heat transfer characteristics when tested using two 1.6-cm (5/8-in.) thick layers compared to the standard Navy mineral wool.

14. SUBJECT TERMS

Fire test
Passive protection
Fire insulation
Fire modeling
Post-flashover fire
Marine fire protection

15. NUMBER OF PAGES

148

16. PRICE CODE

17. SECURITY CLASSIFICATION OF REPORT	18. SECURITY CLASSIFICATION OF THIS PAGE	19. SECURITY CLASSIFICATION OF ABSTRACT	20. LIMITATION OF ABSTRACT
UNCLASSIFIED	UNCLASSIFIED	UNCLASSIFIED	UL

NSN 7540-01-280-5500

Standard Form 298 (Rev. 2-89)
Prescribed by ANSI Std 239-18
298-102

Table of Contents

Table of Contents (Continued)

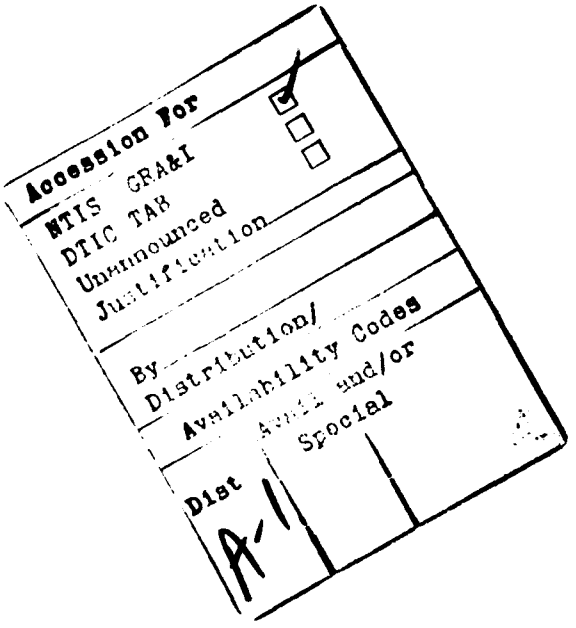

Figures

Figures (Continued)

Tables

Post-flashover Fires in Shipboard Compartments aboard ex-USS SHADWELL: Phase IV–Impact of Navy Fire Insulation

1.0 BACKGROUND

Fire insulation on ships can reduce heat transfer through bulkheads and decks to slow or possibly prevent fire spread. The need for this type of protection was exemplified by the conditions which occurred during the missile-induced conflagration onboard the USS STARK. Both an analysis of the conditions which occurred onboard the USS STARK [1] and fire testing conducted at the Naval Research Laboratory's (NRL) Chesapeake Bay Detachment (CBD) [2] indicate that fire spread from the compartment of origin in all directions except down may occur within ten minutes. Under extreme conditions, fire may spread in as little as three minutes. The question then arises as to how much time fire insulation in and around the fire compartment would provide to firefighting parties trying to contain and gain access to a fire. A corollary question is the increased rate of temperature rise in the fire compartment since heat dissipation would be limited. The Naval Sea Systems Command (NAVSEA) Code 05G2 requested that NRL, under the Internal Ship Conflagration Control Program (ISCC), determine the reduction in heat transfer provided by insulating shipboard compartments using approved Navy fire insulation.

Navy approved fire insulation was initially tested in the intermediate scale mock-up at CBD [3]. The insulation was found to provide little or no protection against fire spread when installed in the fire compartment and exposed to a 4 megawatt (MW) fire having an upper layer temperature on the order of 1000°C (1832°F). A substantial portion of the insulation came off the boundaries during the tests. As a result, the insulation did not provide passive protection to the boundaries as intended. Possible means of failure were attributed to degradation of binder and failure of glass facing due to high temperatures, increased turbulence compared to the standard ASTM E-119 test method, or incorrect insulation.

As a result of the CBD testing, additional tests were conducted under the ISCC project in the port wing wall of the ex-USS SHADWELL [4]. The object of that test series was to provide repeat data of the CBD tests using insulation from a different vendor. This addressed the question of whether the base insulation was the correct material. The insulation was installed in the overhead and on the forward bulkhead of the fire compartment. The insulation was again exposed to a post-flashover fire similar to the CBD design fire threat. The data from these tests confirmed the results of the earlier CBD tests. The standard 2.5 cm (1 in.) thick Navy insulation may drop off the overhead when

Manuscript approved March 24, 1993.

exposed to a rapid temperature rise fire. The mechanical failure of the insulation installed in the overhead is most likely attributable to melting of the insulation facing. Air velocity due to the flames impinging on the overhead may also be a factor. Insulation installed on the bulkhead remained generally intact and did delay ignition temperatures on the unexposed side.

2.0 OBJECTIVE

The objectives of the test series described in this report were to investigate methods to extend the useful life of the Navy approved insulation using protective coatings and coverings and to pinpoint failure mechanisms. Tests were also conducted with new materials which may replace the current insulation. Additionally, analytical methods to correlate threats with fire test results were refined. An alternative composite deck material was also tested.

3.0 APPROACH

Small test specimens were installed in the overhead of a shipboard compartment on the ex-USS SHADWELL. They were exposed to a post-flashover fire. Heat transfer was measured by using thermocouples installed on the bare steel deck above the fire (unexposed side). Protective coatings and metal sheathing were evaluated in an attempt to delay heat transfer. Candidate insulation materials developed from the Navy Lightweight Insulation Program at the Carderock Division of Navy Surface Warfare Center (CD/NSWC) were subjected to the post-flashover fire. Post-test fire modeling to evaluate predictive techniques was performed using a finite element heat transfer computer program.

4.0 TEST AREA

Tests were conducted along the port wing wall of the ex-USS SHADWELL in the ISCC test area (Fig. 1). The insulation samples were installed in the overhead and exposed to a post-flashover fire in the test compartment designated Berthing 2. This exposure, simulating nearly instantaneous achievement of post-flashover compartment fire conditions, was developed at CBD [2]. Subsequently, it was adapted for the larger ex-USS SHADWELL ISCC fire area. It consisted of a three-minute burn period of heptane contained in three 1.2 m (4 ft) square pans. This was followed by a continuous diesel fuel spray fire ignited by the fire in the three pans. The flow rate was nominally 5.80 lpm (1.53 gpm) per pan, 17.4 lpm (4.6 gpm) total. Air was supplied naturally to the fire via vent openings in the hull structure and the open doors to the well deck. The estimated heat release rate of this fire, based on complete combustion, is approximately 9.2 MW. A plan view of Berthing 2 is shown in Fig. 2.

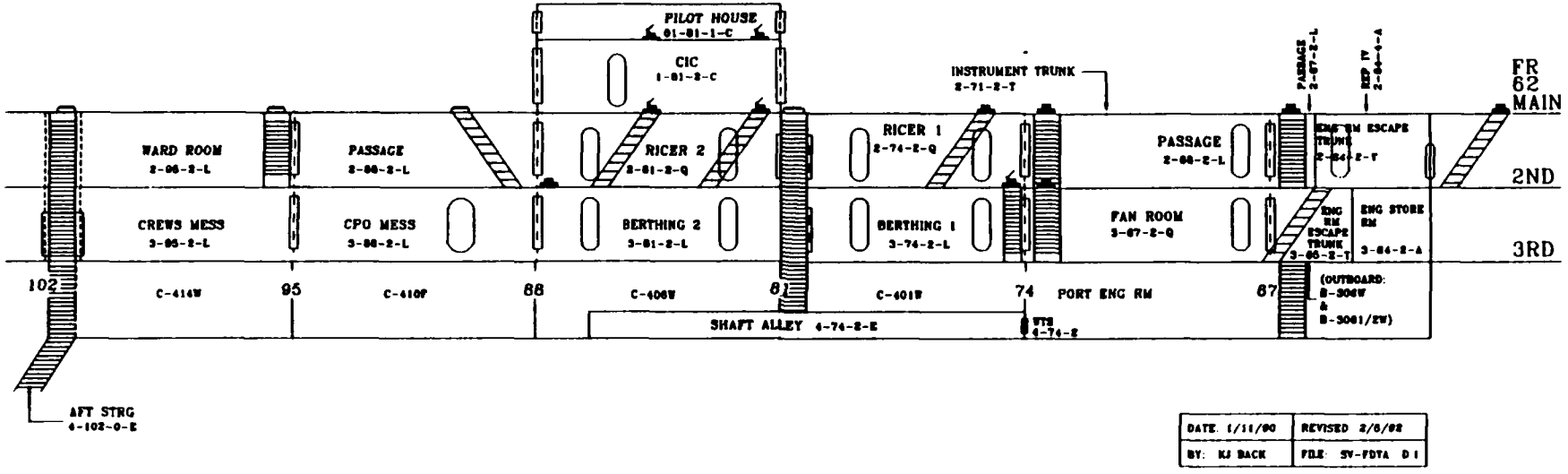

Fig. 1 - ex-SHADWELL, section view, port wing wall ISCC test area

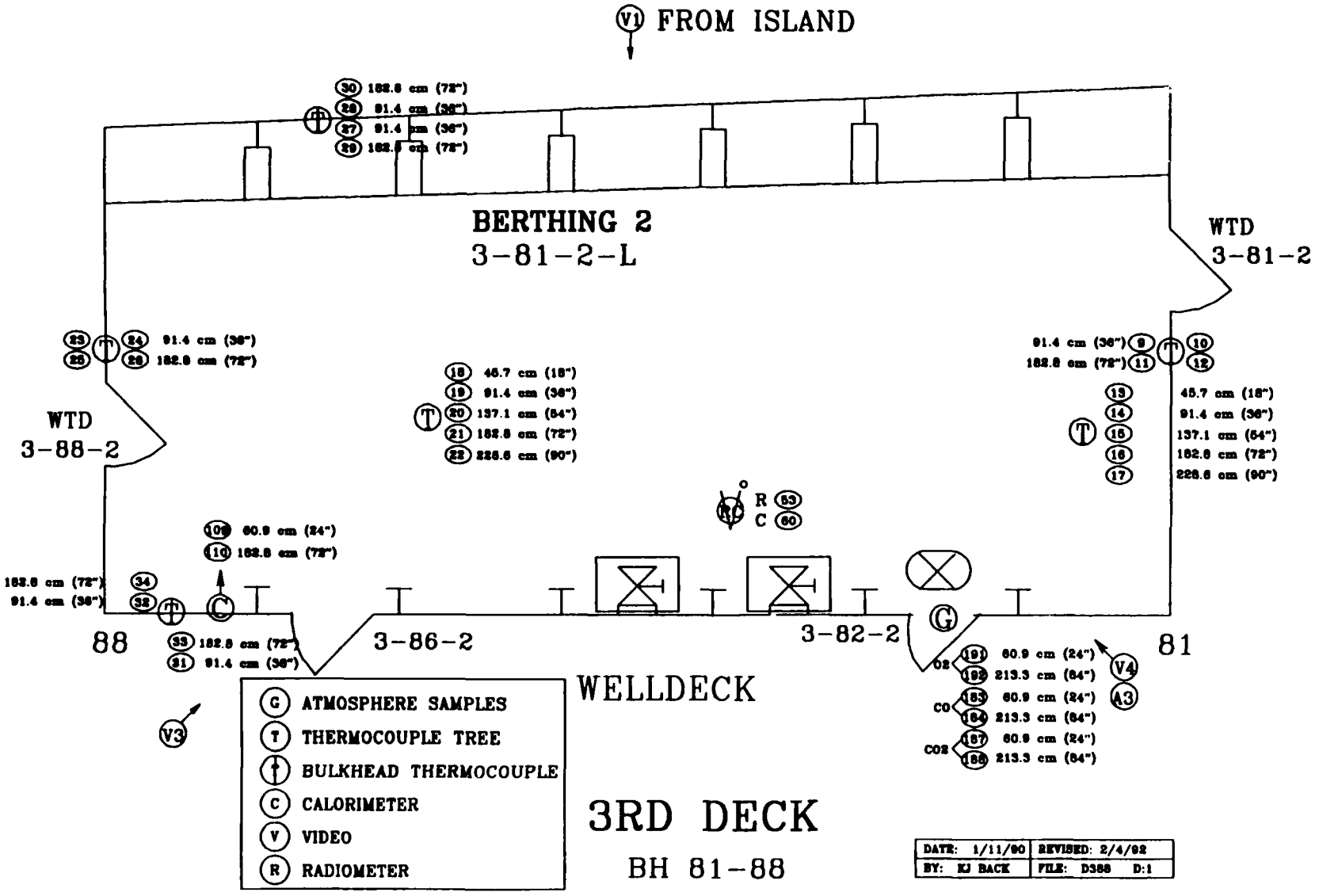

Fig. 2 - Plan view of BERTHING 2, insulation test area

5.0 MATERIALS

5.1 Insulation

The standard Navy insulation used in this evaluation was Liberty Insulation Company's "FireBar™." Liberty uses the same base mineral wool insulation as the other two Navy-approved vendors and applies the facing material to the exterior side of the mineral wool. The base material is nominally 2.5 cm (1 in.) thick and has a nominal density of 64 kg/m^3 (4 lb/ft^3). The nominal weight of the material, including the facing, is 2.0 kg/m^2 (0.418 lb/ft^2) according to data supplied by NAVSEASYSCOM Code 05M. The actual measured density of the material supplied, including facing, was 83.3 kg/m^2 (5.3 lb/ft^2). This resulted in a weight per unit area of 2.1 kg/m^2 (0.44 lb/ft^2). Steel studs 0.463 cm (0.183 in.) in diameter and 2.2 cm (0.875 in.) in length and steel fasteners (caps) manufactured by AGM Industries were used to attach the insulation to the underside of the deck. The insulation was provided in 0.6 x 1.2 m (2 x 4 ft) sheets.

Two experimental insulation systems were supplied by CD/NSWC. "Structo-gard" by Manville was a "amorphous wool insulating fiber" having a white woven fiberglass scrim and a fabric backing. The facing is the same as that used for Navy insulation. It was supplied in 0.6 x 0.9 m (2 x 3 ft) sheets at a measured thickness of 1.59 cm (0.625 in.). The insulation material had a measured density of 115 kg/m^3 (7.2 lb/ft^3) and weighed 2.0 kg/m^2 (0.41 lb/ft^2) as supplied with scrim and backing. The other material was a Sorrento polyamide foam having a blue fiberglass scrim. It was supplied in 0.6 x 0.6 m (2 x 2 ft) sheets at a nominal thickness of 2.5 cm (1 in.). It had a density of 52.8 kg/m^3 (3.3 lb/ft^3) and weighed 1.2 kg/m^2 (0.24 lb/ft^2) as supplied, including the scrim. Both experimental insulation systems were attached to the overhead. When used in two layers, one sheet of Manville Structo-gard material was placed directly on the top of the other, without removing the extra facing sheet.

5.2 Steel Sheathing

In order to assess the performance of the standard Navy insulation if it remained intact in the overhead, steel sheathing was used as an exterior (fire exposed) side sheathing. The intent was to ensure that the insulation material remained intact during the test. The idea was scoped in the earlier ex-USS SHADWELL tests (Test Ins_3 [4]) using a nominal 0.32 cm (0.13 in.) thick galvanized steel sheet. For this test series, Bethlehem Steel provided a new tin-free steel (TFS) product, "Black Plate #55," 0.02 cm (0.008 in.) thick in 0.6 x 1.2 m (2 x 4 ft) panels. The steel sheet weighed 1.6 kg/m^2 (0.33 lb/ft^2), which effectively doubled the weight of the insulation system when combined with mineral wool.

5.3 Protective Coatings

Three protective coatings were recommended by CD/NSWC and evaluated in these tests. Two coats of Ocean 9788, a Navy-approved organic solvent intumescent coating, were applied. It is a two-part mixture generally used to reduce surface flame spread. A second Ocean coating, Ocean 477, was also evaluated. This is also a two-

part intumescent coating designed for marine use. It was applied to the insulation in one and two coats. The third material, Hamilton 303, is also a two-part coating system designed for protection of cable penetrations. It was applied in one coat as a very thick mixture. When applied in two coats, the surface tended to crack because the material was too thick and heavy for the insulation. In all cases, mixtures were prepared and applied in accordance with manufacturer's recommendations.

5.4 Lightweight Metallic Sandwich Structure Material

LASCOR is an all-metallic reinforced panel designed to be used for structural bulkheads for ships. The panels are fabricated from thin steel in a corrugated design that is laser welded. Six panels were received from different sources for testing. The base panels were all manufactured the same, 69 cm (27 in.) x 69 cm (27 in.) wide with a thickness of 5 cm (2 in.). One of the panels was powder coated and received from CFB Halifax, Halifax, Canada. Two panels were filled with a foam and received from Florida International University. Three panels were shipped from Pennsylvania State University, Applied Research Laboratory, one of which was to be filled and drained by Ingalls Shipbuilding, Pascagoula, Mississippi.

6.0 TEST SETUP

In the earlier ex-USS SHADWELL tests, Ins_1a and Ins_2, the insulation was installed on the entire overhead (minus stiffeners) and forward bulkhead of Berthing 2. This required substantial labor, time, and materials. Starting with Ins_3, individual insulation specimens were installed in the overhead in the size provided. This provided a quicker and easier means to evaluate multiple samples. It was found that up to three samples could be tested simultaneously in the overhead channels formed by frame bays (FR) 82-83, 84-85, and 86-87. Five tests, Ins_3 - Ins_7, were conducted with multiple samples in these frame bays. The original thickness of the second deck and FR 81 bulkhead at FR 81 was 0.95 cm (0.38 in.). However, there was some concern that the data from the backside (unexposed) thermocouples installed on the RICER 2 deck might be influenced by the rapid heating of the adjacent bare steel. The concern was the possibility of a thermal "short" being created around the insulation via adjacent bare steel (e.g., there was only 0.3 m (1 ft) from the monitoring backside thermocouples to the adjacent bare deck). There was also concern that the insulation was being exposed around its unprotected perimeter.

To eliminate these concerns, three deck inserts were constructed in FR 82-83, 84-85, and 86-87 (Figs. 3-7). The inside dimension of each insert was nominally 72.6 cm (30 in.). The inserts were created using 1.6 cm (0.63 in.) thick angle having a 7.6 cm (3 in.) lip (Fig. 4). Steel plates, 0.48 cm (0.19 in.) thick and measuring 66 cm (26 in.) square, were used for the test specimens. Insulation was attached with studs and caps to the plate (Figs. 4 and 6) in accordance with the criteria of the standard drawing for Navy insulation [5]. Ceramic fiber fire insulation was then folded in strips and placed on the lip of the insert. The test specimen plate was lain onto the lip and additional ceramic fiber insulation packed aside and above the plate so that it was mechanically and thermally

Notes: TC 27 & TC 28 monitor exposure temperature at FR 86-87 in Berthing 2 for Ins_8 - Ins_13
TC 44 & TC 45 monitor exposure temperature at FR 84-85 in Berthing 2 for Ins_8 - Ins_13
TC 29 & TC 30 monitor exposure temperature at FR 82-83 in Berthing 2 for Ins_8 - Ins_13

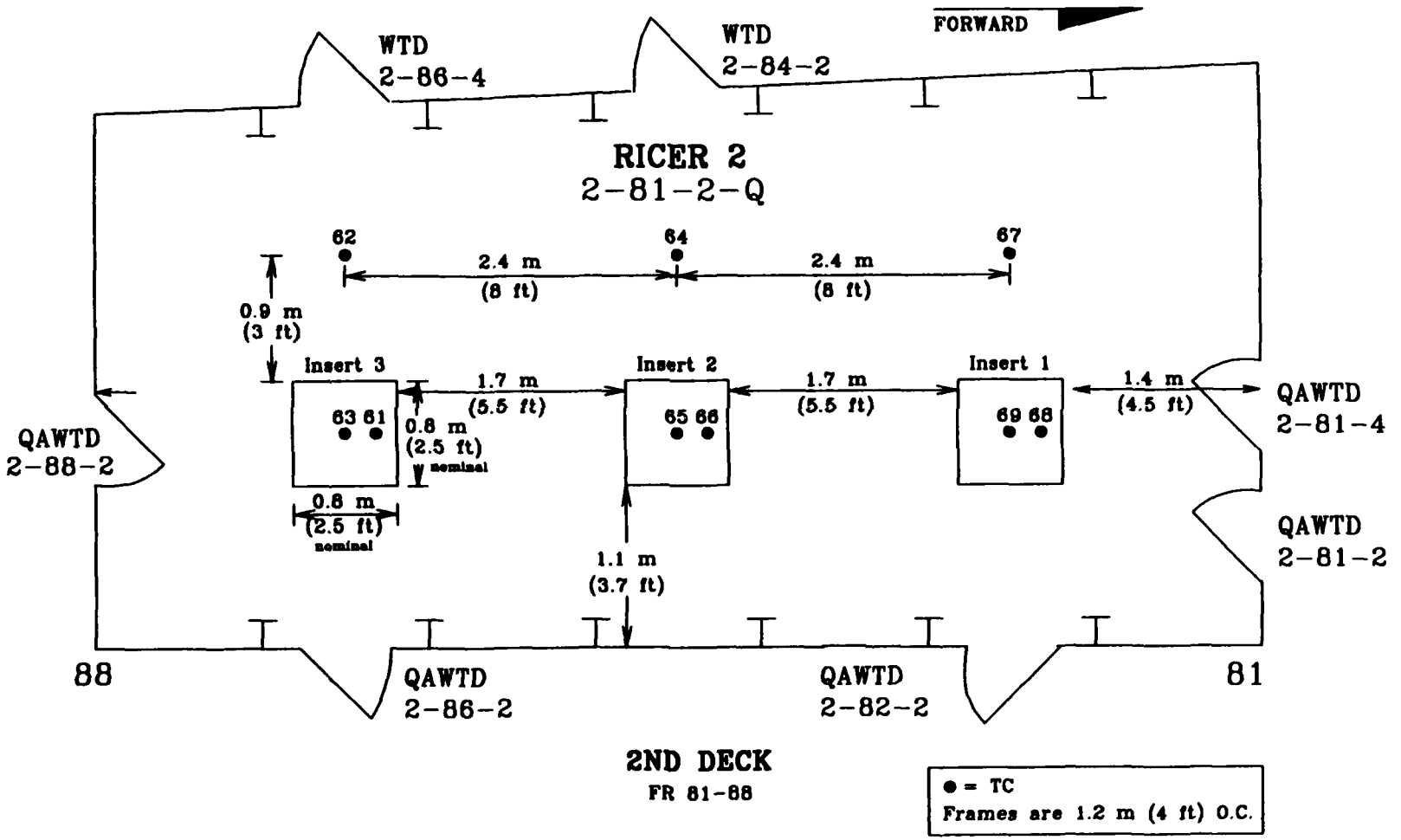

Fig. 3 - Plan view of RICER 2 deck showing inserts for insulation tests

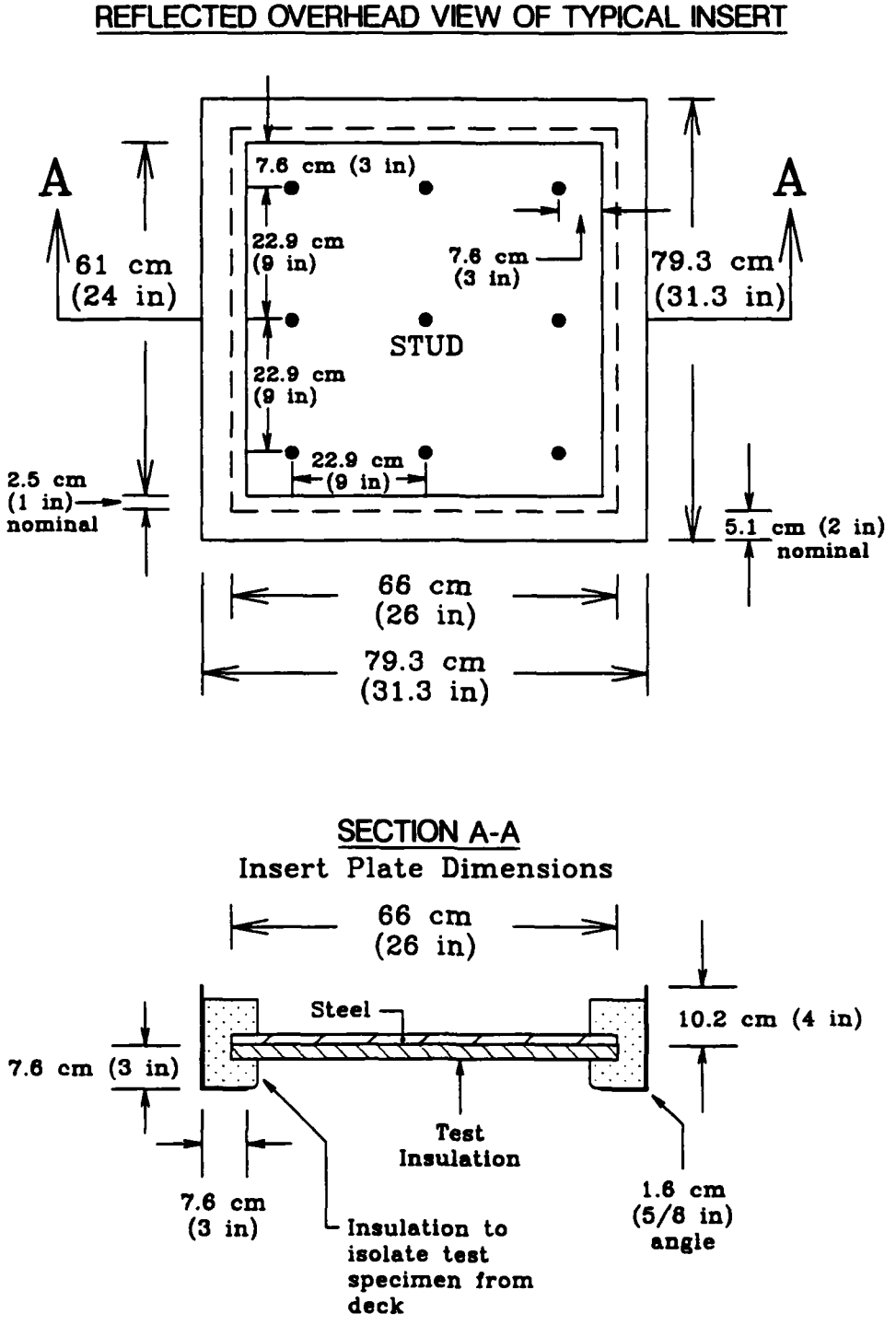

Fig. 4 - Details of RICER 2 deck inserts for insulation tests

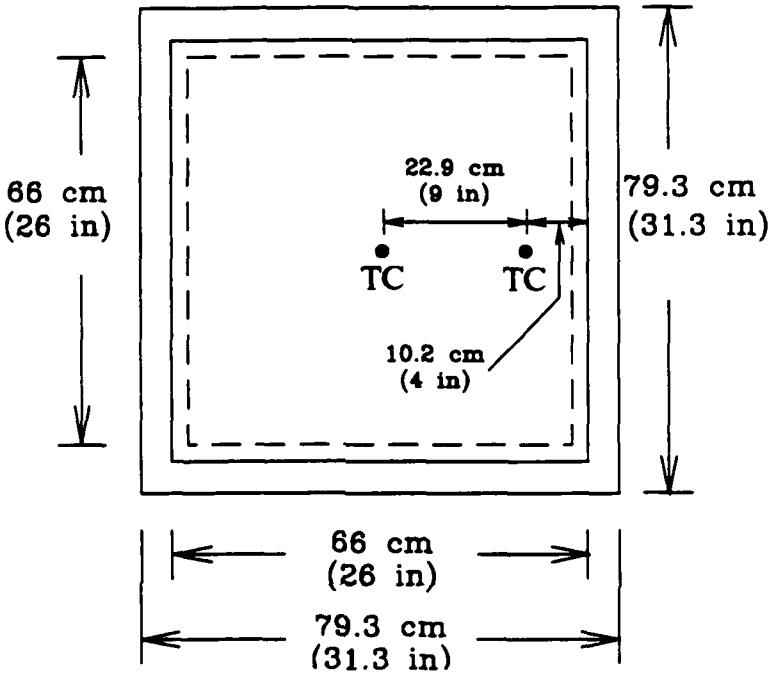

Fig. 5 - Plan view of typical RICER 2 deck insert thermocouple location

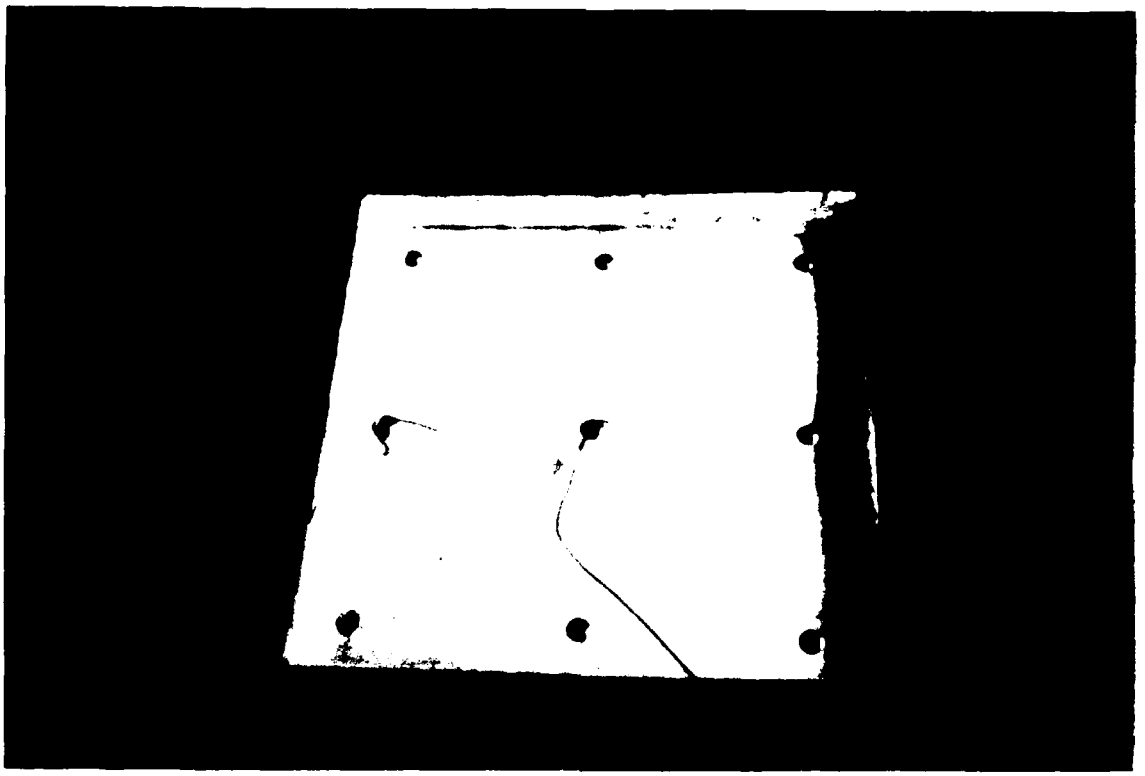

Fig. 6 - Typical deck insert viewed from BERTHING 2

Fig. 7 - Typical deck insert viewed from RICER 2

isolated from the insert. The insert plate with insulation overlapped the insert angle at each edge by about 6 cm (0.375 in.). The adjacent deck area of RICER 2 was 0.64 cm (0.25 in.) thick.

The inserts are designated from forward to aft as Insert 1 (FR 82-83), Insert 2 (FR 84-85), and Insert 3 (FR 86-87).

7.0 INSTRUMENTATION

References 6 and 7 describe the standard instrumentation for the ISCC test area. For these tests, nine additional thermocouples were installed on the RICER 2 deck (Fig. 3). These thermocouples were installed to measure the backside (unexposed side) temperature on the bare steel deck and inserts exposed to the fire in Berthing 2. Originally, these thermocouples were installed in FR 82-83, FR 84-85, and FR 86-87 to measure the RICER 2 deck temperature. After Test Ins_7, they were installed on the deck and inserts as follows:

Frame Bay	Bare Steel (RICER 2 deck)	Insert No.	Insert Center Thermocouple	Insert Edge Thermocouple
82-83	Thermocouple 67	1	Thermocouple 69	Thermocouple 68
84-85	Thermocouple 64	2	Thermocouple 65	Thermocouple 66
86-87	Thermocouple 62	3	Thermocouple 63	Thermocouple 61

Thermocouple 147 also measured the RICER 2 deck temperature near the center of the compartment. Figure 7 shows the thermocouples installed on the backside of a typical deck insert. The thermocouples were installed using a nut and screw arrangement. A nut having a small cut on one face was welded to the deck. The thermocouple was slipped through the cut so that the tip was centered in the nut opening. The screw was then inserted in the nut and screwed down so that the thermocouple tip was in contact with the deck. The backside thermocouples were uninsulated.

Exposure temperatures were monitored using the two thermocouple strings in Berthing 2 (Fig. 3). One string was located near the bulkhead at FR 81 (Thermocouples 13-17) and the other near the center of the compartment at FR 86 (Thermocouples 18-22). After Test Ins_8, additional thermocouples were added in Berthing 2 to monitor the fire exposure directly at the insert.

Insert	Exposure Thermocouple
1	Thermocouples 29 and 30
2	Thermocouples 44 and 45
3	Thermocouples 27 and 28

Generally, Thermocouples 27, 44, and 29 were attached to a stud on the exposed side of the insert within 5.1 cm (2 in.) or less of the insulation (Fig. 6). Thermocouples 30, 45, and 28 were attached in the overhead either at the insert or adjacent to the insert in the contiguous frame bay. The LASCOR panels were setup in a similar manner in the inserts, with thermocouples monitoring the backside temperatures.

8.0 PROCEDURE

Prior to each test, the insulation material was attached to the overhead of Berthing 2, or an insert plate was prepared and installed in the deck of RICER 2.

The post-flashover fire was created in Berthing 2 using a diesel spray fire. Three steel pans measuring 1.2 x 1.2 m (4 x 4 ft) and 5.1 cm (2 in.) deep were placed on the Berthing 2 deck. Approximately 57 liters (15 gal) of heptane were poured into three pans: 15.1 liters (4 gal) in each of the two outside pans and 26.5 liters (7 gal) in the center pan. These pans were ignited simultaneously and allowed to burn until the pool fires started to die down (approximately 2.5 minutes after ignition). Diesel fuel was then sprayed across the hot pans using three flat fan spray nozzles (Bete Fog Nozzle, Inc. Model FF 073145) positioned over each pan. The hot pans allowed the diesel to flash immediately to fire and eliminated residual fuel build-up in the test compartment. Total diesel fuel flow was nominally 17.4 lpm (4.6 gpm), split evenly through the three nozzles. Air was supplied naturally to the fire area via vent openings in the hull structure and the two door openings leading to the well deck. The estimated heat release rate of this fire, based on complete combustion, was on the order of 10 MW.

Each test was normally run for at least 20 minutes including the heptane preburn period. In some tests, active firefighting tests were conducted in RICER 1, RICER 2, and CIC after the fueling system was secured.

A more detailed description of the fueling system is contained in a separate report describing the fire dynamics in Berthing 2 and surrounding compartments [6].

9.0 RESULTS

9.1 Heat Transfer

A total of 13 insulation tests were conducted. The results of the first three tests, Ins_1a, 2 and 3, are described in more detail in Reference 4. Those results are included here for comparative purposes. Tests Ins_4-7 were conducted with insulation systems attached directly to the overhead of Berthing 2. Tests Ins_8-13 were conducted with the insert design. Table 1 summarizes the results based on the type of insulation, installation configuration, and the time for the backside temperature to reach 232°C (450°F) (the approximate ignition temperature of paper). Also included is the time difference to reach 232°C (450°F) between bare steel and the area protected by insulation. This provides a

Table 1. Insulation Test Summary

Test	Insulation Material	Test Specimen Design	Time to 232°C (min.)	Time Difference to Reach 232°C Between Bare Steel & Insulation (min.)	Damage Assessment
Ins_1a	Navy with aluminum caps	Entire overhead protected plus FR 81 bulkhead	5	0 - 1.5	Substantial amount of material dropped from the overhead (see Ref. 4)
Ins_2	Navy with steel caps	Entire overhead protected plus FR 81 bulkhead	7.5	2 - 4	Substantial amount of material dropped from the overhead (see Ref. 4)
Ins_3	Navy with steel sheet	0.6 x 1.2 m (2 x 4 ft) specimen attached to overhead	12.5	7.5 - 9	Material held in place
Ins_4	Navy with steel sheet	0.6 x 1.2 m (2 x 4 ft) specimen attached to overhead	10	7.5	Material held in place, steel warped but remained intact
Ins_5a	Manville	0.6 x 0.9 m (2 x 3 ft) specimen	11	8	Material remained in place and remained intact
	Polyamide	0.6 x 0.6 m (2 x 2 ft) specimen attached to overhead located adjacent to Manville specimen	9.8	6.7	Approximately one-third of the material remained in place, charred
Ins_6	Polyamide	Two 0.6 x 0.6 m (2 x 2 ft) specimens attached to overhead seam not taped	10	6.6	
Ins_7	Manville with joint	One 0.6 x 0.3 m (2 x 1 ft) specimen butted to 0.6 x 0.9 m (2 x 3 ft) specimen attached to the overhead seam not taped	Disregard Results		Material partially dropped
	Navy with 1 coat of Ocean 477	One 0.6 x 1.2 m (2 x 4 ft) specimen attached to the overhead	5.8 - 9.5 AVG 7.7	2.9 - 6.6 AVG 4.8	Material completely dropped no intumescent char observed on the remains

Table 1. Insulation Test Summary (Continued)

Test	Insulation Material	Test Specimen Design	Time to 232°C (min.)	Time Difference to Reach 232°C Between Bare Steel & Insulation (min.)	Damage Assessment
Ins_8	Manville	Insert	8.5	5.2	Material remained intact
Ins_9	2 layers of Manville	Insert	13.5 - 14.8 AVG 13.9	10.9	Material intact
	Navy with 1 coat of Ocean 9788	Insert	7 - 8.8 AVG 7.9	4 - 5.8 AVG 4.9	Material intact - modest intumescent action observed
	Navy with 1 coat of Hamilton 303	Insert	11	6.6	
Ins_10	2 layers of Manville	Insert	13.9 - 16.6 AVG 15.3	10.4 - 13.1 AVG 11.8	Material intact - facing essentially intact
	1 layer of Manville	Insert	8.9	5.4	Material intact - most of facing burnt off
	Navy with 1 coat of Hamilton 303	Insert	8.8 - 10.7 AVG 9.8	5.3 - 7.2 AVG 6.3	Material dropped off - intumescent material noted on exposure thermocouples
	Standard Navy (no insert/ no protective cover)	0.6 x 1.2 m (2 x 4 ft) specimen attached to the overhead	5.7	2.2	Material dropped off
	Polyamide	0.6 x 0.6 m (2 x 2 ft) specimen attached to the overhead	8.5	5	Material dropped off

Table 1. Insulation Test Summary (Continued)

Test	Insulation Material	Test Specimen Design	Time to 232°C (min.)	Time Difference to Reach 232°C Between Bare Steel & Insulation (min.)	Damage Assessment
Ins_11	Polyamide	Insert	10.7 - 11.3 AVG 11	7.4 - 8.0 AVG 7.7	Material dropped off during test
	Navy with steel sheet	Insert	10.0	6.7	Material remained intact
	Navy with 2 coats of Ocean 477	Insert	9.7 - 11 AVG 10.4	5.0 - 6.3 AVG 5.7	Material remained intact - most of facing burnt off, base insulation showed cracks, some intumescent action noted
	Ins_12 Navy unprotected	Insert	8.5 - 9.5 AVG 9.0	6.1 - 7.1 AVG 6.6	Material dropped off during test
	Ins_13 Navy unprotected	Insert	11.0 - 12.1 AVG 11.6	7.2 - 8.3 AVG 7.8	Material remained intact, facing melted and holed
	Navy with 2 coats of Ocean 9788	Insert	10.1	7.6	Material dropped off - intumescent action noted on remaining material

normalization of results for comparative purposes. Appendix A provides detailed test notes and graphical data for the tests.

In Tests Ins_1a and 2, the time for bare steel deck to reach 232°C (450°F) is assumed to be 3.5-5 minutes. This is based on the range of deck temperatures from Ins_3 since the overhead in Ins_1a and 2 was completely protected. In. Tests Ins_4-7, the bare steel deck temperature is based on the temperature from the closest deck thermocouple (TC 62, 64, or 67). For Tests Ins_8-13, the deck thermocouple used for comparison is specifically identified.

Table 2 summarizes the time difference to reach 232°C (450°F) between the bare steel and insulation for the different protective systems. The average time to 232°C (450°F) on the unexposed side for the bare steel insert design tests was 3.4 minutes, with a standard deviation of ±0.5 minutes. For the insert design, the data indicate that the protective systems provide no improvements for the standard Navy insulation. The slight increase in fire resistance exhibited by the standard insulation compared to the protective systems is attributed to normal experimental error and differences in the threats between tests. This will be discussed in Section 10.2. The difference in test procedures is most noticeable for the standard Navy insulation where there is a 4-5 minute time gain where the insert design is used. Perhaps this can be attributed to more rapid degradation/falling of the Navy insulation when the edges are unprotected. Since the insulation could not be readily observed during the test due to the flames, it is difficult to quantify the mechanism at work. This theory is supported by the results with the steel sheathing. Where the material is attached directly to the overhead, the sheathing provides three times the resistance. When the insert tests are compared, the results between the sheathed and unprotected insulation are comparable.

Table 3 summarizes the fire resistive characteristics between the standard Navy insulation and the potential replacement systems. For the insert design, single layers of the Navy standard, Manville, and polyamide are essentially the same with the Manville having slightly less resistance. The double layer of Manville provides the greatest degree of resistance. Again, a greater difference between the standard Navy and experimental insulation is seen when comparing the results of the materials attached directly to the overhead. This supports the previous conclusion that when attached directly to the overhead, the resistance of the standard Navy insulation may be less than with other insulations.

Tables 4 and 5 describe the LASCOR setup and results.

Table 2. Comparison of Protective Systems with Navy Standard Insulation

Time Difference to Reach 232°C Between Bare Steel and Insulation (min.)

	Navy Unprotected	Navy with Steel Sheet	Navy with 2 coats Ocean 477	Navy with Ocean 9788 1 coat	Navy with Ocean 9788 2 coats	Navy with Hamilton coating
Insert Design	6.6	6.7	5.7	4.9	7.6	6.6
	7.8					6.3
	AVG 7.2					AVG 6.5
Specimen attached to overhead*	3**	8.3	4.8	--	--	---
	2.2	7.5				
	AVG 2.6	AVG 7.9				

Notes:

* Disregard Ins_1a
** Average of Ins_2

Table 3. Comparison of Proposed Insulation Systems with Navy Standard Insulation

Time Difference to Reach 232°C Between Bare Steel and Insulation (min.)

	Navy Unprotected	Manville 1 layer	Manville 2 layer	Polyamide
Insert Design	6.6	5.2	10.9	7.7
	7.8	5.4	11.8	
	AVG 7.2	AVG 5.3	AVG 11.4	
Specimen Attached to Overhead	3*			6.7
	2.2	8	---	6.6
	AVG 2.6			5.0
				AVG 6.1

Notes:
* Average of Ins_2

Table 4. LASCOR Panels Tested in the ISCC Test Area

Panel No.	Test No.	LASCOR Panel	Insert No. (Fwd to Aft)
1	LASC1 & 2	Pennsylvania State University	2
2	LASC1 - 5	Pennsylvania State University	3
4	LASC3 - 5	Florida Int. University Panel	1
5	LASC3 - 5	Florida Int. University Panel	2
6	LASC1 & 2	Treated Panel (Canadian)	1

Note: Panel #3 was not evaluated because fill and drain treatment was not available.

Table 5 shows the difference between bare steel and the LASCOR panels for time to achieve the 235°C (450°F) on the non-fire side of the panel.

Table 5. Comparison of Heat Transfer Through LASCOR Panel

	Time difference of bare steel vs. Panel to reach 232°C (450°F) (min:sec)				
Panel No.	LASC1	LASC2	LASC3	LASC4	LASC5
1 (PSU)	1:56	2:06	--	--	--
2 (PSU)	2:48	2:14	1:55	2:26	2:50
3	----------not tested----------				
4 (FIU Foam Filled)	--	--	8:35	6:14	6:37
5 (FIU Foam Filled)	--	--	5:25	3:33	4:41
6 (Canadian Treated)	2:14	1:09	--	--	--

The hollow panels provided 2-3 minutes delay in the time to reach 232°C compared to bare steel. The Canadian treated panels provided 1-2 minutes delay. The foam filled panels extended the time to 232°C (450°F) by a factor of 2-4 (4-8.5 min.) compared to the hollow panels. Reference [7] provides additional details on the testing of the LASCOR panels.

9.2 Damage Assessment

Table 1 describes the damage to the insulation material after 20 minutes of fire exposure. Generally, the Navy insulation dropped from the overhead during the test (Fig. 8). In one test, Ins_13, the Navy insulation did remain intact, with holing occurring on the facing (Fig. 9). The exposure to the mineral wool in Ins_13 was slightly lower than in other tests (see Section 10.2). In all cases, there was full depth charring of the mineral wool, and it was very friable. Any remaining insulation was powder-like to the touch, indicating that the phenolic resin binder was consumed and the material was possibly undergoing a phase change. In Test Ins_2, the Navy insulation generally remained intact on the bulkhead (Fig. 10). The sheet steel used to hold the Navy insulation remained intact during the fire exposure (Figs. 11 and 12). No general conclusions can be drawn for the intumescent coatings. In some tests, the insulation remained intact (Ins_11, Fig. 13). In other tests, the insulation dropped from the insert (e.g., Ins_9 with Hamilton, Ins_13 with Ocean 9788).

Generally, the Manville material remained intact during the 20-minute fire exposure although the facing started to peel off (Fig. 14). The ability of the Manville material to stay in place may be attributed in part to its binderless formulation and the Kevlar thread which is used to stitch the material together. The polyamide tended to fall off the overhead during the fire.

10.0 DISCUSSION

10.1 Effects of Experimental Design

Tables 2 and 3 indicate that, generally, the tests with the insert design yielded longer times to achieve 232°C (450°F) backside temperatures compared to tests where the material was attached directly to the overhead. This is most noticeable for the standard Navy insulation. With the insert design, the Navy insulation provided an additional 4-5 minutes to reach 232°C (450°F), compared to the tests with material attached directly to the overhead. Two factors may contribute to this effect, both related to the edge of the insulation. More rapid degradation/falling of the insulation may occur where the edges are unprotected. For example, in Ins_2 the material fell where the edges (butt joints) were protected by the cloth tape. This cloth tape quickly burns and falls away as observed in the CBD tests.

In Ins_10, the edges of the single sheet of insulation were unprotected, and there was no physical support of those edges. There initially was concern that a "thermal short" effect was influencing the backside temperature data for the single sheets attached directly to the overhead. A review of the data does not indicate any particular trend to support this. For example, the thermocouple closest to the edge of the insert did not always result in the highest temperature compared to the thermocouple nearer to the center of the specimen. The "thermal short" or bypass theory can probably be discounted for the overhead attachment methods, and the data were considered reasonably accurate.

Fig. 8 - Overhead of BERTHING 2 after Ins_2 fire test

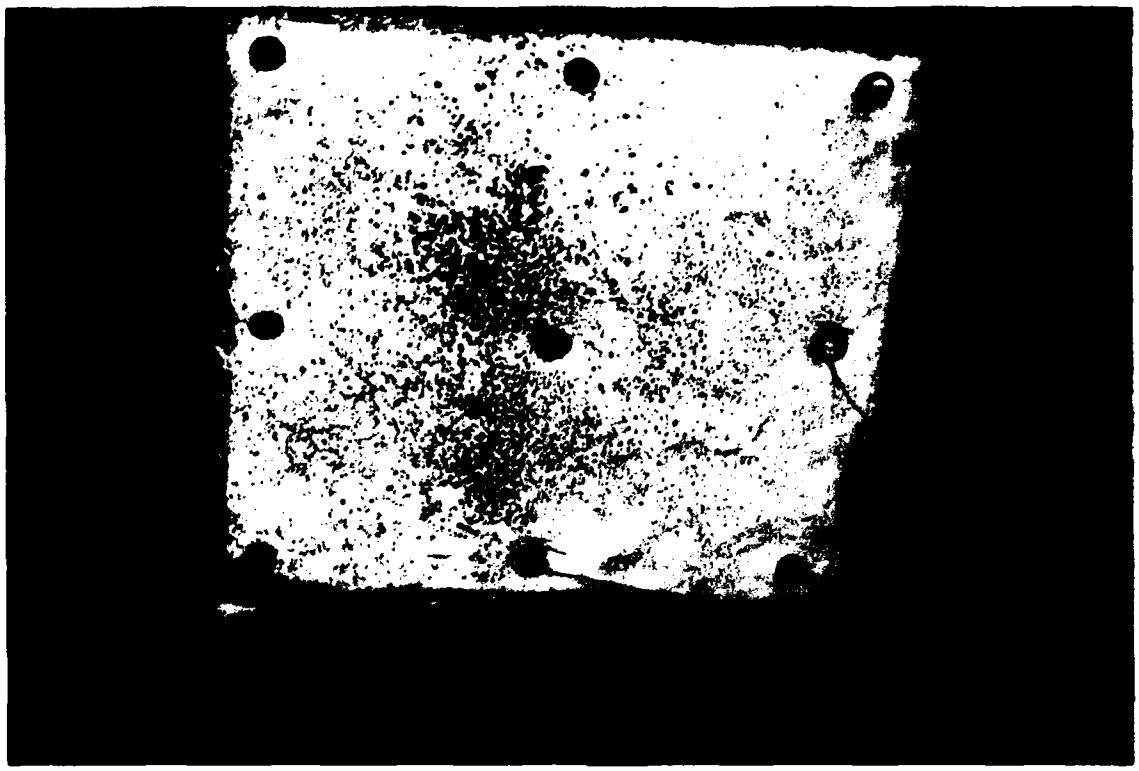

Fig. 9 - Navy insulation after Ins_13 fire

Fig. 10 - Bulkhead of BERTHING 2, FR 81, after Ins_2 fire test

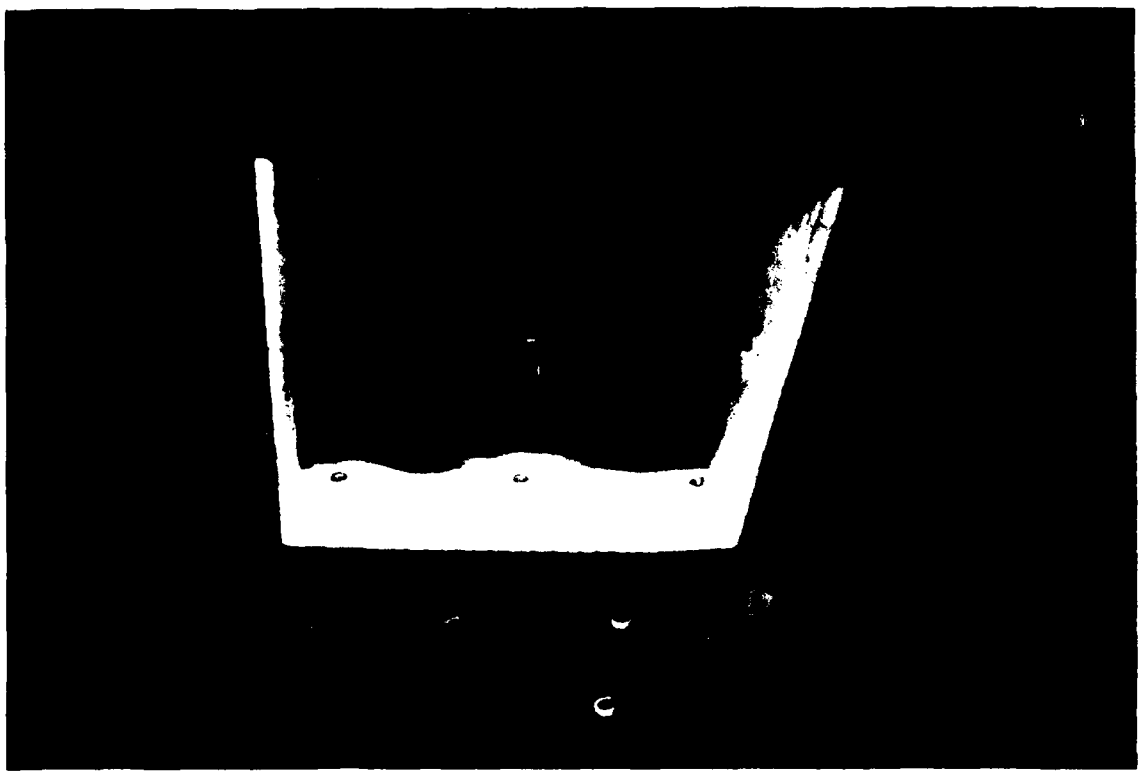

Fig. 11 - Insulation protected by steel sheath, prior to Ins_11

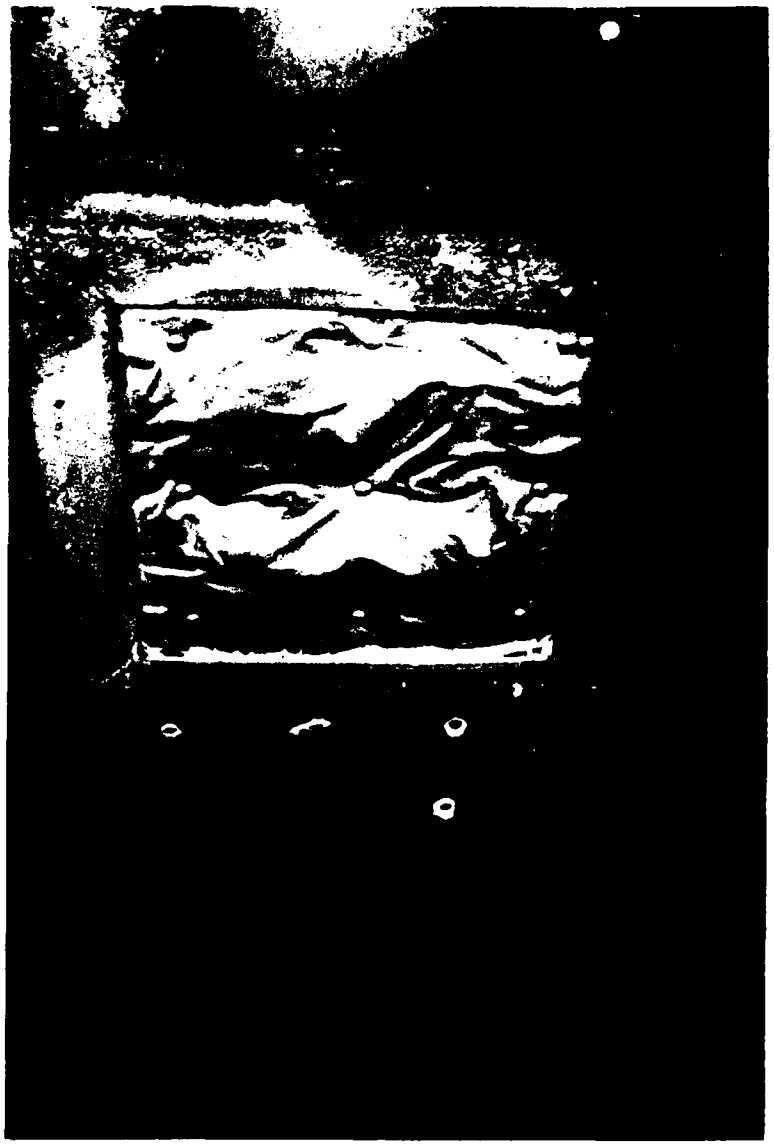

Fig. 12 - Insulation protected by steel sheath, post test Ins_11

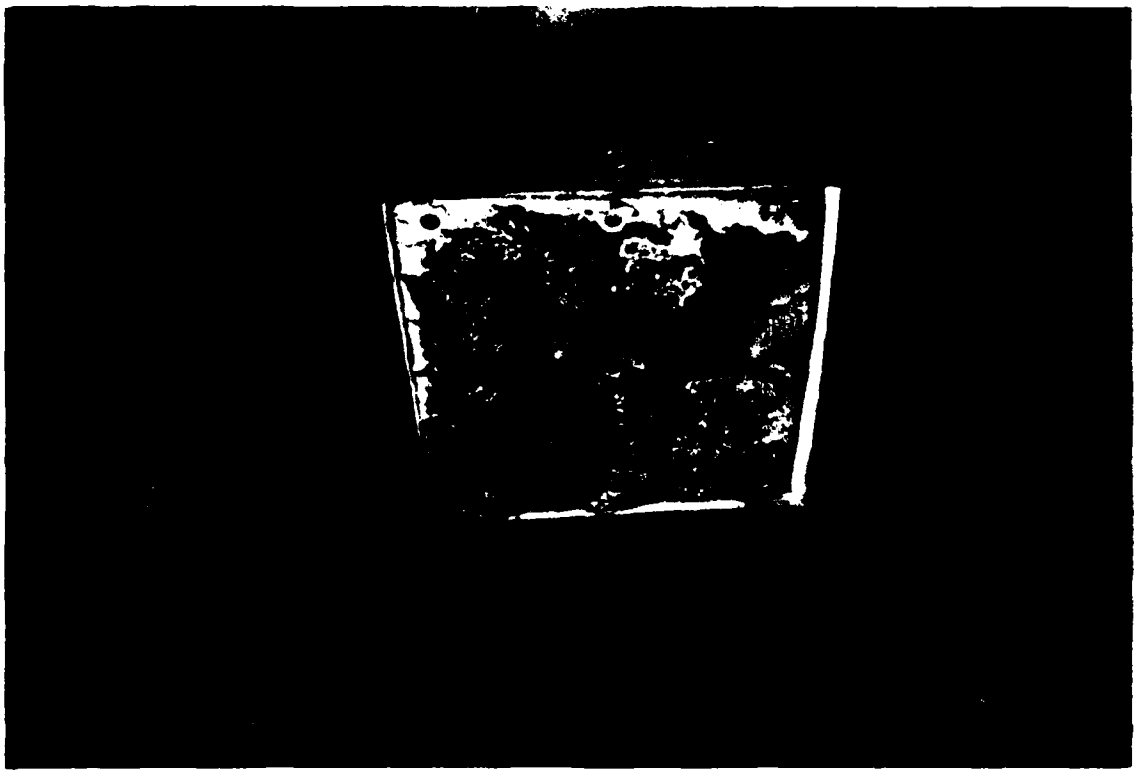

Fig. 13 - Navy insulation protected by Ocean 477, post test Ins_11

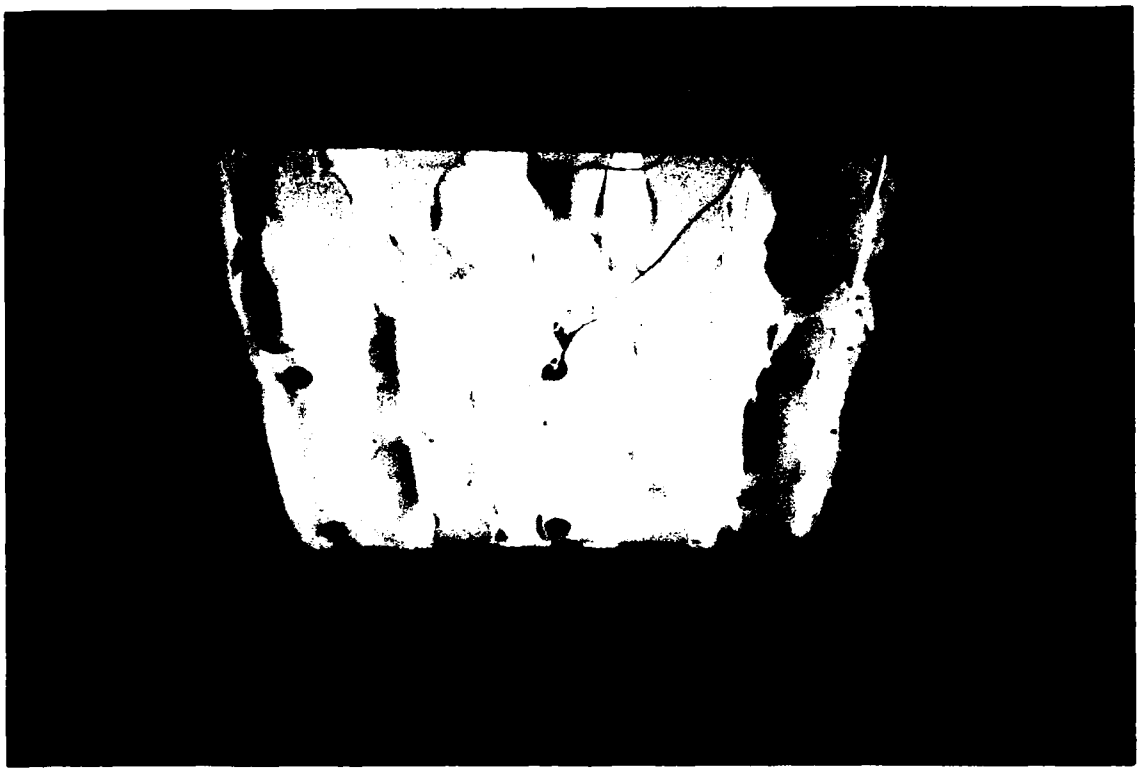

Fig. 14 - Two layers of Manville insulation, post test Ins_10

The lip overlap of the insert design may also provide physical strength to hold the insulation in place. This is most evident when comparing the results of the Navy insulation protected by sheet steel with unprotected insulation. The sheet steel was designed to help hold the insulation in place. The results for the steel protected insulation are about the same for both the insert and overhead attachment designs, compared to the considerable improvement for the unprotected insulation with the insert design.

The same trend of better results for the insert design is evident for the polyamide and Ocean 477 tests although not to the degree evident for the unprotected Navy insulation. The trend was not observed in the Manville tests, where the specimen attached directly to the overhead performed better than the experiments where the insert design was used. The differences in results where experimental materials and protective sheaths/coatings are used may be attributed to normal experimental deviation and differences in the exposure for the particular test.

10.2 Effects of Design Fire

Most of the variability of the data may be explained by fluctuations in the design fire. The effects of ambient wind on heat transfer characteristics to adjacent compartments has been analyzed [8] and will be described in future reports [9]. Consequently, ambient wind speed and direction may affect the local insult in any particular region of Berthing 2. General variations in the design fire are shown in Fig. 15 for Tests 8-12, thermocouples 20, 21, and 22. These are the top three thermocouples on a string located directly adjacent to the fire pan under Insert #3. The first standard deviation shows the general variability for the overall mean of these tests, which is on the order of ± 50°C. Effects of compartment location are evident in Fig. 16, the mean and first standard deviation of thermocouples 15, 16, and 17. These top three thermocouples are located on a string near the FR 81 bulkhead, adjacent to a structural stringer. The stringer partially shields the string, which results in an overall reduced insult to the bulkhead. This also explains the better performance of the bulkhead insulation in Tests Ins_1a and 2 described in Reference 4, i.e., the insult is not as great directly against the bulkhead compared to direct flame impingement to the deck.

Repeatability of the results can be attributed to a large degree on the local threat. This is shown in Figs. 17-19. In Fig. 17, the threat to a single layer of Manville insulation is shown by thermocouple 44 for Tests 8 and 10. The threats are nearly the same, with the resulting heat transfer nearly the same. No direct exposure data were recorded for Ins_5a where the Manville was attached directly to the deck. The same characteristic holds true when tests with a double layer of Manville are compared (Fig. 18). Where the threats differ between tests, the time difference in heat transfer for the same material becomes evident. Fig. 19 shows the results of the standard Navy insulation in Tests Ins_12 and 13. As the variance in threat increases, so does the heat transfer. Appendix A provides graphical data on the heat transfer characteristics for Tests Ins_4-13 and, where recorded, the localized threat curve.

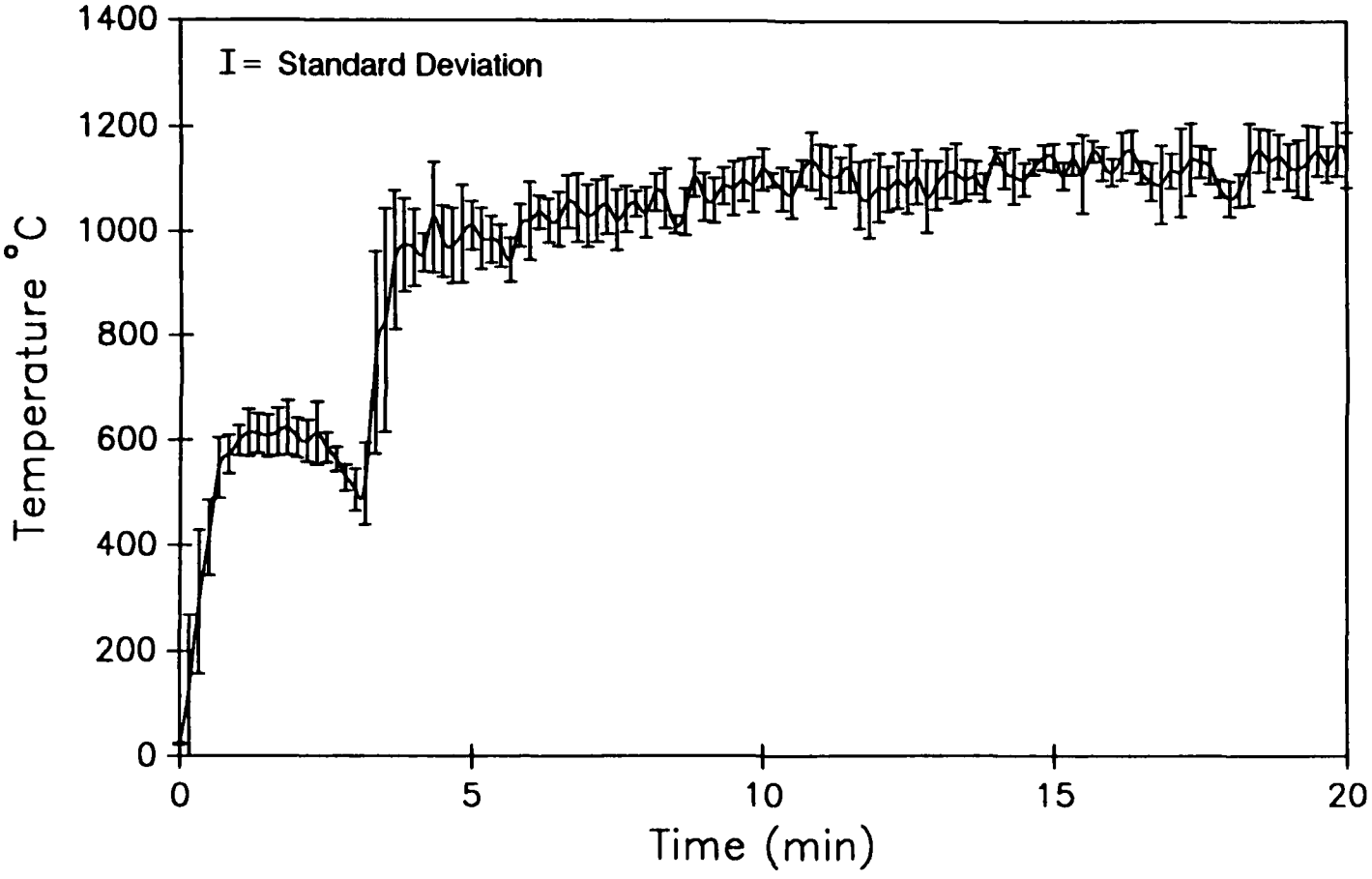

Fig. 15 - Average of TC's 20, 21 & 22 for Ins_8 through Ins_12

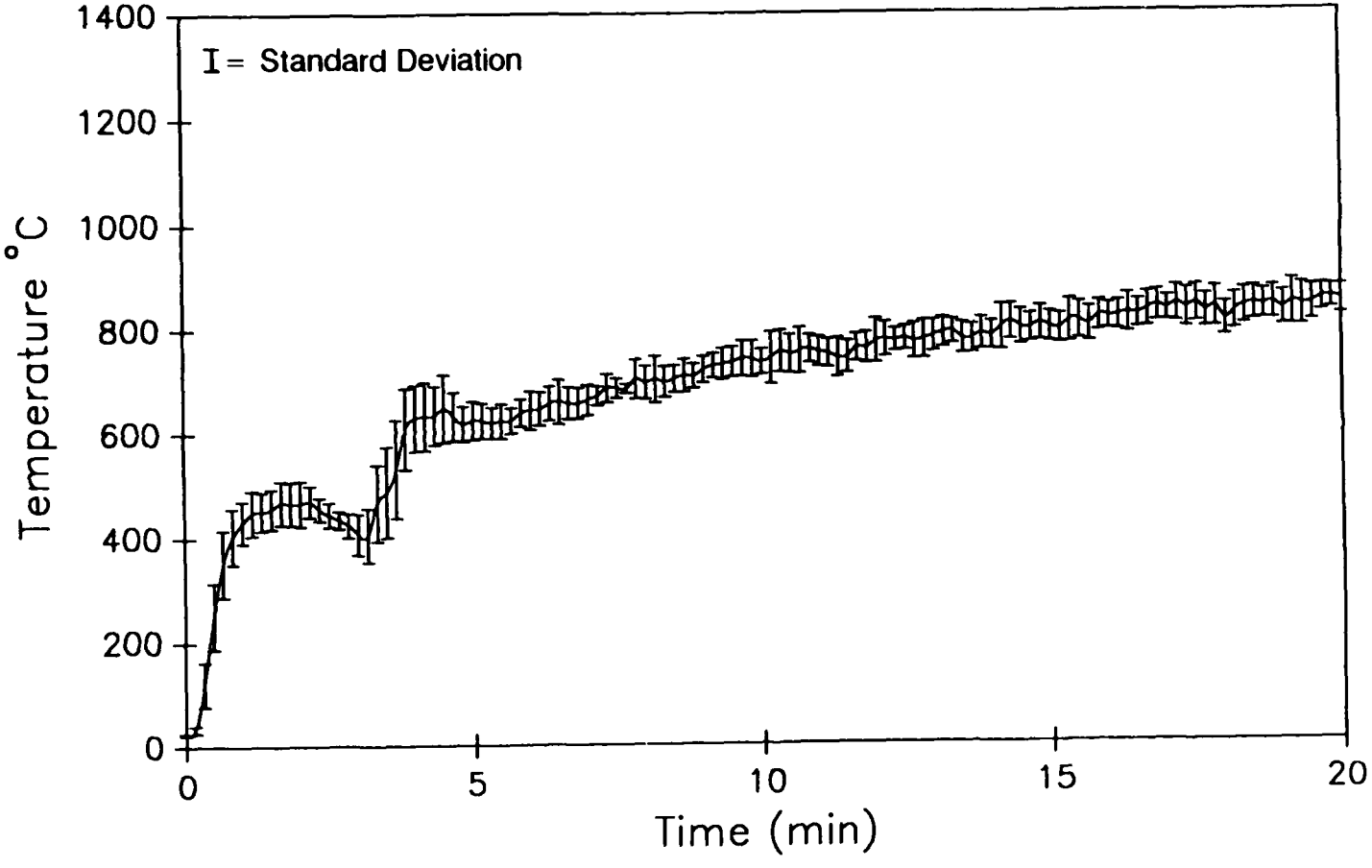

Fig. 16 - Average of TC's 15, 16 & 17 for Ins_8 through Ins_13

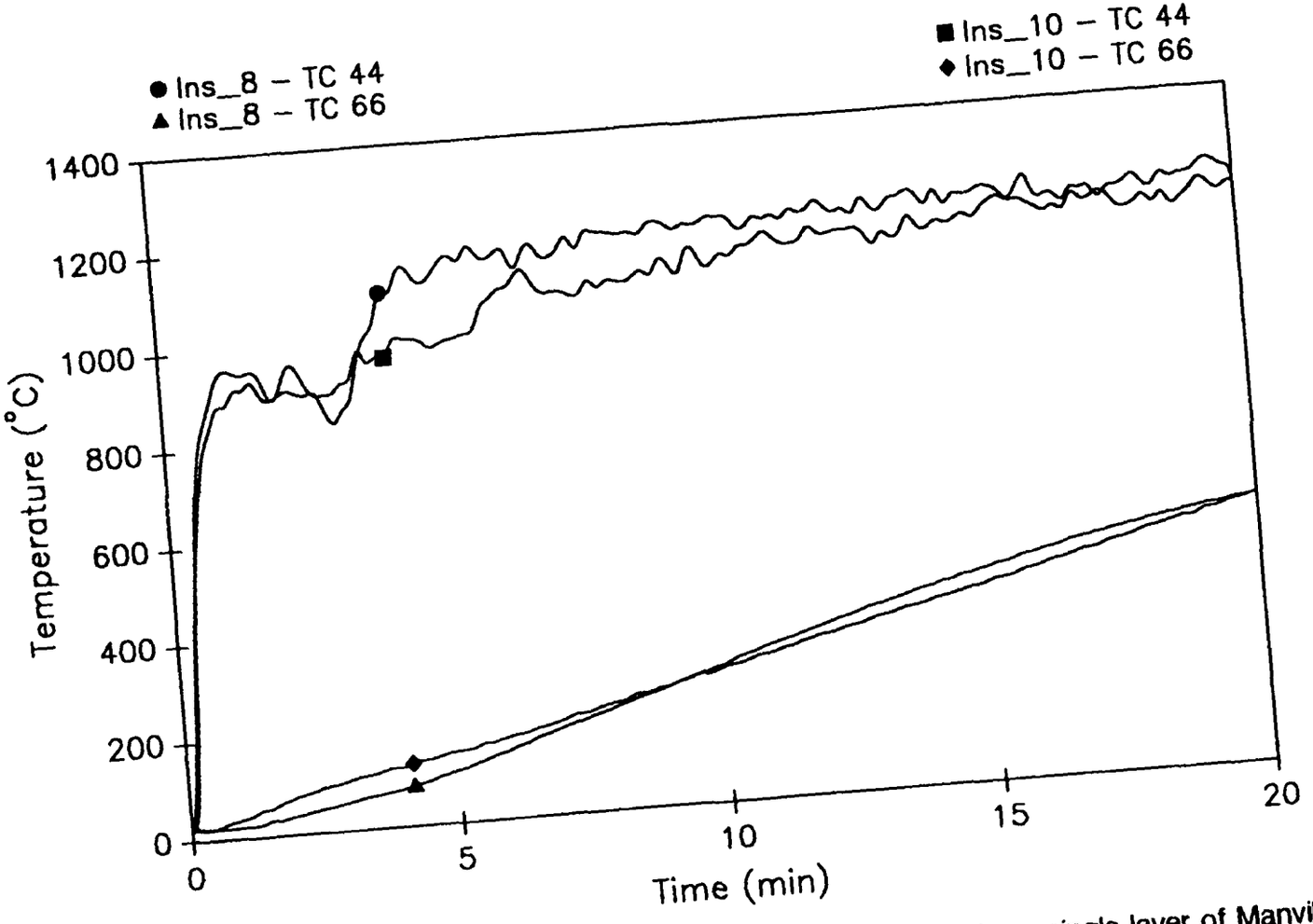

Fig. 17 - Comparison of exposure temperatures and heat transfer for a single layer of Manville

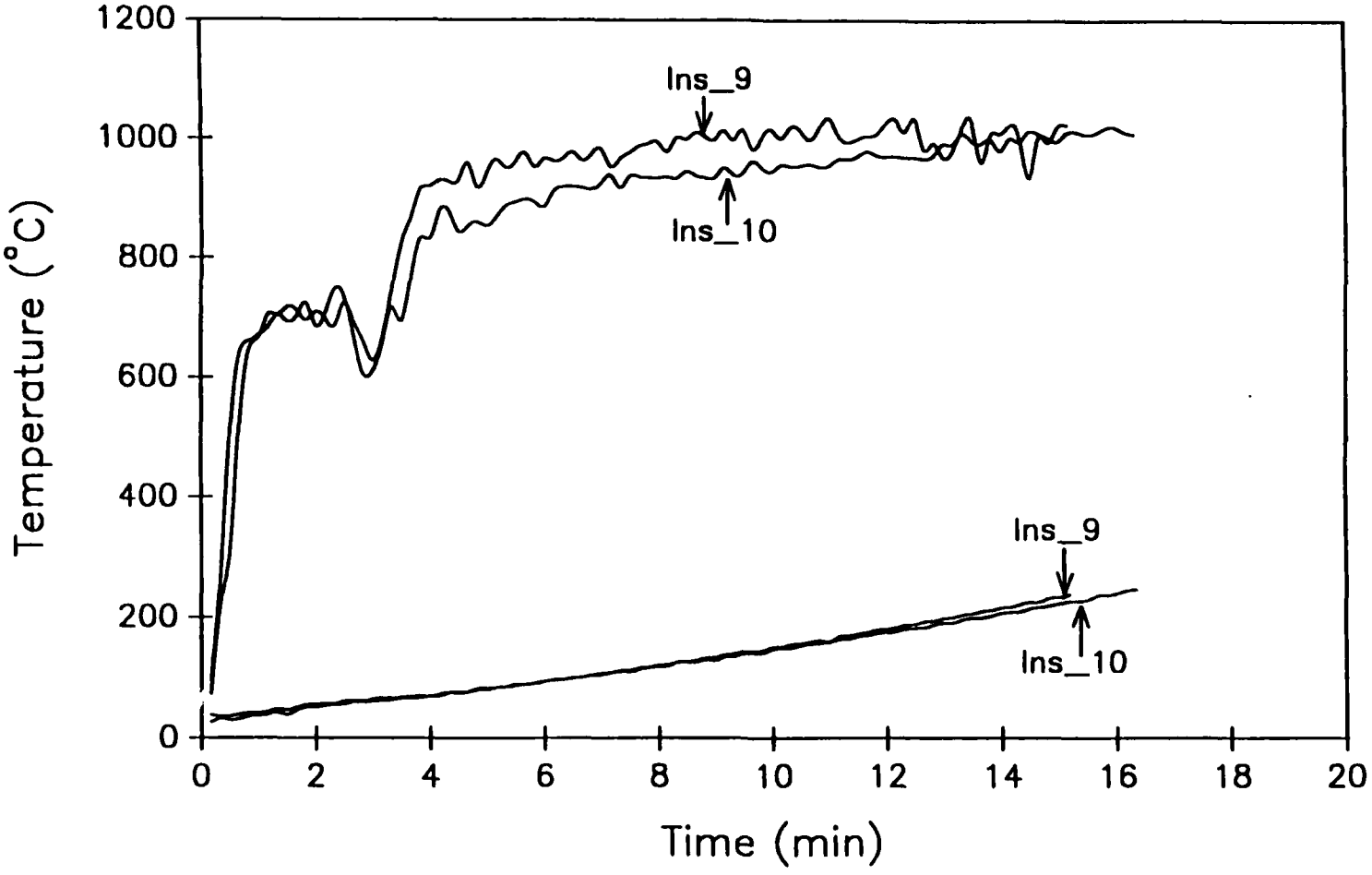

Fig. 18 - Comparison of exposure temperatures and heat transfer for a double layer of Manville

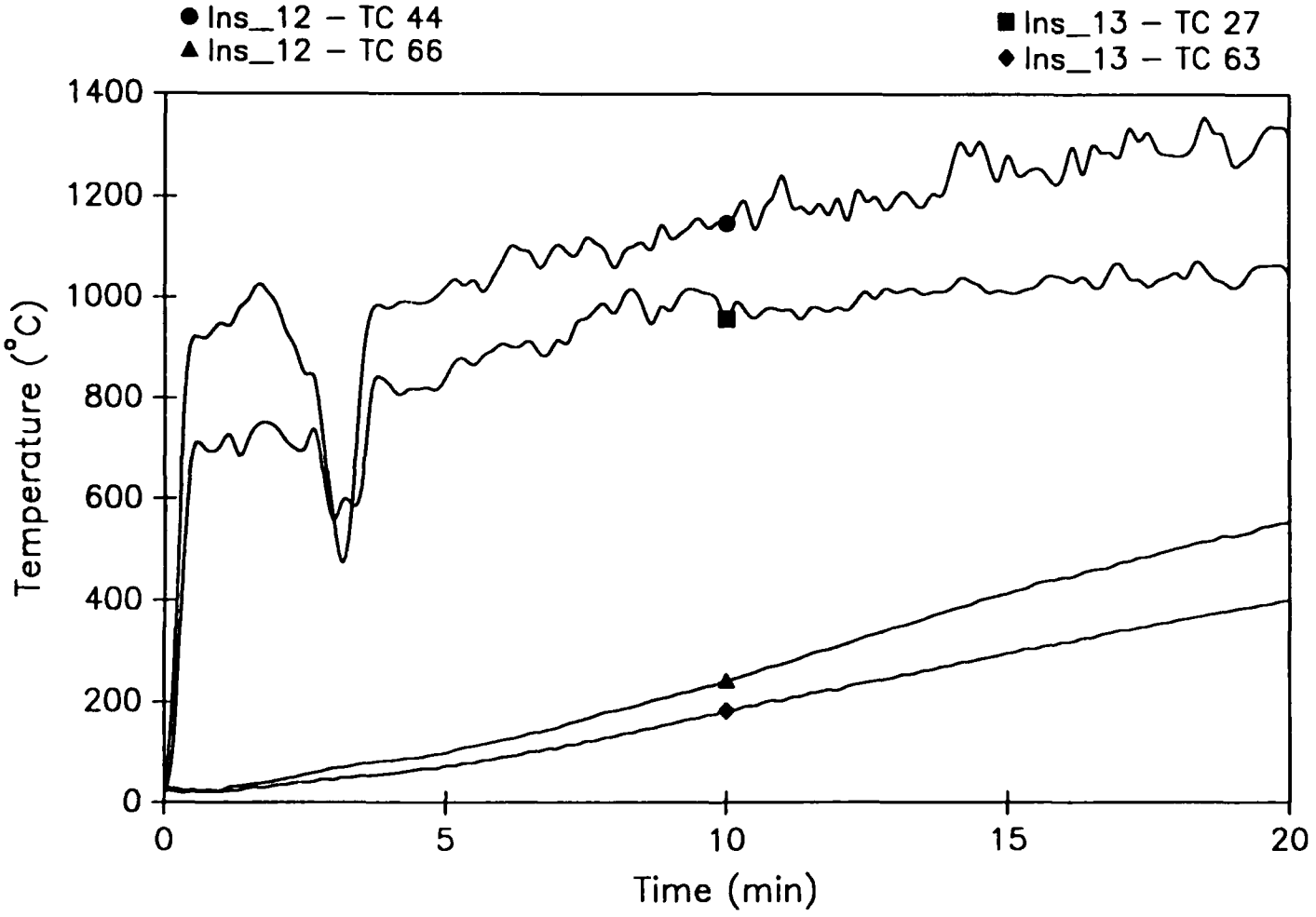

Fig. 19 - Comparison of exposure temperatures and heat transfer for a Navy insulation

10.3 Effects of Insulating a Compartment

Figures 20 and 21 show a comparison of the average upper layer air temperature in Berthing 2 for Ins_2, where the entire overhead and forward bulkhead was insulated, the insert tests, Ins_8 - 13. The data indicate that at the hottest part of the compartment (TC 20-22 located directly adjacent to the fire pan under Insert No. 3), there is virtually no change in temperature. For the thermocouple string located adjacent to the bulkhead (Fig. 21), there was about a 200°C (392°F) temperature rise in the test with the entire overhead insulated. This suggests that, at the hottest locations, i.e., where the temperature already has reached near-maximum adiabatic flame temperature, there is no effect of insulating the compartment. However, the thermocouple data near the bulkhead suggest greater uniformity of compartment temperature. Thus, the overall compartment may actually be hotter compared to the uninsulated situation. This was qualitatively supported by test observers who reported Ins_2 as the hottest fire encountered in the test series.

10.4 Effects of Insulation on Fire Spread and Heat Transfer

For the high temperature, post-flashover scenario investigated in the ISCC tests, standard Navy mineral wool insulation provides only a modest reduction in time to critical temperature (232°C (450°F)) for steel decks. The insulation does provide some heat transfer retarding effect as shown in Figures 22-23 and Table 6. In particular, the air temperature in RICER 2 is held below critical temperatures (232°C (450°F)) for nearly 20 minutes.

Table 6. Effects of Insulation on Heat Transfer to Adjacent Compartments

	Temperature (°C)			
	5 min.	10 min.	15 min.	20 min.
RICER 2 deck				
With insulation	111	430	608	698
Without insulation	416	651	733	778
Berthing 2 FWD Bulkhead				
High				
With insulation	38	177	304	386
Without insulation	312	522	596	617
Low				
With insulation	27	69	126	186
Without insulation	155	317	426	487
RICER 2 Air Temperature				
With insulation	18	90	179	246
Without insulation	88	210	284	329

Note: Data are from Ins_2 and Ins_3.

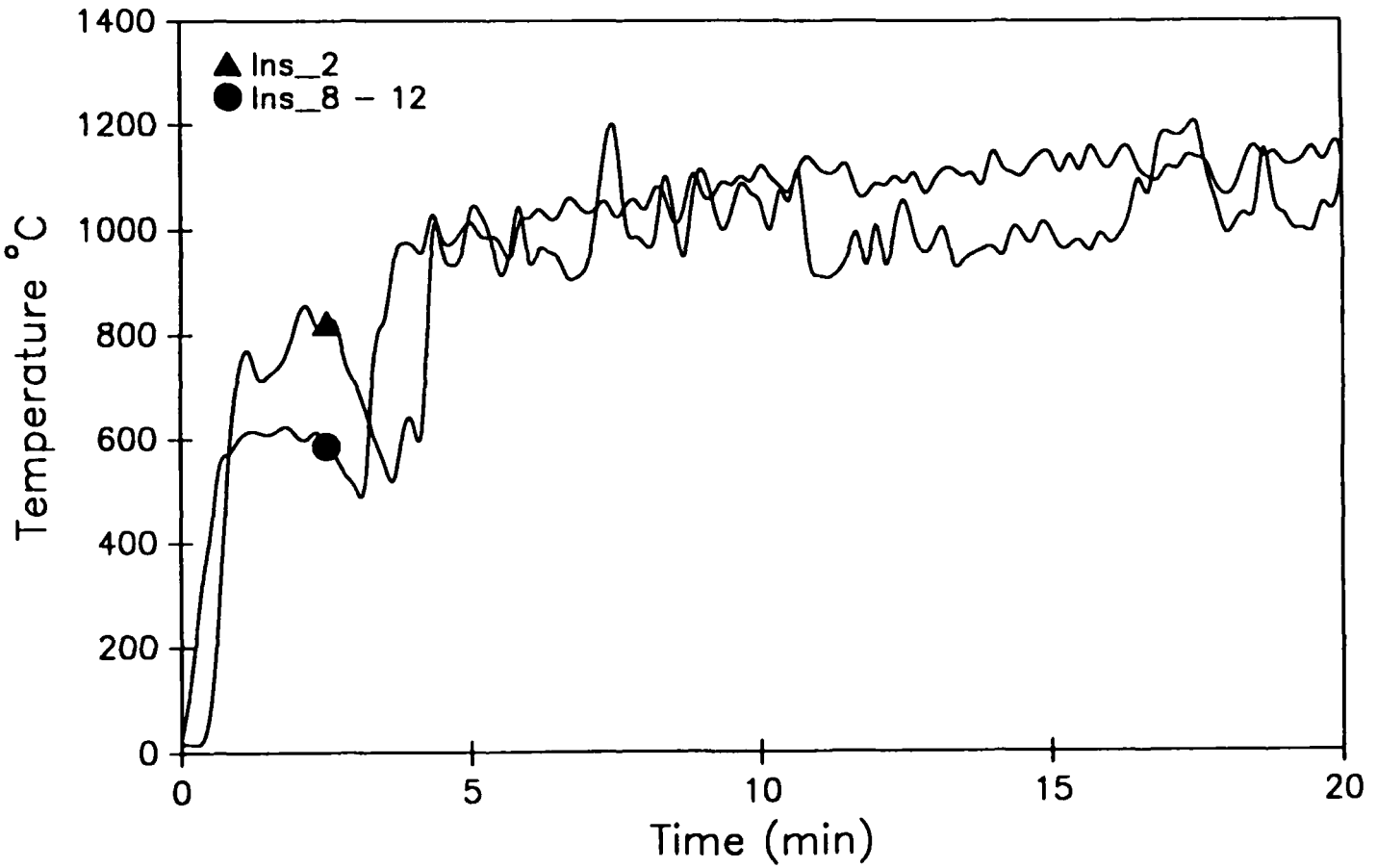

Fig. 20 - Comparison of TC's 20, 21 & 22 for Ins_8 through Ins_12 vs. Ins_2

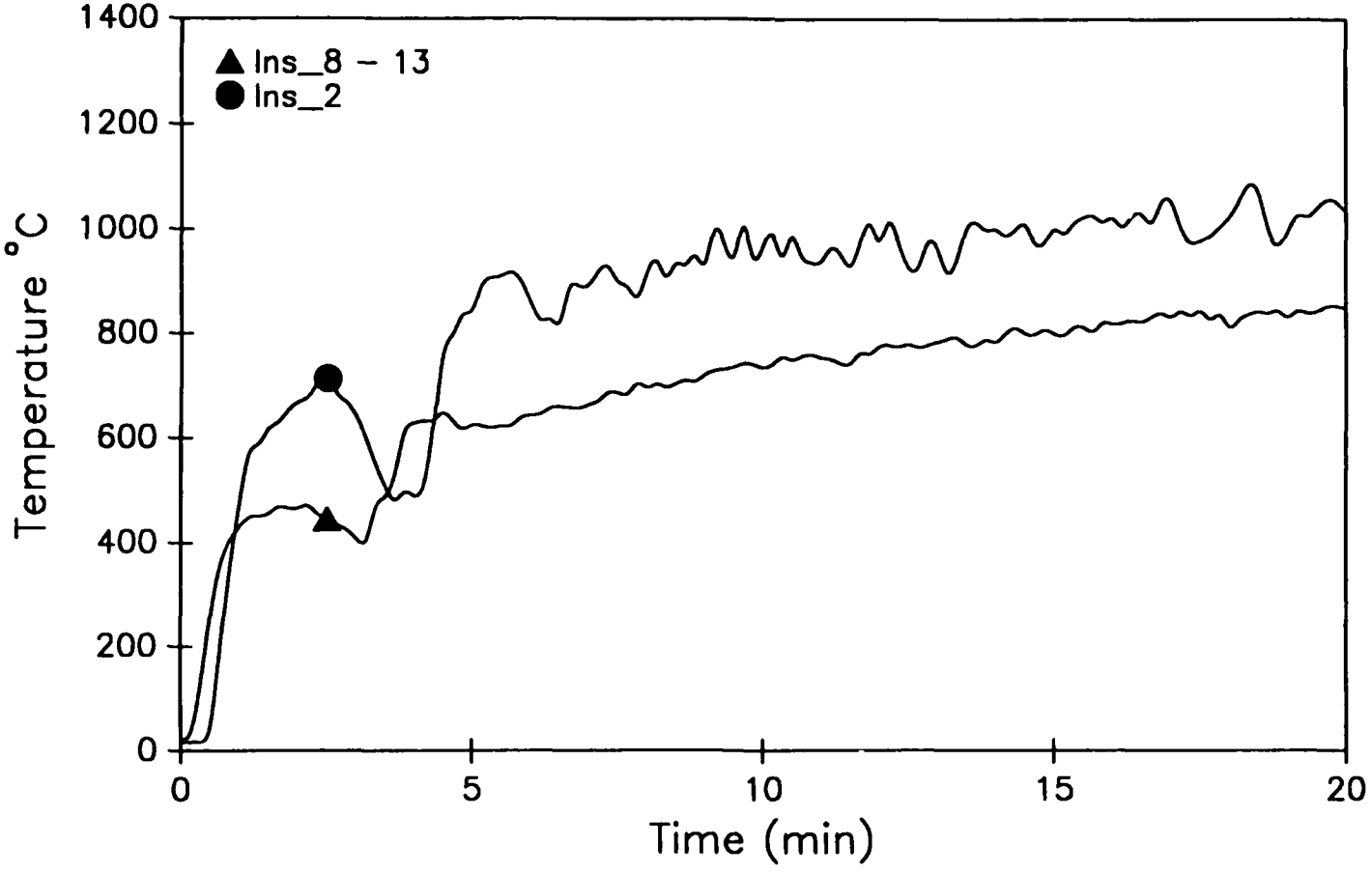

Fig. 21 - Comparison of TC's 15, 16 & 17 for Ins_8 through Ins_13 vs. Ins_2

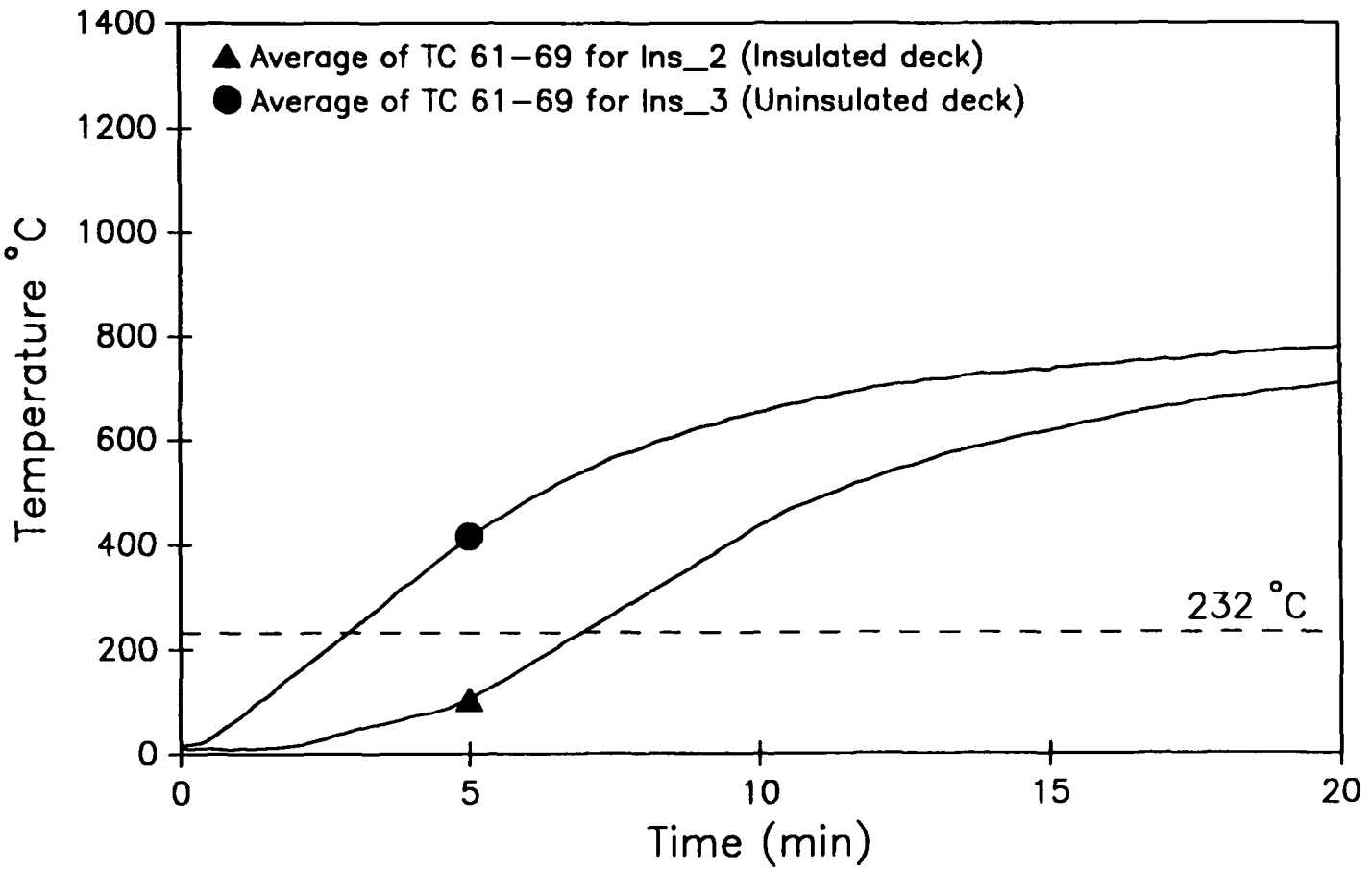

Fig. 22 - Comparison of insulated and uninsulated deck temperatures

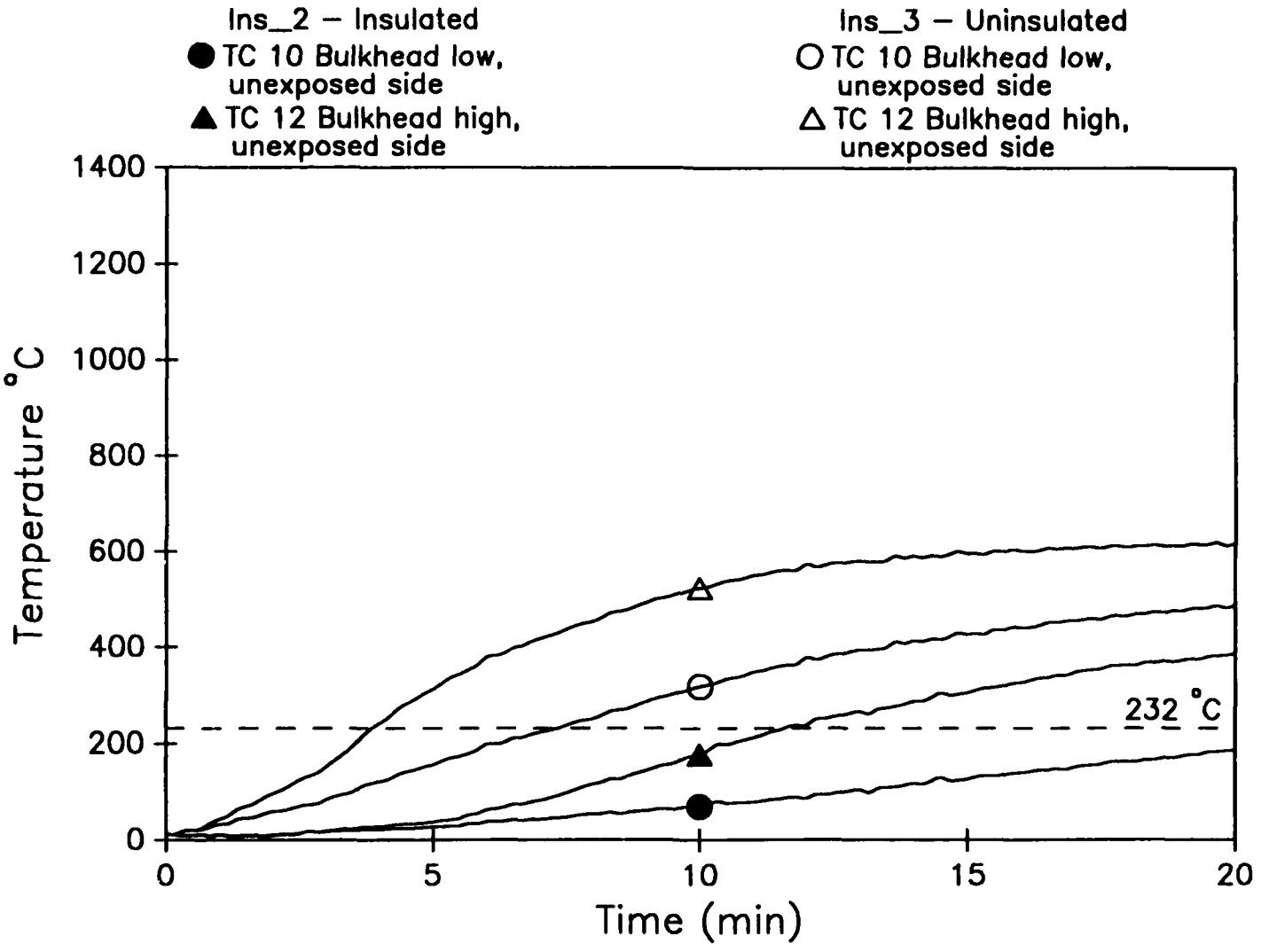

Fig. 23 - Comparison of insulated and uninsulated bulkhead temperatures

11.0 FIRE MODELING

Correlation between these fire tests and others is accomplished through heat transfer fire modeling. Specifically, a finite-element heat transfer model was used to compare the results from the ex-USS SHADWELL tests and other standard tests of the same or similar materials. In particular, the ASTM E119 fire exposure is of interest.

Appendix B details the fire modeling analysis. The thermal modeling capabilities of a finite element heat transfer program were validated on simple exact solutions and then compared to the results of fire tests with a material with well-known material properties. Predictions agreed with the test data with a maximum error of 15%.

Having validated the program, the model was used to predict the results from the SHADWELL tests. The primary limitation is the lack of thermal conductivity data for the Navy mineral wool and candidate materials. Specific density and thickness data was also unconfirmed since some of the data has not been officially reported. High-temperature thermal conductivity data was "backed out" of the results for the Navy mineral wool and Manville Structo-gard. These data were then used to attempt to model E119 fire exposure tests. The results, detailed graphically in Appendix B, are summarized in Table 7. The data indicates that all of the SHADWELL results could be accurately modeled. Results for other tests are not as uniformly successful. The lack of agreement with the E119 test data is attributed to: the "back out" method to establish thermal conductivity; lack of accurate thickness, specific heat, and density data for some of the test materials; and, anomalies in some of the thermocouple data in the E119 exposure tests.

Table 7. Correlation of Test Results and Fire Modeling

Materials/Test	Time to Reach 232°C (min) Predicted	Actual
Navy mineral wool, 1 in.		
SHADWELL Ins_12	9.0	9.2
SHADWELL Ins_13	11.5	11.7
VTEC Small E119	25.0	31.5
Navy mineral wool, 2 in.		
VTEC Small E119	64.0	77.0
Manville Structo-gard, 1 layer		
SHADWELL Ins_8	7.8	8.7
SHADWELL Ins_10	8.0	9.0
VTEC Small E119	24.0	34.0
Manville Structo-gard, 2 layers		
SHADWELL Ins_9	16.1	14.6
SHADWELL Ins_10	16.2	15.1

Even with these limitations, the model is being used to estimate the performance of Navy mineral wool and Manville Structo-gard material which will be exposed to a UL 1709 fire exposure.

It is interesting that the results of the SHADWELL tests for the Navy mineral wool were reproduced with the model, even thought the material generally fell off the overhead during the tests. This phenomena could not be accurately modeled. This suggests that the material may lose its inherent insulative capacity (e.g. due to glass fusing/phase change) before the effects of the material dropping off are evident in the backside temperatures. This is supported by the tests where steel sheathes were used to hold the Navy insulation in place. The heat transfer between the sheathed and unsheathed material is about the same (Table 1). This may not hold true for thicker specimens of mineral wool, where physical collapse may have a more dramatic impact on the heat transfer.

Important variables in the finite element model were identified by systematically varying model parameters. In particular, the actual thickness and conductivity of a material and accurate exposure temperatures are important input parameters. Small changes to these input parameters can significantly change the output, i.e., time to reach 232°C (450°F) on the unexposed side of the steel.

There was a concern that the heating of RICER 2 during the tests was affecting the thermocouple data on the insulation inserts. In other words, the temperature in RICER 2 might be heating the uninsulated thermocouples on the backside of the steel inserts, prematurely causing "failure," i.e., time to 232°C (450°F). This was addressed in the Appendix B analysis. It was determined that for thin insulation, e.g., one layer of fibrous material, that the impact was insignificant. With an increasing insulation thickness, where the RICER 2 temperature is higher than the steel temperature, the impact becomes more pronounced. For example, it was estimated that, for the two-layer Manville insulation tests, failure time may have been overestimated by 2 minutes or 15%. The problem becomes even more serious for thicker insulations, where the differences in RICER 2 and steel deck temperatures would be even more pronounced. In those situations, actions should be taken to cool RICER 2 or the data corrected using a heat transfer program.

12.0 CONCLUSIONS

1. The experimental Manville Structo-gard material when applied in a double layer appears to have improved thermal properties compared to the Navy mineral wool. It also did not physically degrade when exposed to high temperatures, as the mineral wool did.

2. The protective coatings tested were ineffective in reducing heat transfer when applied directly to existing mineral wool insulation.

3. Variations in test data were primarily a result of variations in direct exposure temperatures. These variations were readily handled by the computer model.

4. The effects of mineral wool mechanical failure (dropping off of the overhead) were more pronounced when the material was applied directly to the overhead, compared to the insert design.

5. The LASCOR sandwich panels did not provide significant heat transfer reductions. Panels 1, 2 and 6 provided less than 3 minutes increased time to critical temperatures compared to bare steel. Foam-filled panels 4 and 5 were roughly equivalent to steel protected with the existing Navy mineral wool.

6. Insulation of the entire compartment overhead and forward bulkhead did not increase temperatures at the hottest locations in the fire compartment, but did increase temperatures which generally were below flame temperature in other areas. This suggests that localized temperatures in the hot layer of a compartment, where there is a post-flashover fire, may not be hotter. The overall compartment temperature may increase, i.e., closer to the well-stirred approximation commonly assumed for post-flashover situations. Modeling data suggests that insulating a compartment may reduce the time to flashover for a given threat compared to an uninsulated compartment. This aspect was not investigated.

7. While the Navy mineral wool provides only modest protection against a post-flashover fire, it does delay heat transfer compared to bare steel.

13.0 RECOMMENDATIONS

1. The experimental development of the Manville Structo-gard material should be continued.

2. No further evaluation of protective coatings, applied directly to existing mineral wool, is recommended. Improved insulations, and protective coatings applied directly to metal bulkheads, are better approaches for addressing the passive reduction of heat transfer.

3. The validation and application of heat transfer models should continue. The Navy should consider requiring that data for candidate insulation materials include actual density, actual applied thickness, and thermal conductivity and specific heat for temperatures from 0-1100°C. High temperature thermal conductivity data would provide the additional benefit of identifying material degradation/phase changes. Accurate modeling data could be used to

    a) Predict the performance of insulating materials for different fire threats; and

    b) Predict the effects of insulated vs. uninsulated compartments for flashover potential.

4. The importance of material degradation for thicker specimens of Navy mineral wool insulation should be determined.

14.0 REFERENCES

1. Naval Sea Systems Command, "Damage Assessment and Analysis, USS STARK (FFG 31)," Washington, DC, February 1988.

2. G.G. Back, J.T. Leonard, C.R. Fulper, R.L. Darwin, J.L. Scheffey, R.L. Willard, P.J. DiNenno, J.S. Steel, R.J. Ouellette, and C.L. Beyler, "Post-Flashover Fires in Simulated Shipboard Compartments: Phase I–Small Scale Studies," NRL Memorandum Report 6886, 3 September 1991.

3. J.T. Leonard, G.G. Back, J.L. Scheffey, and R.G. Gewain, "An Evaluation of Navy Approved Insulation Exposed to a Severe Fire Insult," NRL Draft Letter Report, October 1990, unpublished.

4. J.L. Scheffey, F.W. Williams, A.F. Durkin, and G.G. Back, "Interim Evaluation of Navy-Approved Fire Insulation Exposed to a Post-Flashover Fire (ex-USS SHADWELL)," NRL Letter Report Ser 6180-166, 11 April 1991.

5. Naval Sea Systems Command, "Insulation, Passive Fire Protection–Insulation Details," NAVSEASYSCOM Dwg. No. 803-5184182, 2 December 1987.

6. J.L. Scheffey and F.W. Williams, "Internal Ship Conflagration Control (ISCC) Large Scale Testing–Fire Dynamics Test Series," NRL Letter Report Ser 6180-220, 9 April 1990.

7. A.F. Durkin and F.W. Williams, "Fire Test of Lightweight Metallic Sandwich Structure Material," NRL Letter Report Ser 6180-292.1, 11 June 1992.

8. D.E. Smith and K.C. Burns, "Statistical Support of the Analysis of Full Scale Fire Tests: The Effect of Wind Conditions," Desmatics, Inc., Technical Report No. 146, State College, PA, September 1991.

9. J.L. Scheffey, T.A. Toomey, and F.W. Williams, "Post-Flashover Fires in Simulated Shipboard Compartment: Phase V–Fire Dynamics in ex-USS SHADWELL Test Compartment, NRL Memo Report (in preparation).

15.0 ACKNOWLEDGEMENTS

The assistance of the test team on the ex-USS SHADWELL during the ISCC tests is greatly appreciated. In particular, setup and installation of insulation specimens by Manton Smith and Carl Krueger is recognized.

Thanks is extended to Charles Rollhauser of NSWC, Annapolis Detachment, for providing preliminary test data for input to the computer model.

Appendix A

Instrumentation Details and Data Plots

Appendix A

Table of Contents

Appendix A

Table of Contents

Table A1. Insulation Test Notes

Test	Insulation Material	Specimen Location	Notes
Ins_1a	Navy with aluminum caps	entire overhead	3.5 - 5 minutes to 232°C from Ins_3
Ins_2	Navy with steel caps	entire overhead	3.5 - 5 minutes to 232°C from Ins_3
Ins_3	Navy with sheet steel	FR 84-85	TC 63 protected; 61, 62, 64-67 unprotected
Ins_4	Navy with Sheet Steel	FR 84-85	TC 44 was placed within the insulation--use TC 45 for analysis of heat transfer TC 65 was at the edge of the protected area--use TC 66 for analysis of heat transfer
Ins_5a	Manville	FR 84-85	TC's 65 and 44 monitor the polyamide TC's 66 and 45 monitor the Manville
	Polyamide	FR 84-85	TC's 44 and 45 were slipped in the insulation just under the exposed facing
Ins_6	Polyamide	FR 84-85	TC 44 was placed within the insulation TC 45 was slipped in the insulation just under the exposed face

General Notes: Thermocouples 61-69 monitor backside (unexposed temperatures).
Thermocouples 27, 28, 29, 30, 44, and 45 measure localized exposure or internal insulation techniques.
Starting with Ins_8, insert design adopted; location of the thermocouples 61-69, 27-28, 44 and 45 standardized as shown in Fig. 3. Thermocouples 29 and 30 measuring exposure temperatures for Insert 1 starting with Test Ins_10. TC 147 also monitors deck temperature near the center of RICER 2.

Table A1. Insulation Test Notes (Continued)

Test	Insulation Material	Specimen Location	Notes
Ins_7	Manville with joint	FR 84-85	TC's 27 and 28 placed within the insulation with Ocean 477 TC 64 installed over the Manville insulation area (along with TC 65 and 66)
	Navy with 1 coat of Ocean 477	FR 86-87	TC's 44 and 45 placed within insulation; TC 44 went bad during test TC 62 time to reach 232°C = 2.9 min.
Ins_8	Manville	FR 84-85	2 x 2 ft new insert design TC 64 time to reach 232°C = 3.3 min.
Ins_9	2 layers of Manville	Insert 3	TC 62 time to reach 232°C = 3 min.
	Navy with 1 coat of Ocean 9788	Insert 2	TC 64 time to reach 232°C = 3 min.
	Navy with 1 coat of Hamilton 303	Insert 1	TC 67 time to reach 232°C = 4.4 min.

General Notes: Thermocouples 61-69 monitor backside (unexposed temperatures).
Thermocouples 27, 28, 29, 30, 44, and 45 measure localized exposure or internal insulation techniques.
Starting with Ins_8, insert design adopted; location of the thermocouples 61-69, 27-28, 44 and 45 standardized as shown in Fig. 3. Thermocouples 29 and 30 measuring exposure temperatures for Insert 1 starting with Test Ins_10. TC 147 also monitors deck temperature near the center of RICER 2.

Table A1. Insulation Test Notes (Continued)

Test	Insulation Material	Specimen Location	Notes
Ins_10	2 layer of Manville	Insert 3	TC 62 time to reach 232°C = 3.5 min. TC 147 time to reach 232°C = 3.7 min.
	1 layer of Manville	Insert 2	Use TC 62 for all data
	Navy with 1 coat of Hamilton 303	Insert 1	TC 67 was on an area protected by polyamide
	Standard Navy (no insert/ no protective cover)	FR 84-85	TC 64 was on an area protected by the Navy insulation
	Polyamide (no insert)	FR 82-83	TC 67
Ins_11	CD/NSWC Polyamide	Insert 1	TC 64 time to reach 232°C = 3.3 min. TC 67 was still over area protected by polyamide insulation from Ins_10
	Navy with steel sheet	Insert 2	TC 64 time to reach 232°C = 3.3 min. TC 44 went bad during test
	Navy with 2 coats of Ocean 477	Insert 3	TC 62 time to reach 232°C = 4.7 min.

General Notes: Thermocouples 61-69 monitor backside (unexposed temperatures).
Thermocouples 27, 28, 29, 30, 44, and 45 measure localized exposure or internal insulation techniques.
Starting with Ins_8, insert design adopted; location of the thermocouples 61-69, 27-28, 44 and 45 standardized as shown in Fig. 3. Thermocouples 29 and 30 measuring exposure temperatures for Insert 1 starting with Test Ins_10. TC 147 also monitors deck temperature near the center of RICER 2.

Table A1. Insulation Test Notes (Continued)

Test	Insulation Material	Specimen Location	Notes
Ins_12	Navy unprotected	Insert 2	TC 64 time to reach 232°C = 2.4 min. TC 65 not installed under screw–this may contribute to the extended time to 232°C TC 45 located outside of insert, near wing wall bulkhead TC 30 was located near the center of the compartment, not below insert
Ins_13	Navy unprotected	Insert 3	TC 61 time to reach 232°C = 3.8 min.
	Navy with 2 coats of Ocean 9788	Insert 2	TC 64 time to reach 232°C = 2.5 min. TC 45 located outside of the insert, near wing wall bulkhead

General Notes: Thermocouples 61-69 monitor backside (unexposed temperatures).
Thermocouples 27, 28, 29, 30, 44, and 45 measure localized exposure or internal insulation techniques.
Starting with Ins_8, insert design adopted; location of the thermocouples 61-69, 27-28, 44 and 45 standardized as shown in Fig. 3. Thermocouples 29 and 30 measuring exposure temperatures for Insert 1 starting with Test Ins_10. TC 147 also monitors deck temperature near the center of RICER 2.

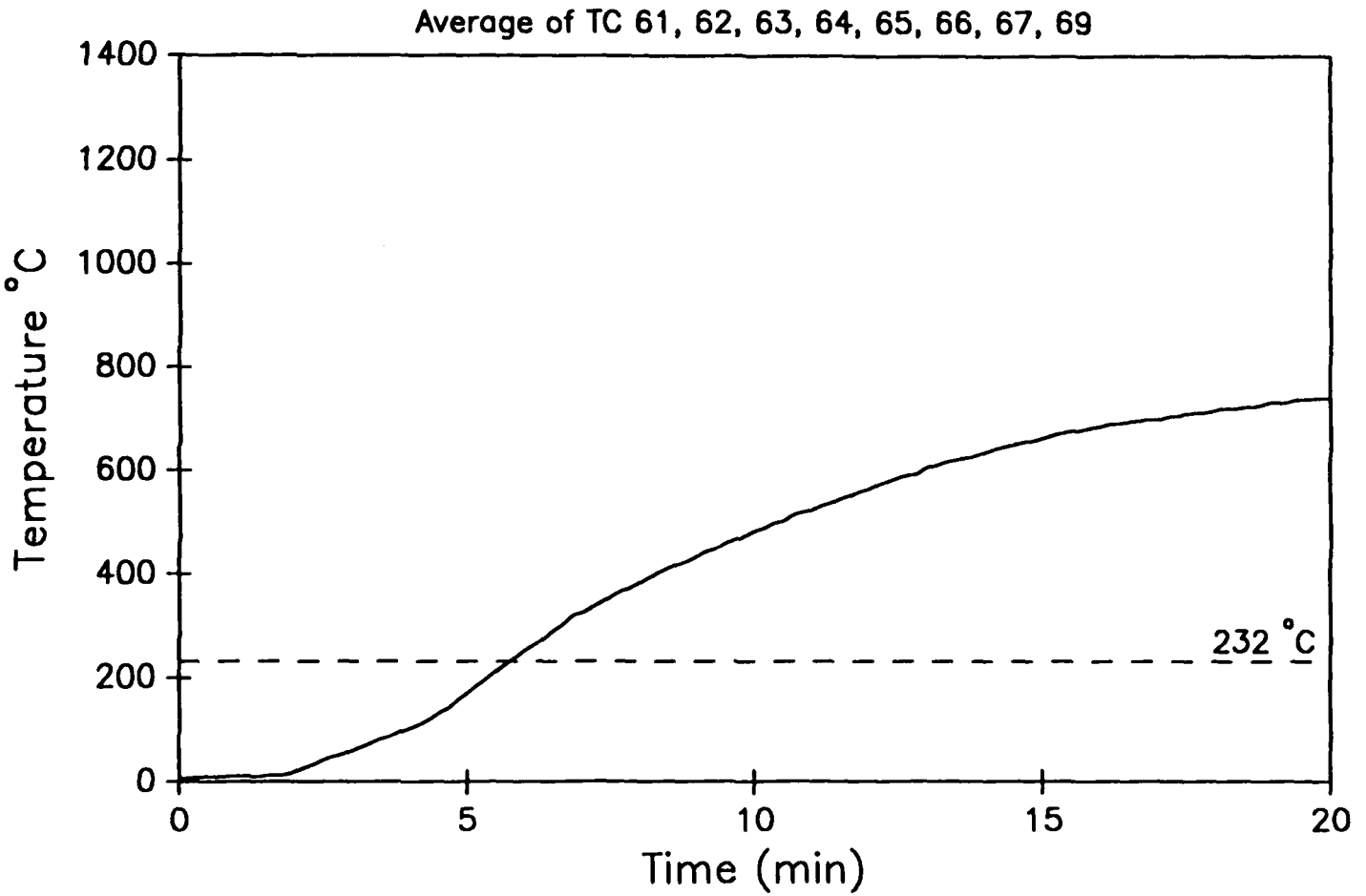

Fig. A1 - Ins_1a, average deck temperature, Navy insulation with aluminum caps

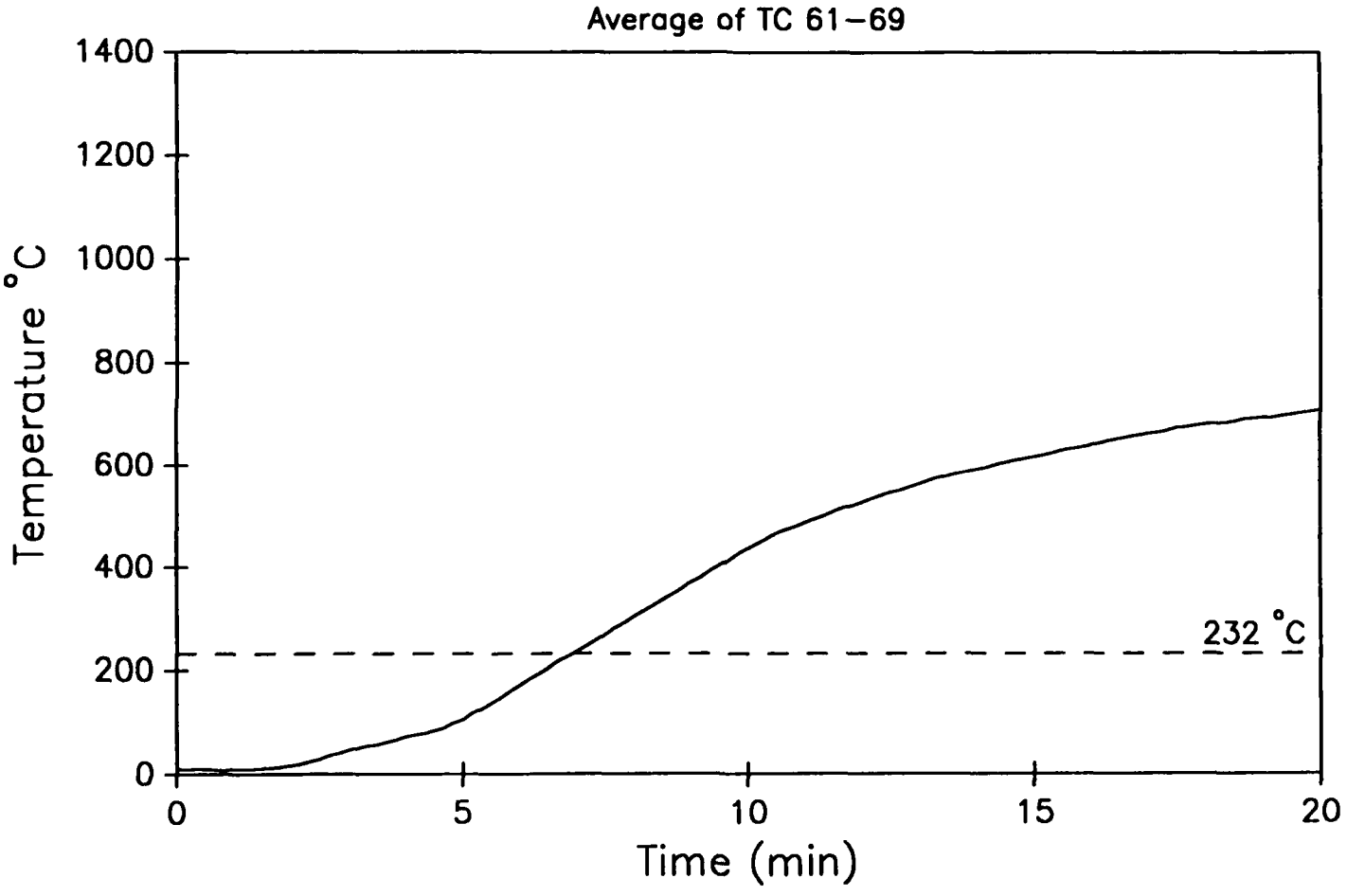

Fig. A2 - Ins_2, average deck temperature, Navy insulation with steel caps

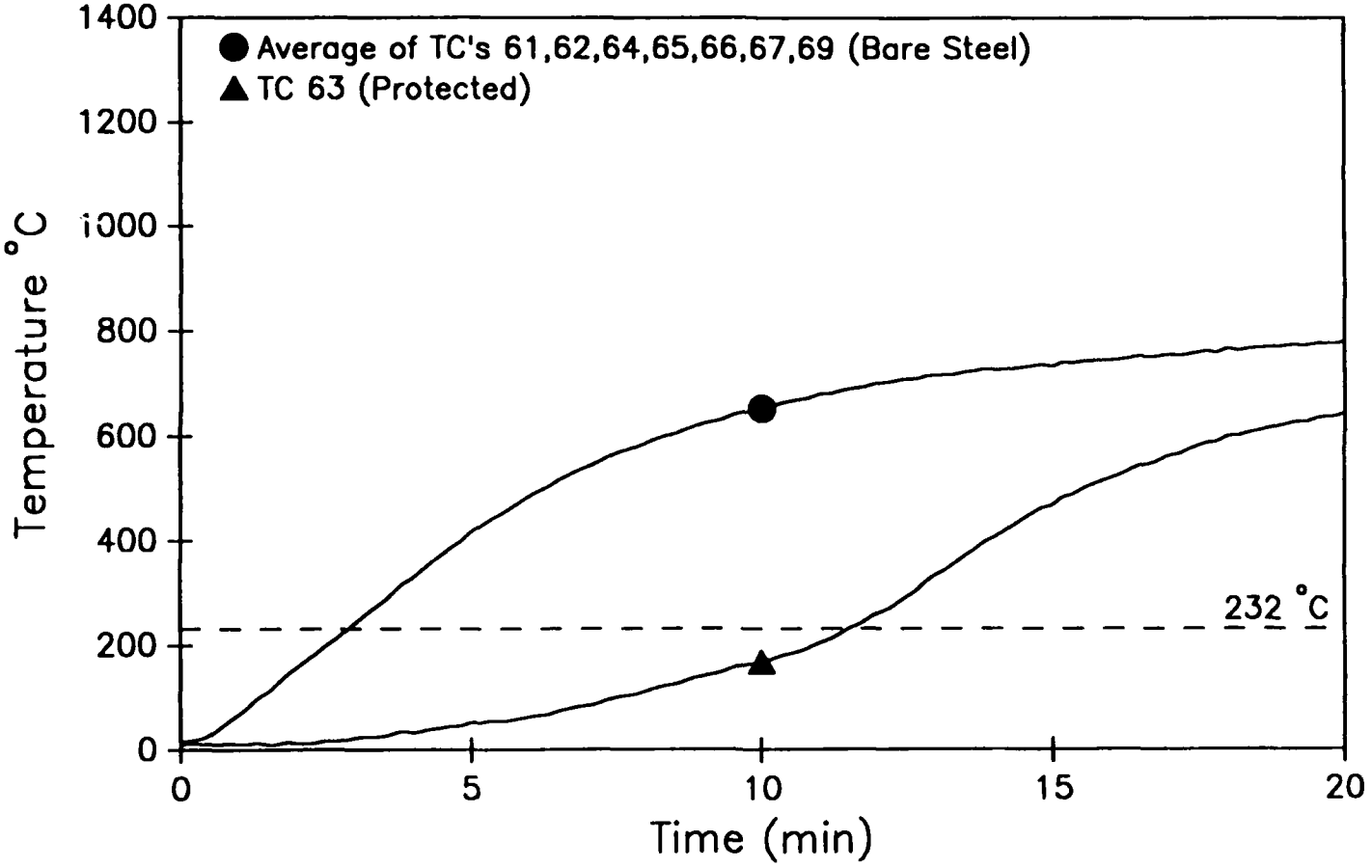

Fig. A3 - Ins_3, deck temperature, average of bare steel and Navy insulation protected by steel plate

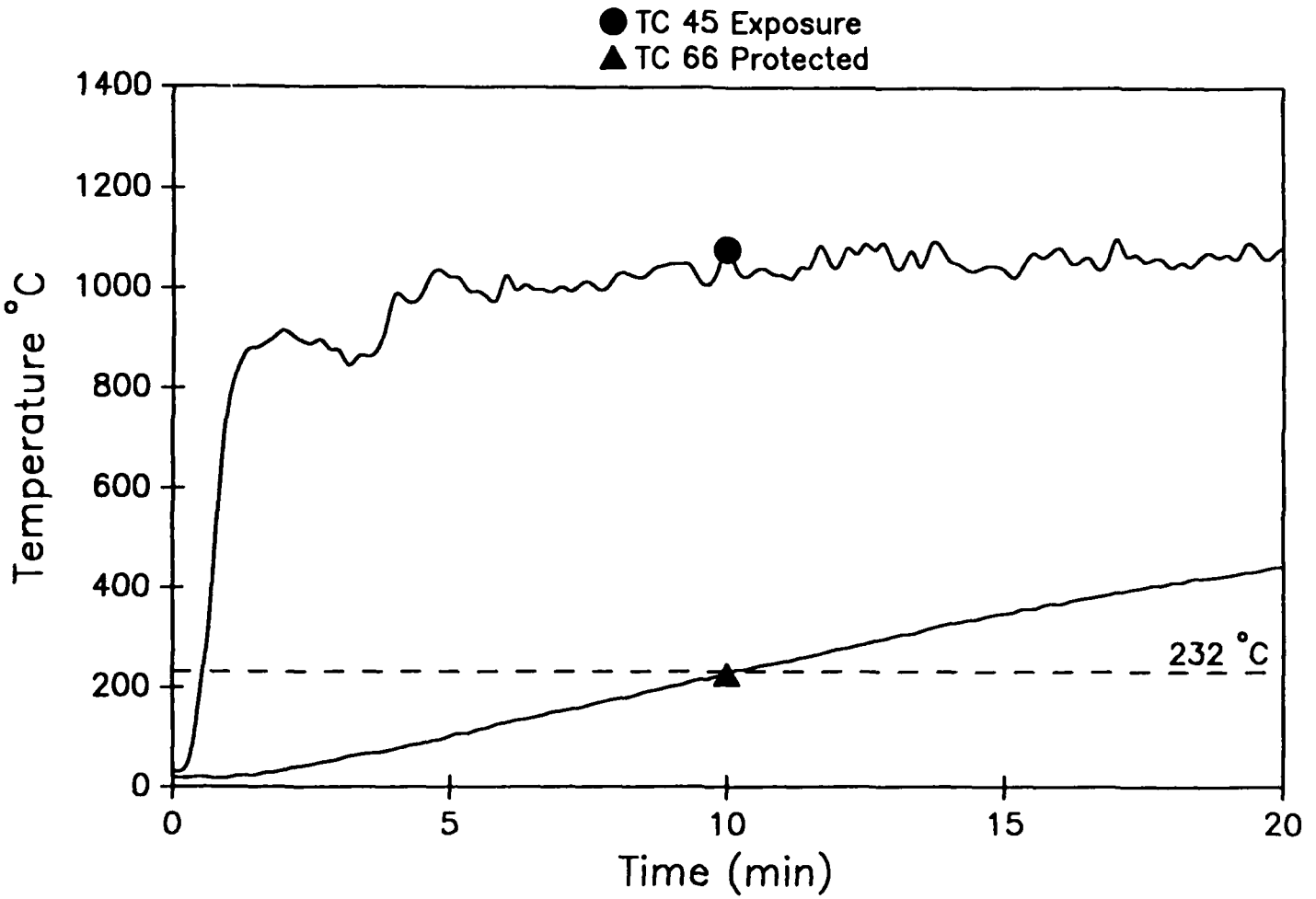

Fig. A4 - Ins_4, Navy with steel sheet

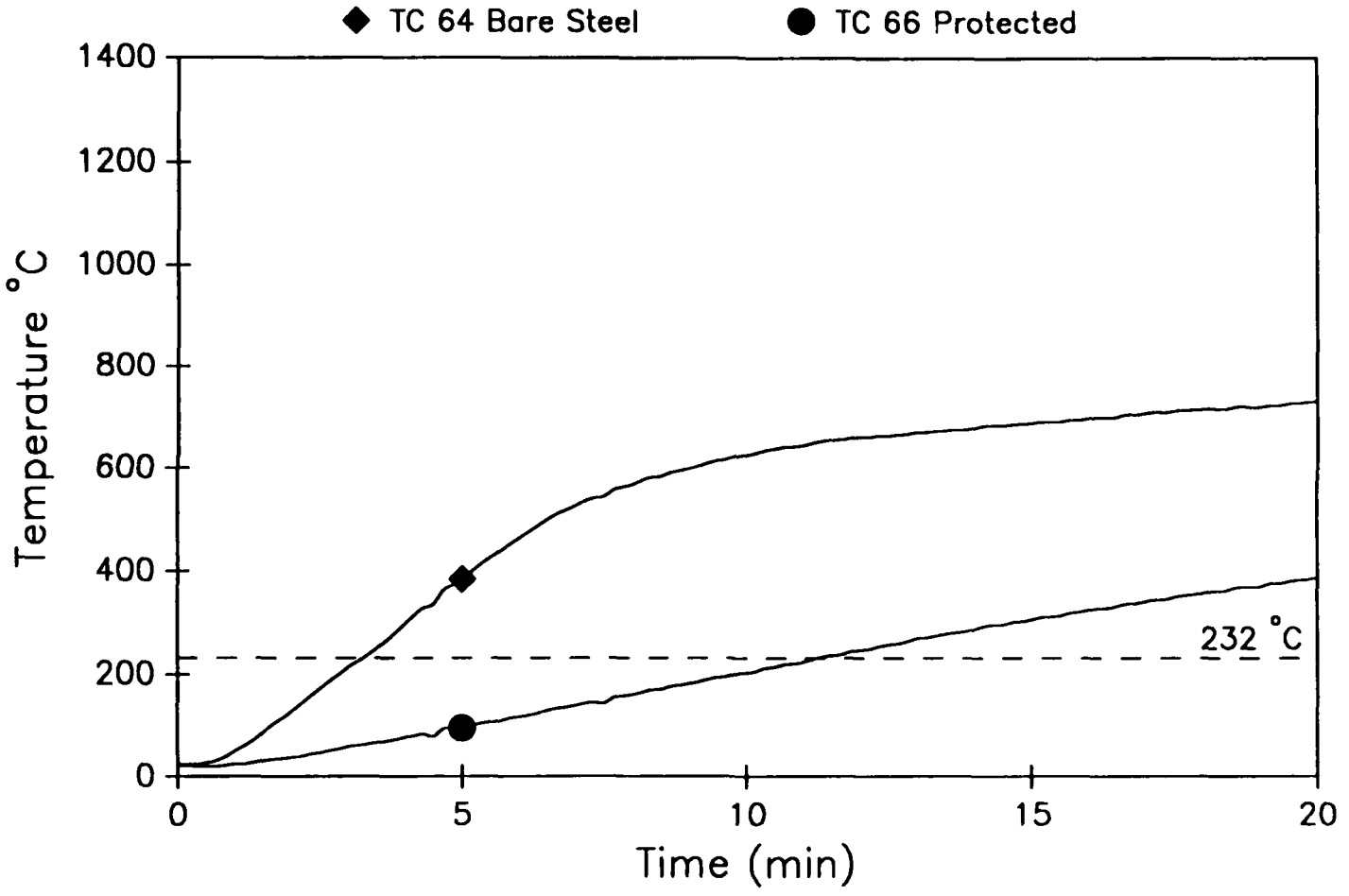

Fig. A5 - Ins_5, polyamide

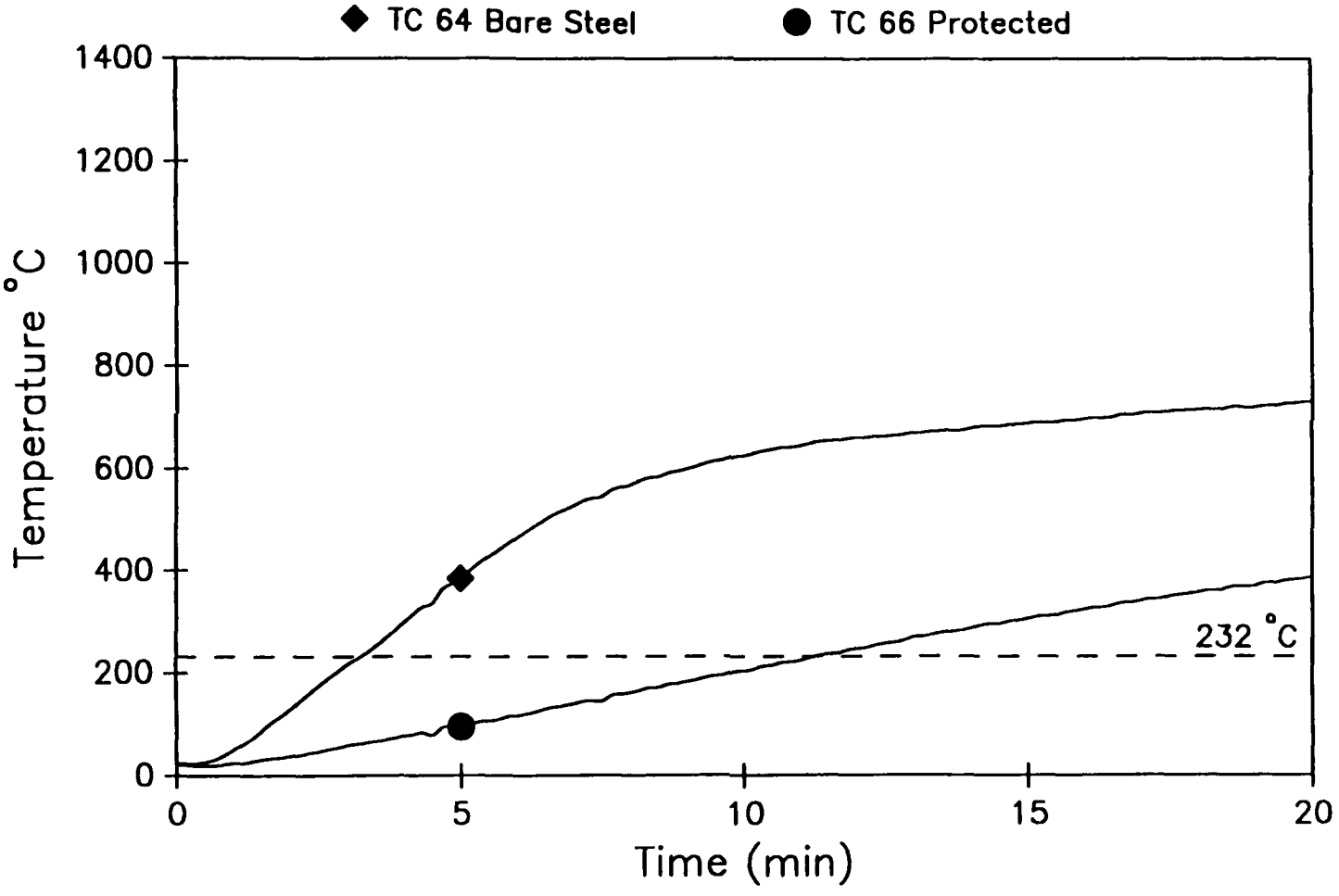

Fig. A6 - Ins_5, single layer of Manville

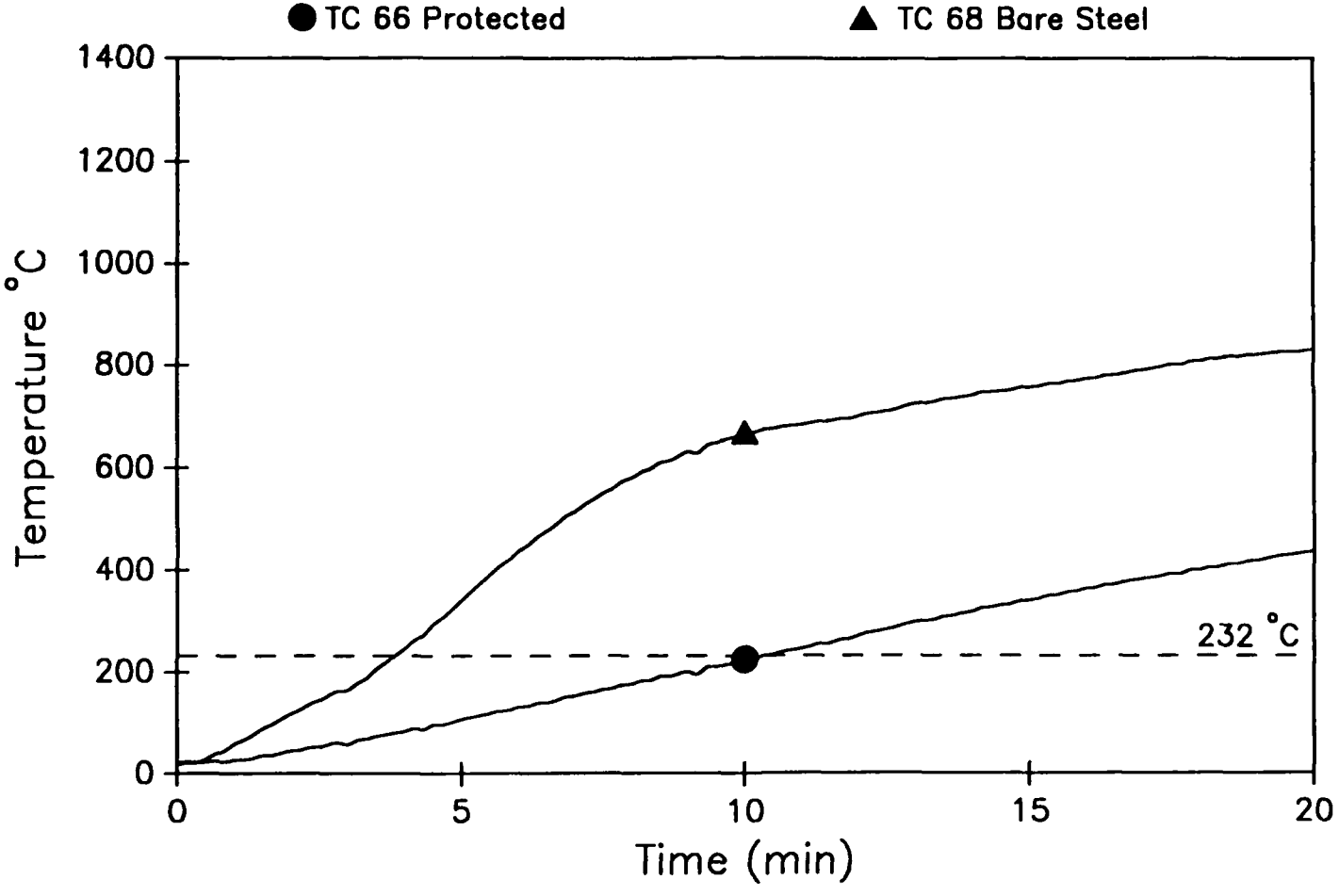

Fig. A7 - Ins_6, polyamide

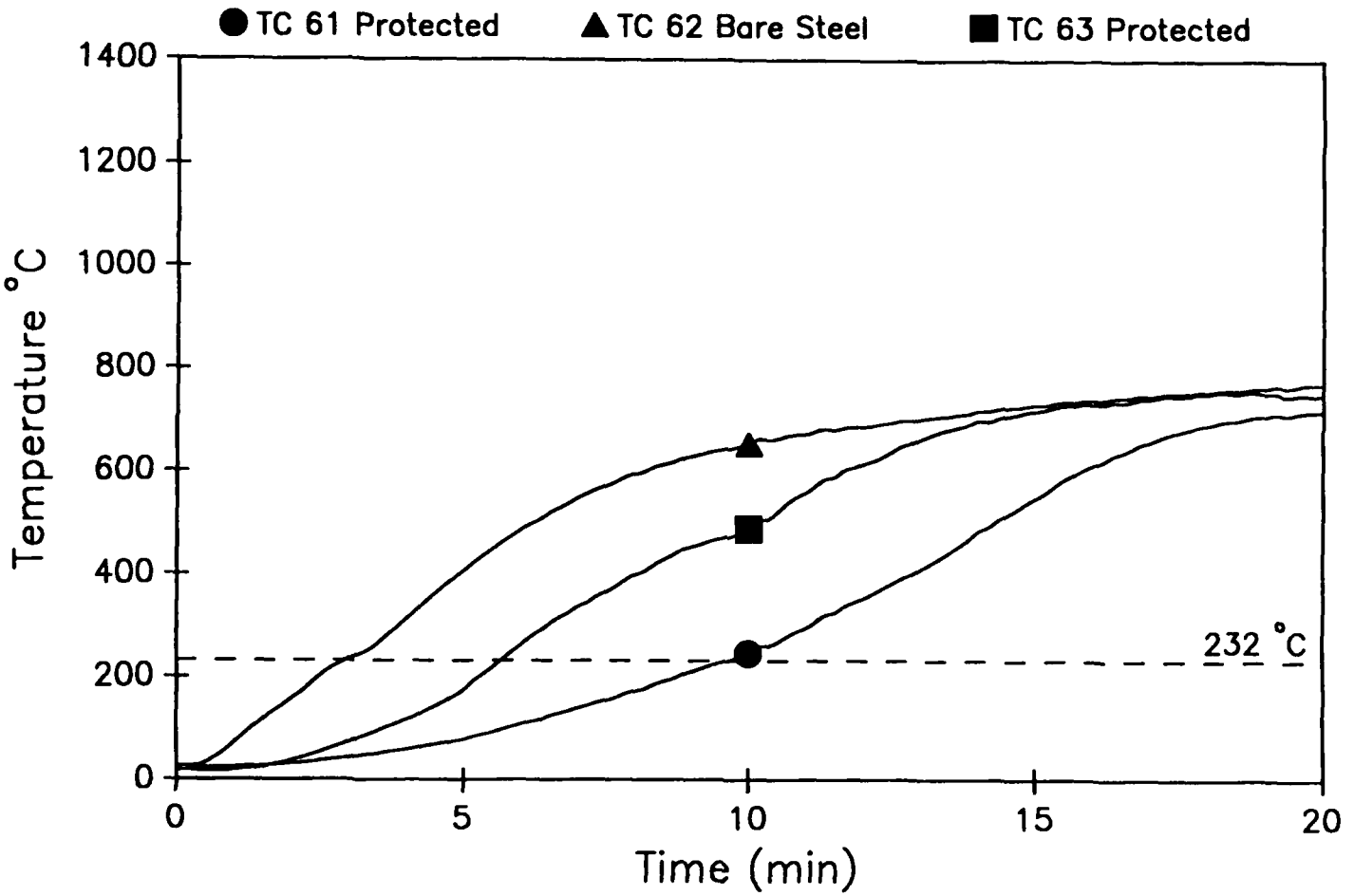

Fig. A8 - Ins_7, Navy with one coat of Ocean 477

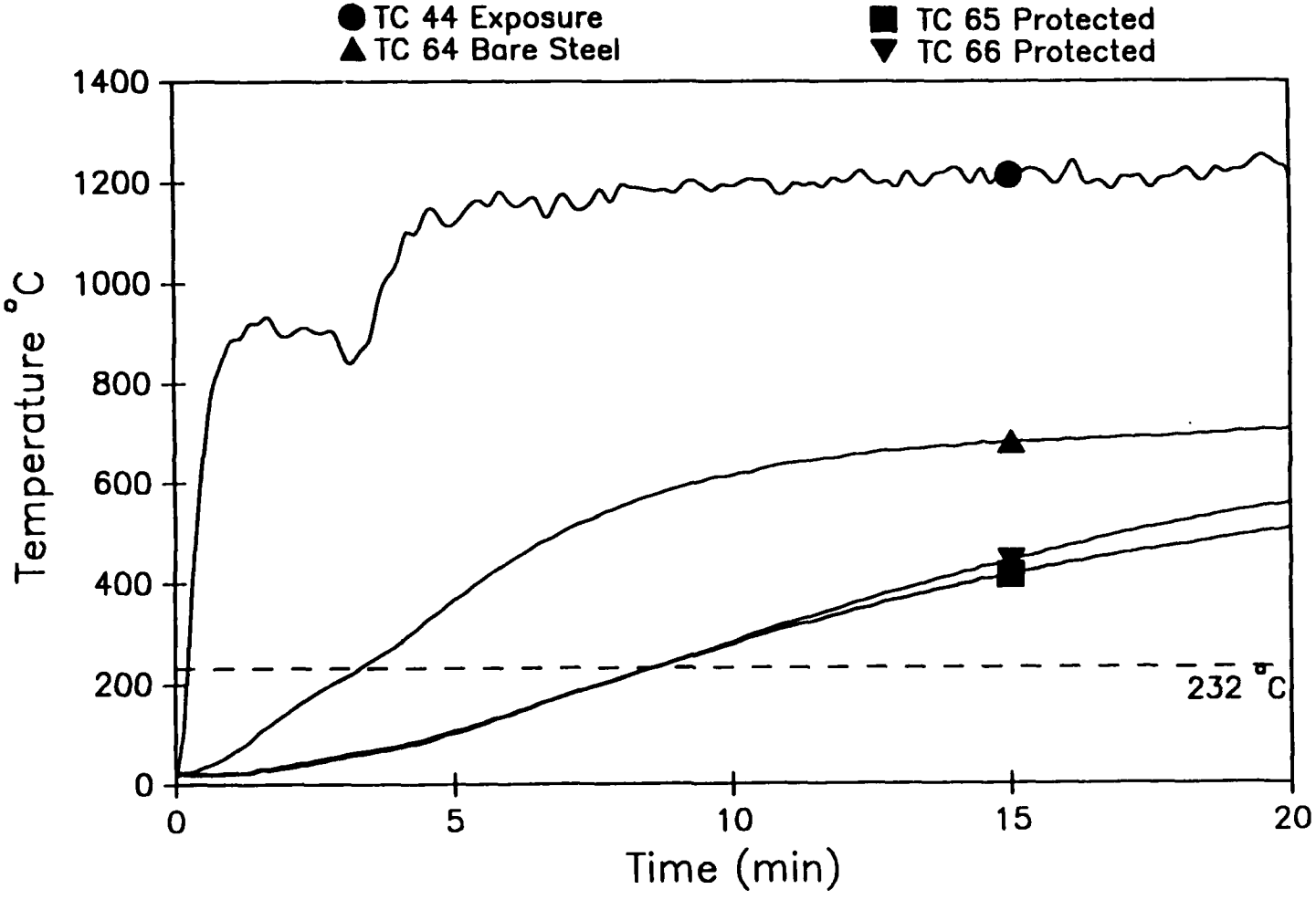

Fig. A9 - Ins_8, single layer of Manville

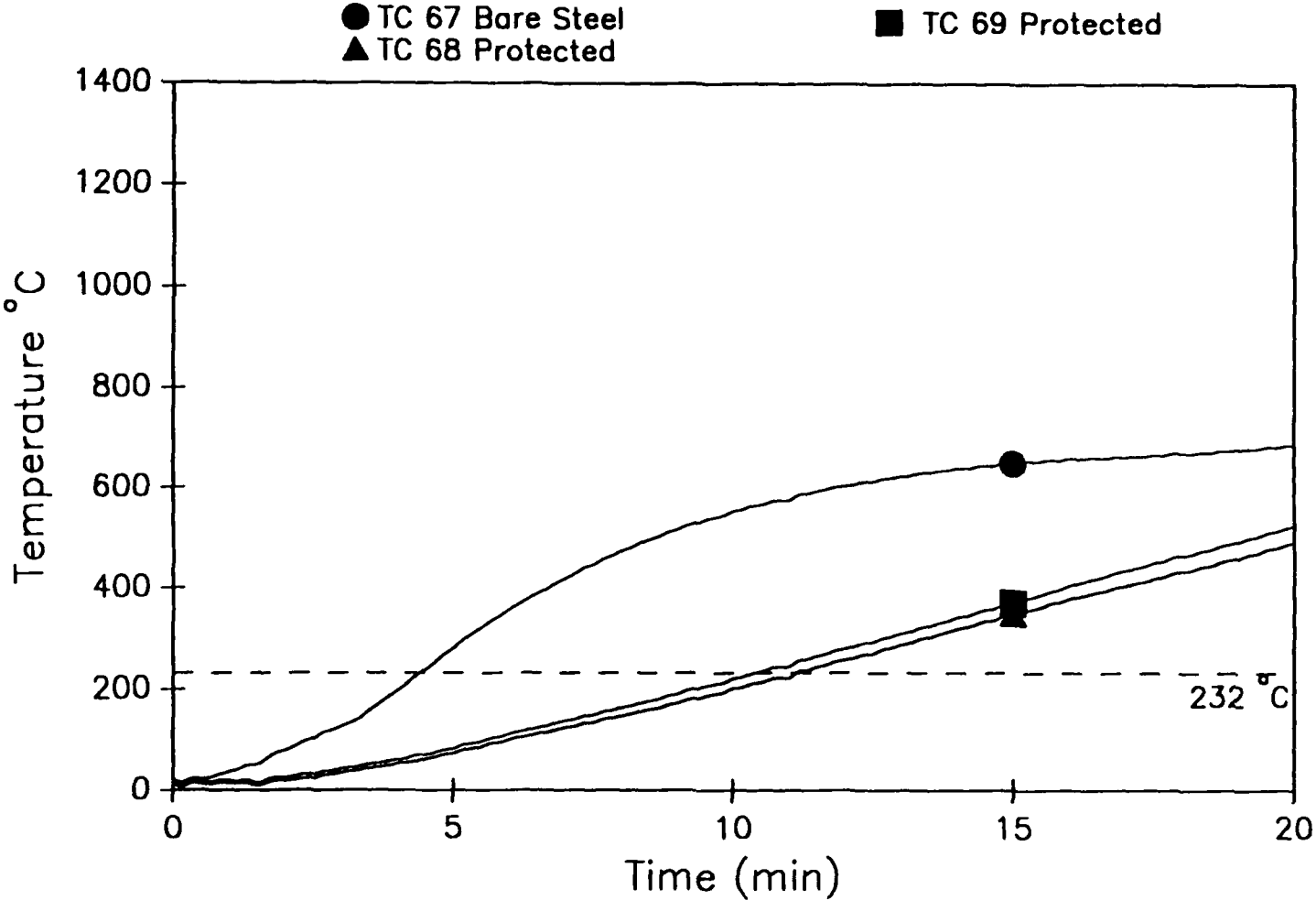

Fig. A10 - Ins_9, Navy standard with Hamilton 303

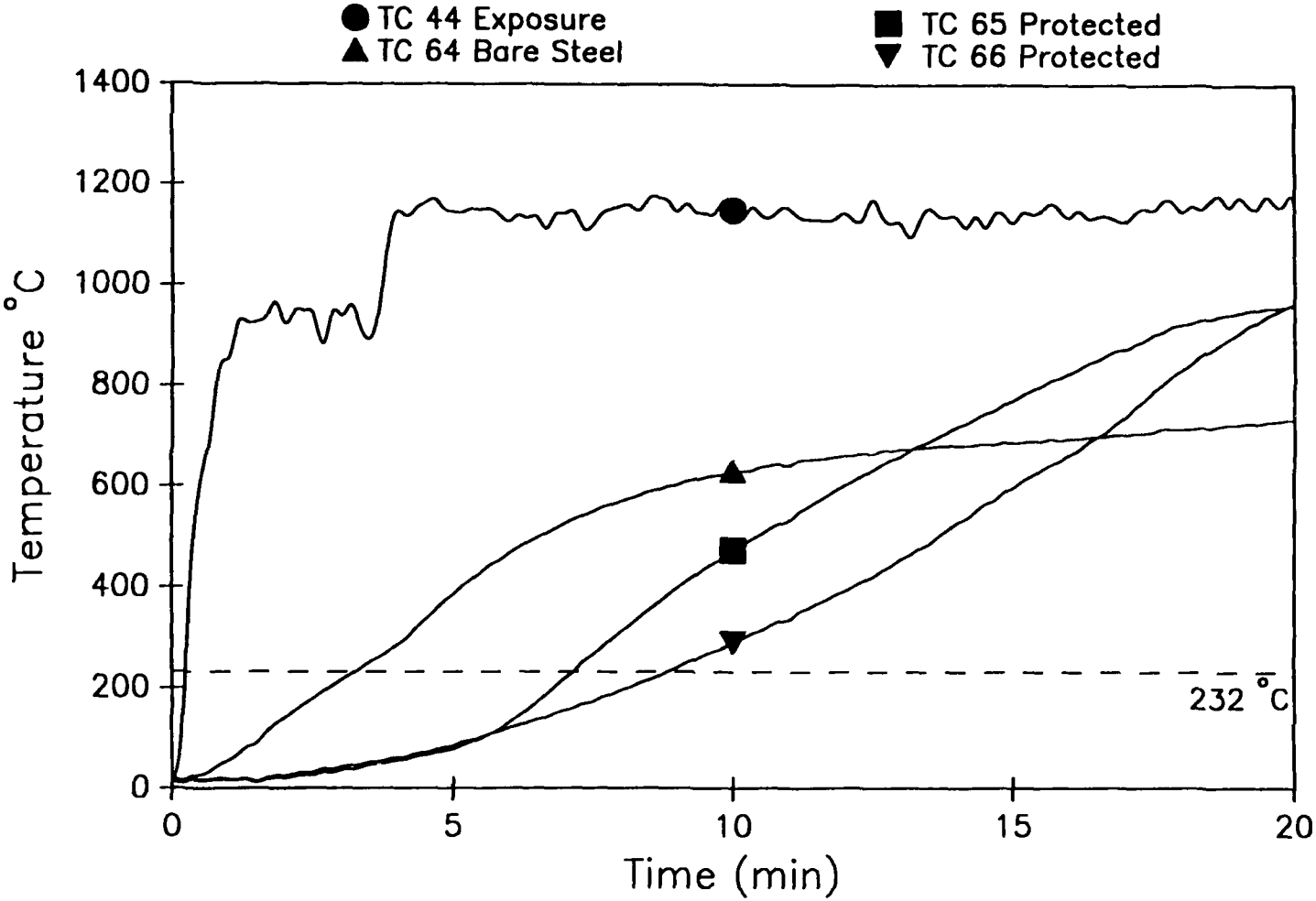

Fig. A11 - Ins_9, Navy standard with Ocean 9788

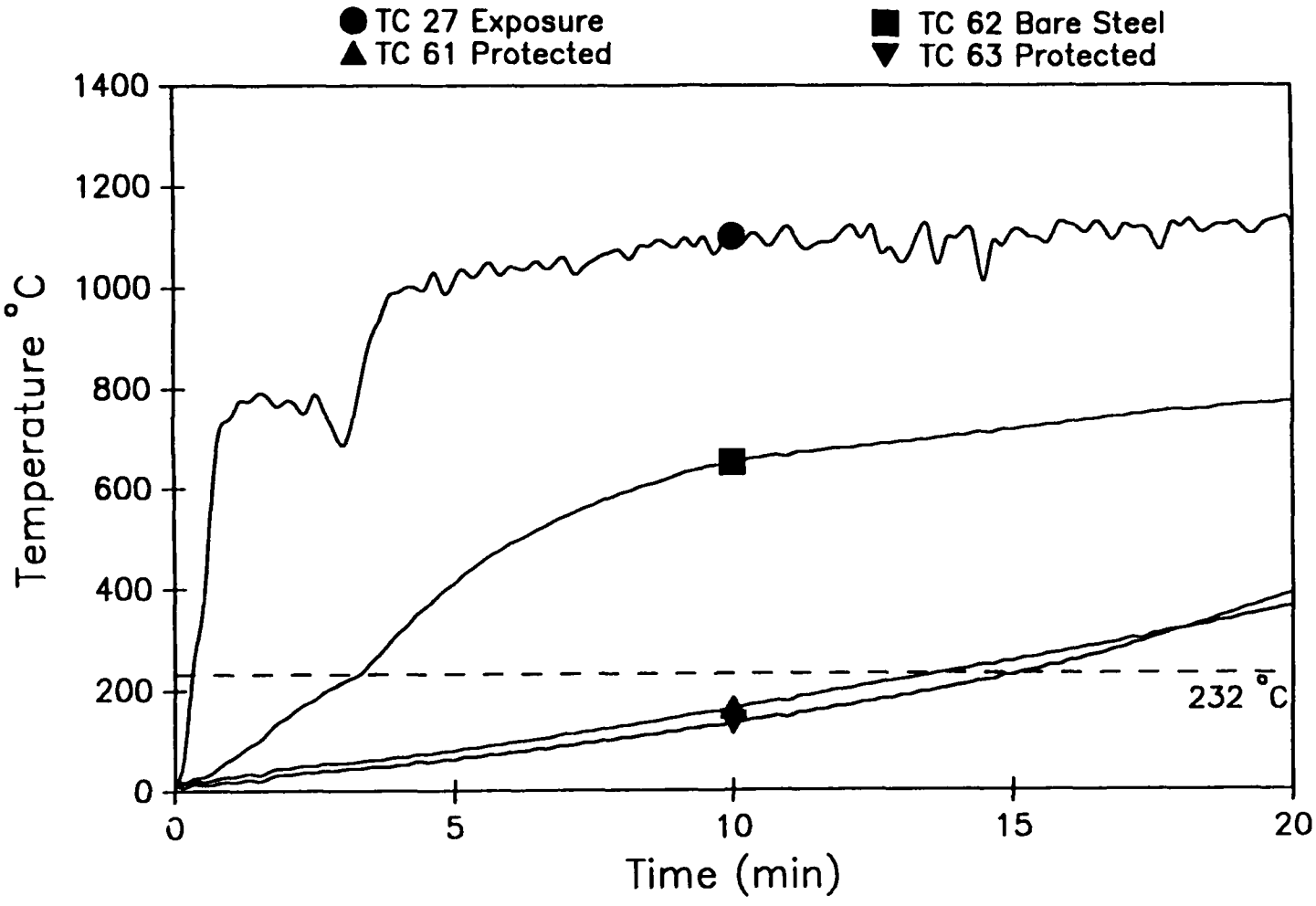

Fig. A12 - Ins_9, two layers of Manville

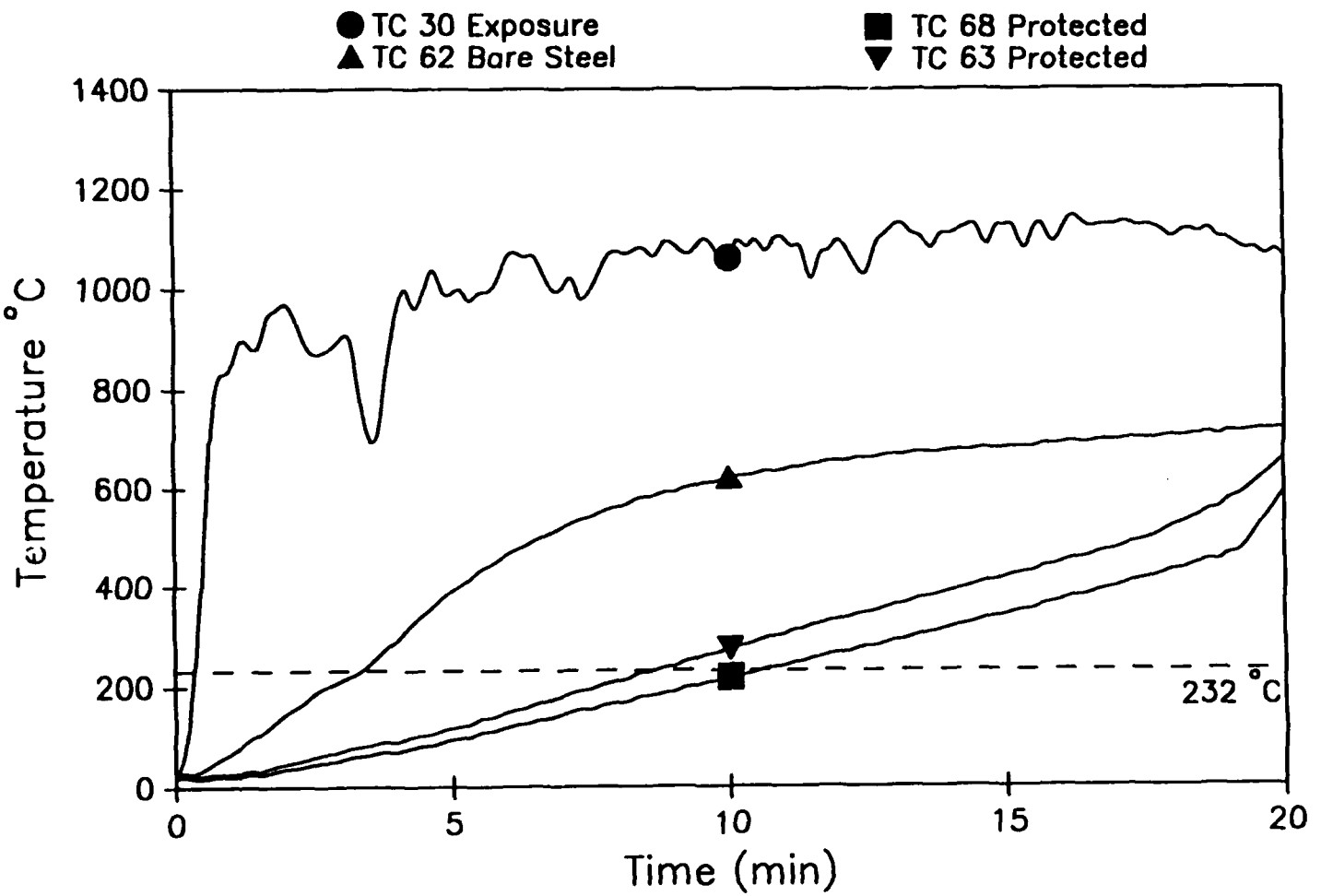

Fig. A13 - Ins_10, Navy standard with Hamilton 303

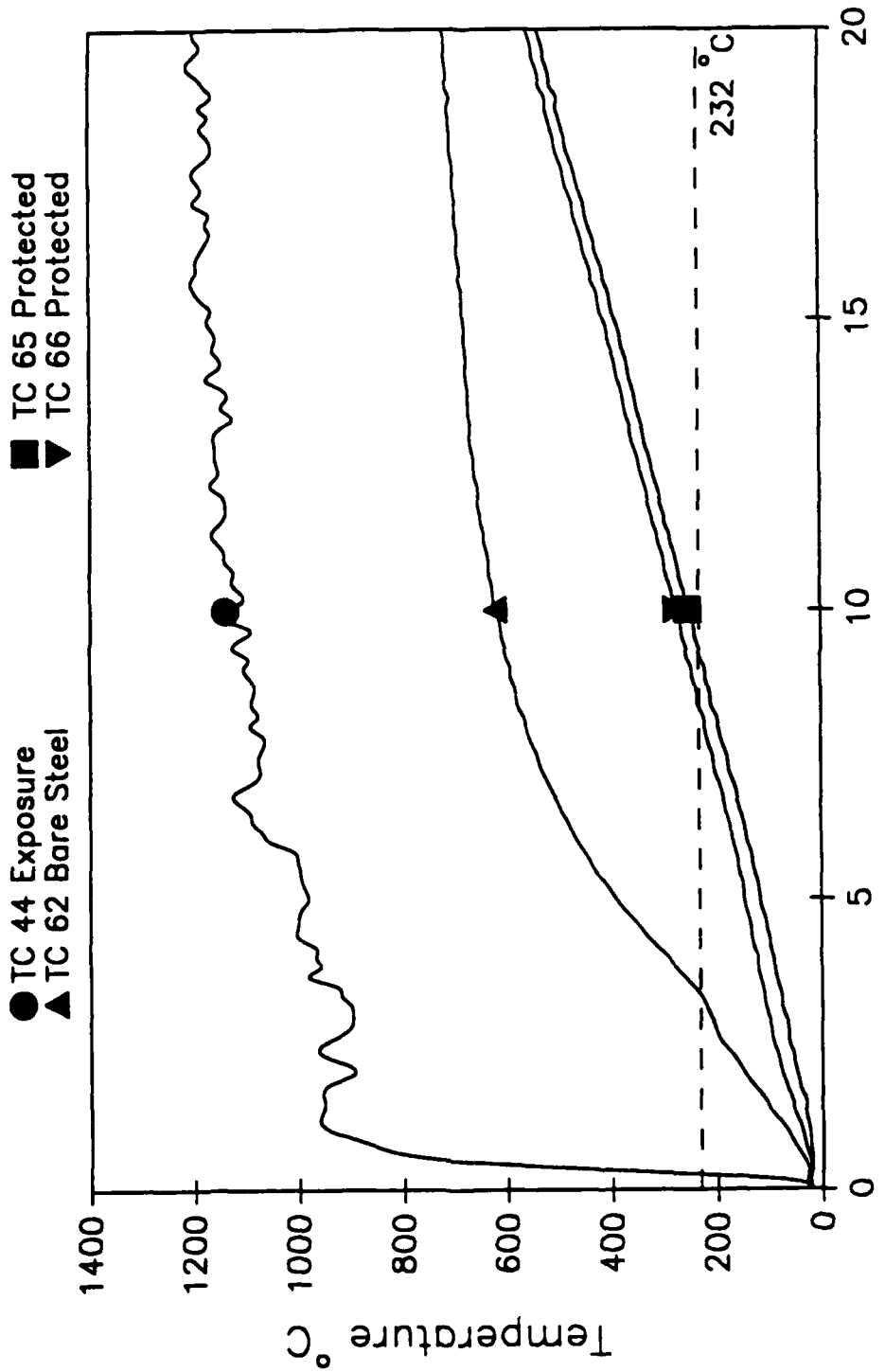

Fig. A14 - Ins_10, one layer of Manville

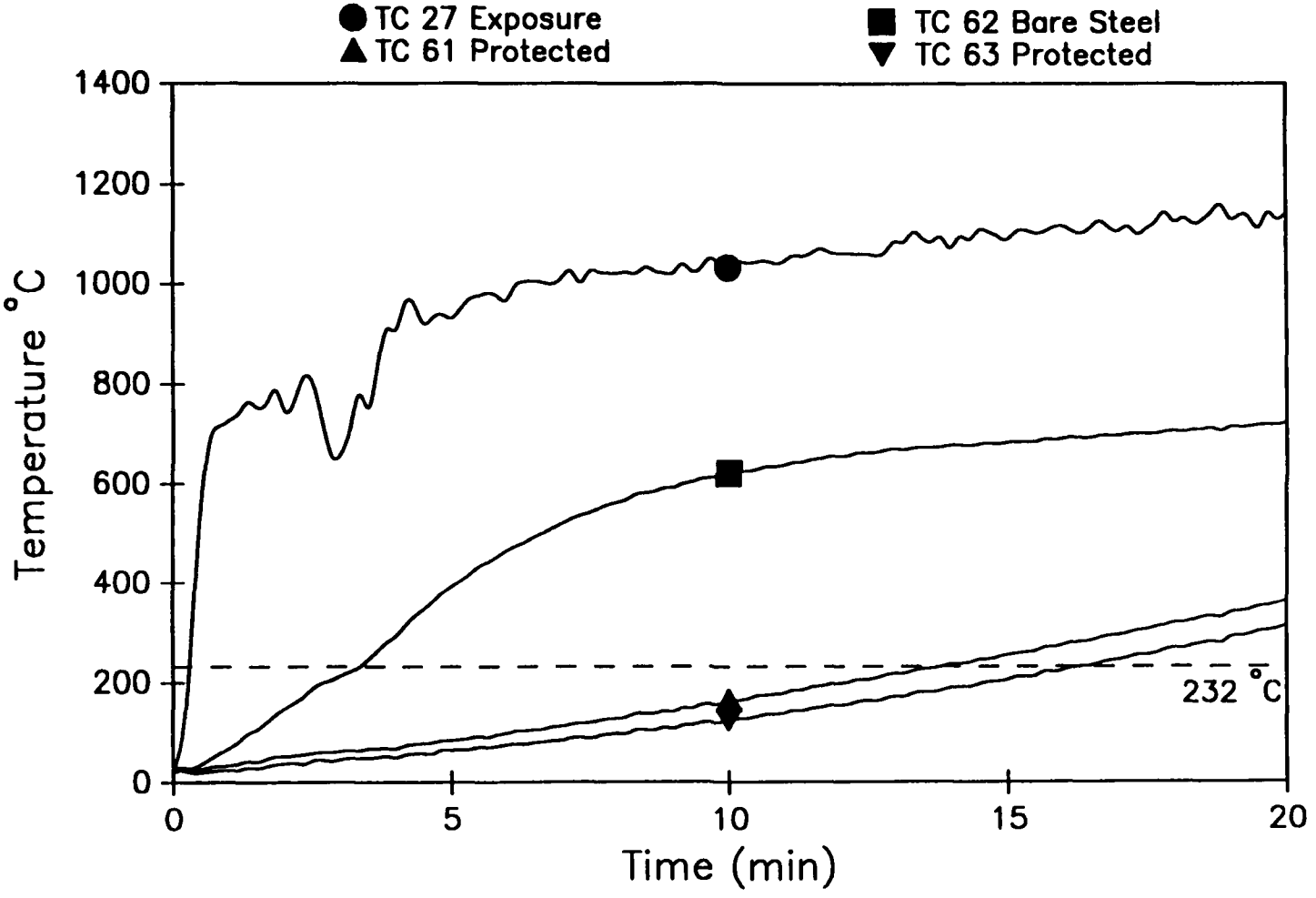

Fig. A15 - Ins_10, two layers of Manville

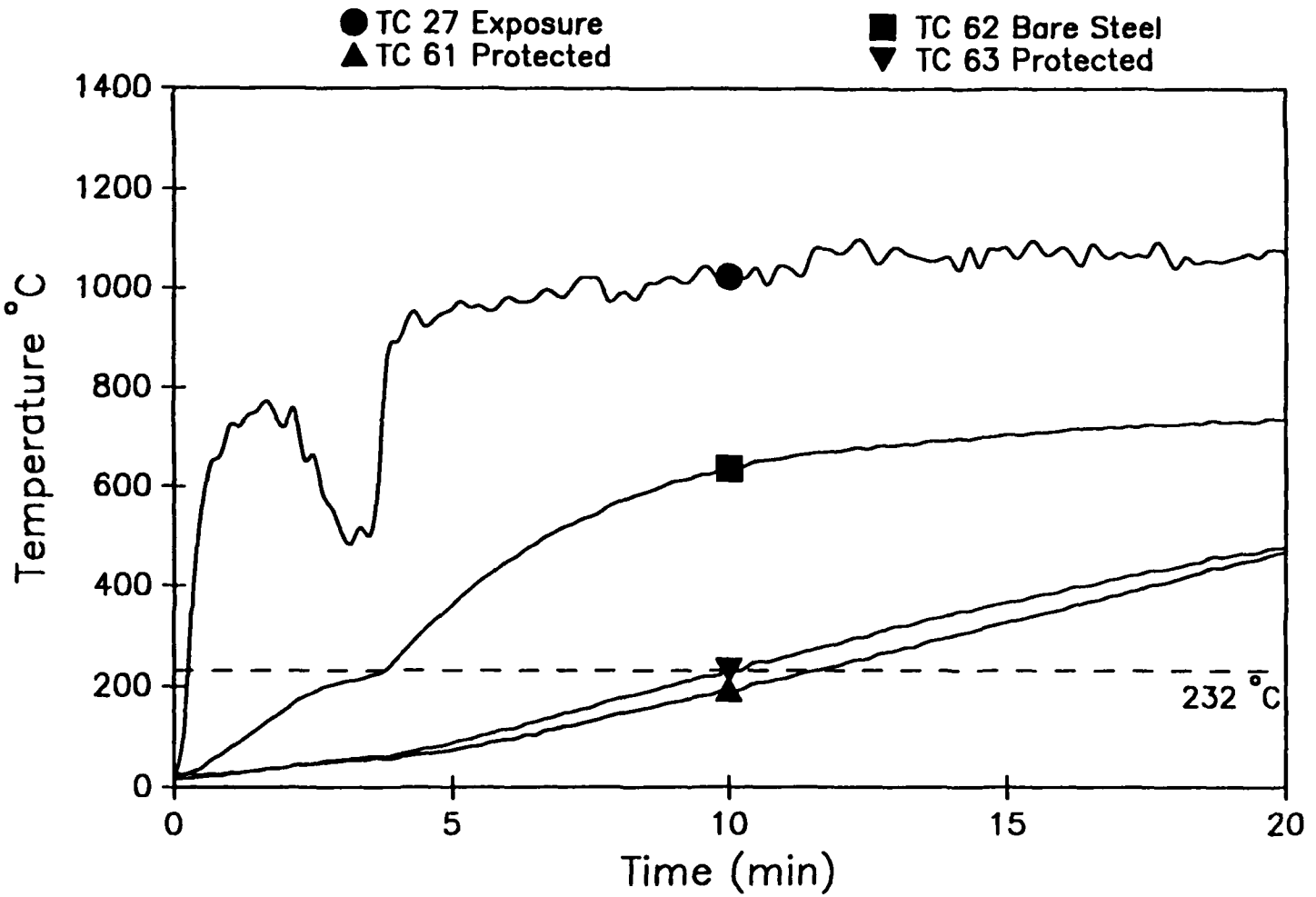

Fig. A16 - Ins_11, Navy standard with Ocean 477

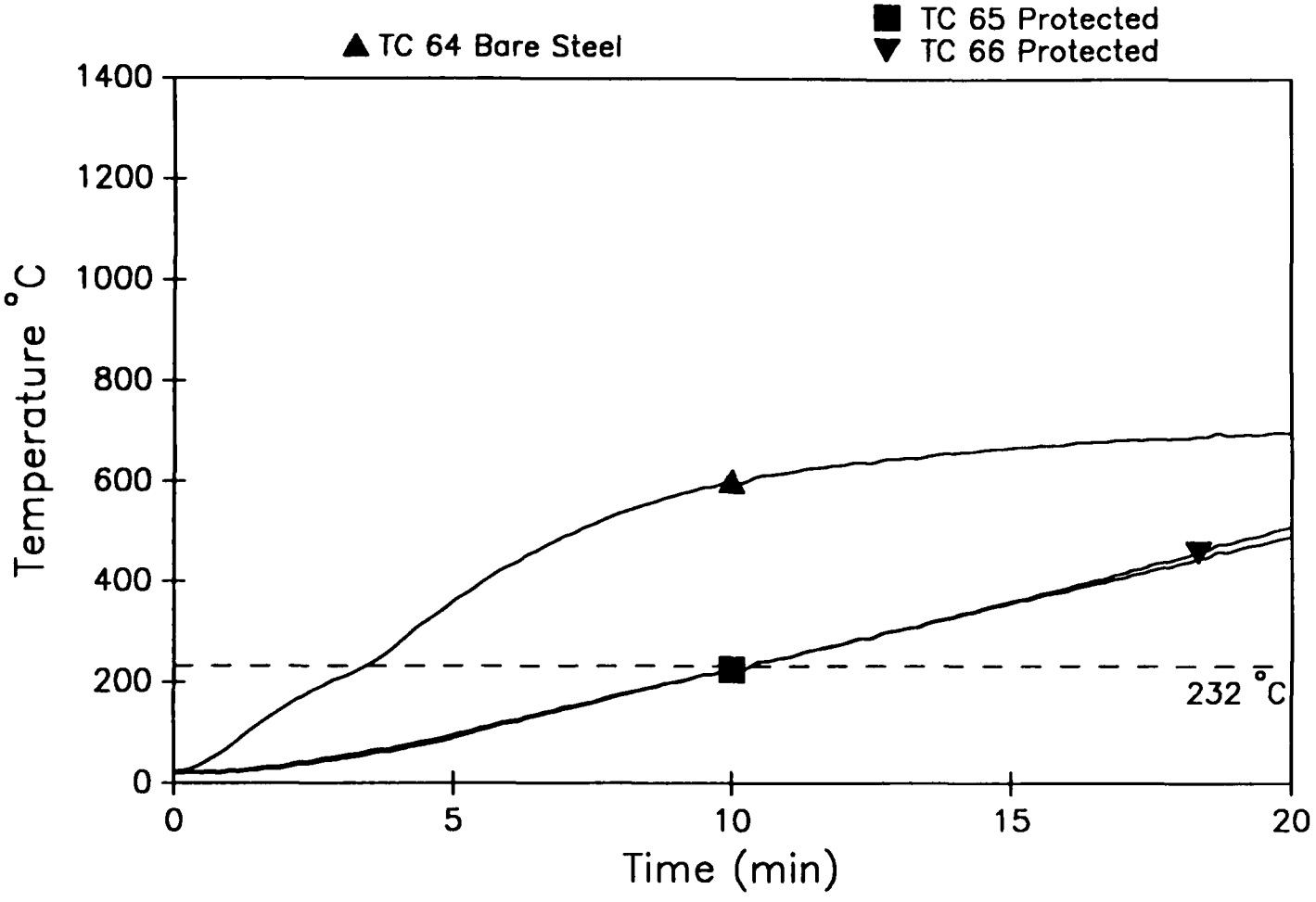

Fig. A17 - Ins_11, Navy standard with steel sheet

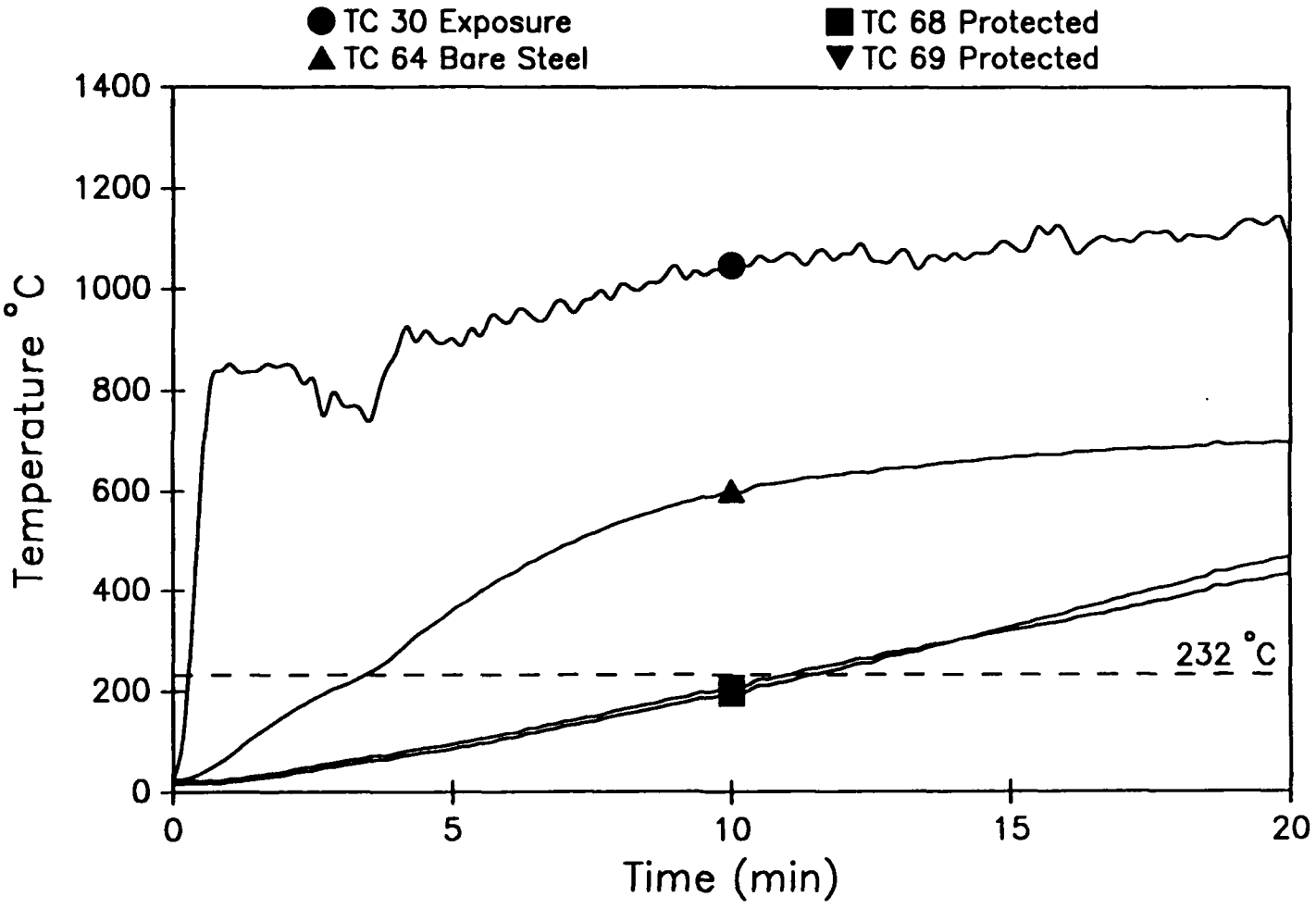

Fig. A18 - Ins_11, Polyamide

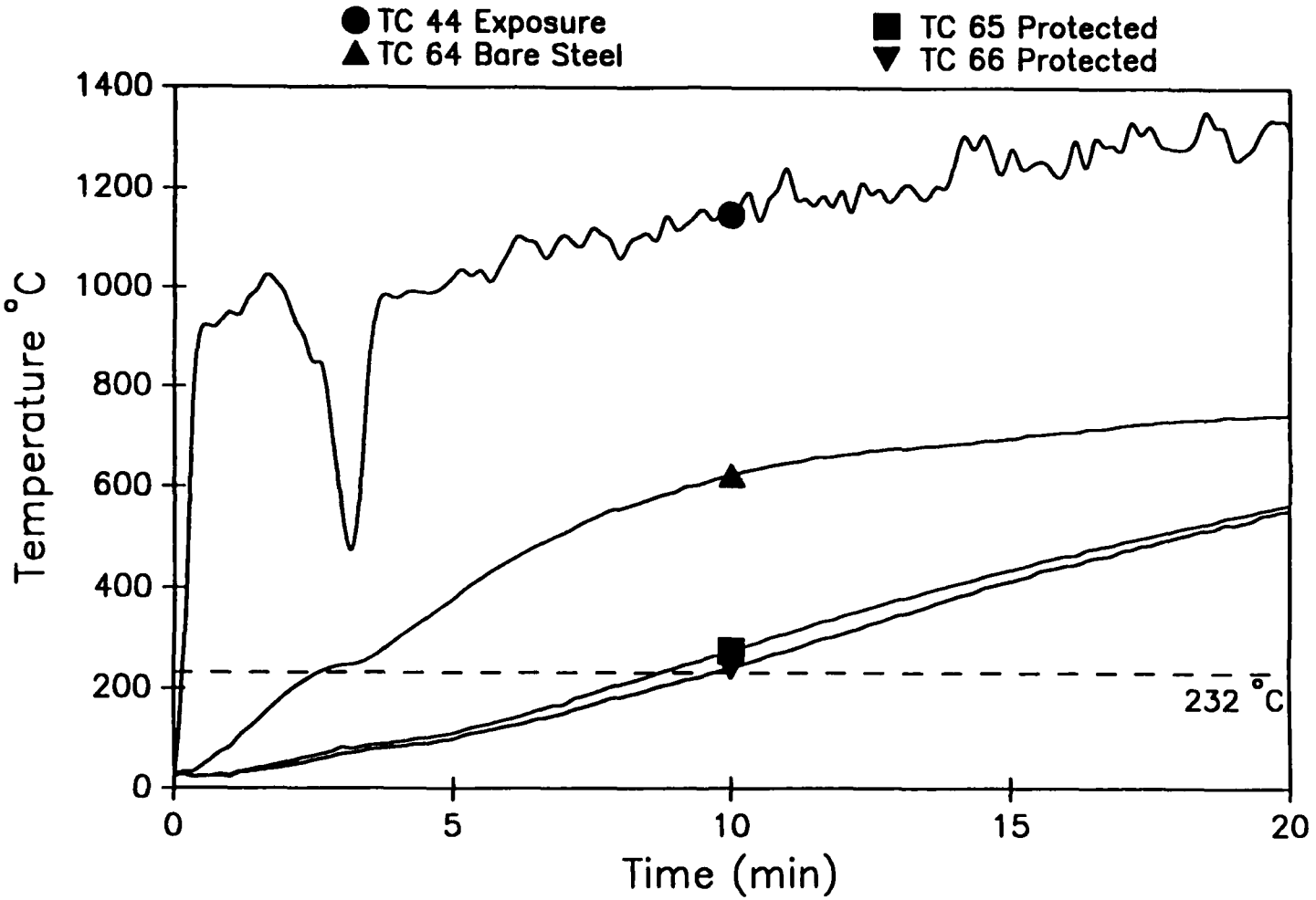

Fig. A19 - Ins_12, Navy unprotected

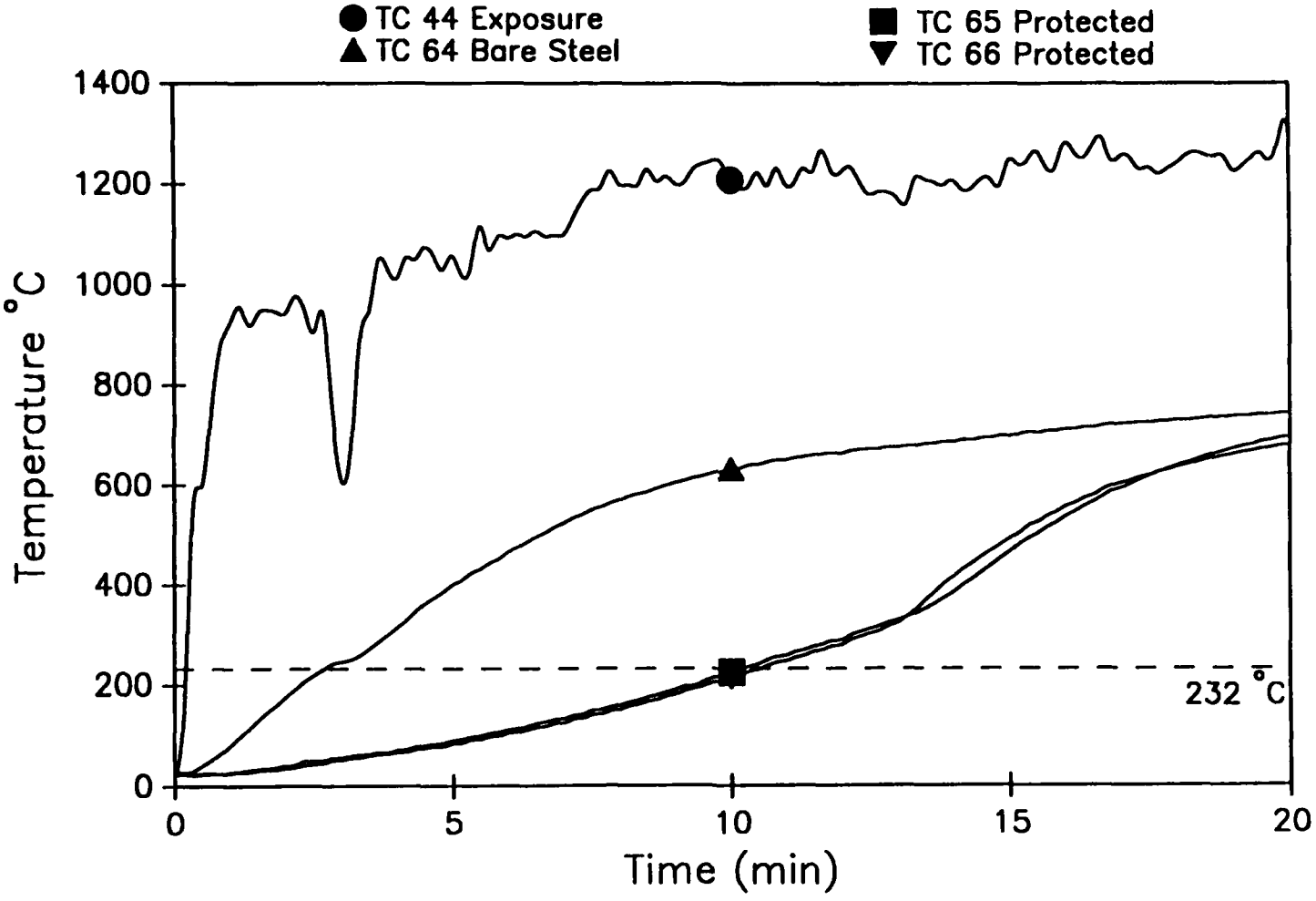

Fig. A20 - Ins_13, Navy standard with Ocean 9788

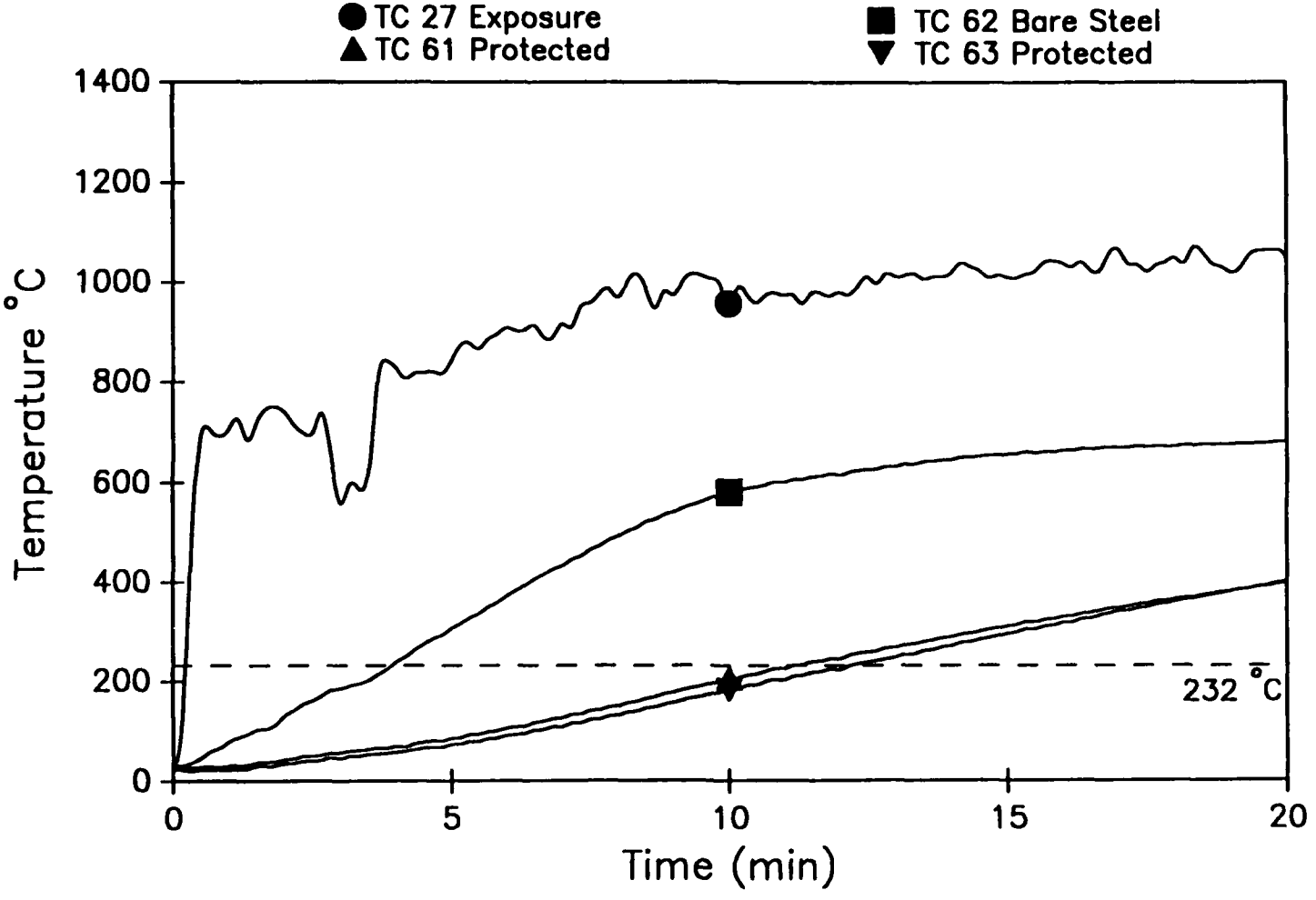

Fig. A21 - Ins_13, Navy unprotected

Appendix B

Heat Transfer Analysis

Appendix B
Table of Contents

Table of Contents (Continued)

List of Figures

List of Figures (Continued)

List of Figures (Continued)

List of Tables

Appendix B

Heat Transfer Analysis

B1.0 OBJECTIVES

The thermal modeling abilities of FIRES-T3, a finite element heat transfer computer program, were validated on simple exact solutions and then compared to the results of fire tests with a material that has well known thermal properties. After the program validation, FIRES-T3 was used to predict the time to reach 232°C (450°F) on the backside of the steel inserts and compared against the actual results. Next, the parameters used in FIRES-T3 were systematically altered to evaluate those parameters having the greatest impact on the program results. Finally, FIRES-T3 was used to estimate the impact of the heating of RICER 2 on the thermocouple readings recording the heat transfer through the insulation attached to the steel inserts.

B2.0 INTRODUCTION TO AND VALIDATION OF FIRES-T3

FIRES-T3 is a one-, two-, or three-dimensional finite element heat transfer program written by Iding, Nizamuddin, and Bresler [B1]. The program is used in the fire protection engineering field for estimating the required fire-proofing material thickness for columns and beams. It is also used to determine the fire endurance of existing construction configurations such as truss and wall assemblies. FIRES-T3 allows a user to specify time dependent exposure temperatures, temperature dependent material properties, and non-linear boundary conditions (radiation and temperature dependent convection). The program has been validated on several two-dimensional beam configurations exposed to a standard E119 fire curve with reasonable success [B2, B3].

B2.1 Description of the Capabilities of FIRES-T3

FIRES-T3 determines the temperature distribution in a material by using a version of the finite element method to solve the heat transfer equation [B4]:

$$c_p(T)\,\rho(T)\,\frac{\partial T}{\partial t} = \nabla\cdot\kappa(T)\,\nabla T + S(x,y,z,t) \qquad \text{(B1)}$$

where $C_p(T)$ is the temperature dependent heat capacity, $\rho(T)$ is the temperature dependent density, T is the temperature, t is the time, $\kappa(T)$ is temperature dependent thermal conductivity, and S(x,y,z,t) is the spatial and time dependent source term.

The finite element method numerically solves a wide variety of partial differential equations by dividing the domain under consideration into a finite number of elements. Each individual element has a prescribed number of nodes that depends on the type of

element selected. Each node in an element may or may not be shared with another element, but every element must have at least one node in common with another element.

The differential equation B1 is approximated over each element via the element geometric (shape) function. FIRES-T3 uses elements that have a linear shape function, so that the differential equation assumes a linear solution over the domain of each element. Better results are obtained either when the actual solution is approximately linear (as in steady state, constant property heat transfer problems) or when the elements are small and numerous with respect to the entire solution domain. In general, the greater the thermal gradient, the larger the number of elements necessary for a convergent solution.

For a problem with one dimension, no internal heat generation, constant cross sectional area and an unknown surface temperature, equation B1 reduces to:

$$c_p(T)\,\rho(T)\,\frac{dT}{dt} = A\frac{d}{dx}\cdot\left(\kappa(T)\,\frac{dT}{dx}\right) \qquad (Internal\ Nodes) \qquad \text{(B2)}$$

$$c_p(T)\,\rho(T)\,\frac{dT}{dt} = A\frac{d}{dx}\cdot\left(\kappa(T)\,\frac{dT}{dx}\right) + \dot{q}_c(T) + \dot{q}_r(T) \quad (Boundary\ Nodes) \qquad \text{(B3)}$$

where, x is the one dimensional position, and $\dot{q}_c(T)$ and $\dot{q}_r(T)$ are the boundary heat fluxes due to convection and radiation, respectively. The terms on the left side of equations B2 and B3 represent the energy that remains at a point (by storage and temperature increase) and the terms on the right side are the energy flowing into and out of a point (by convection, radiation, and conduction). The insulation tests conducted on the ex-USS SHADWELL were assumed to have a constant cross sectional area, no internal heat generation, and one dimensional heat flow.

The boundary heat fluxes for radiation and convection in equation B3 are calculated in FIRES-T3 using:

$$\dot{q}_c = A\,h\,(T_f(t) - T_s)^{\beta} \qquad \text{(B4)}$$

$$\dot{q}_r = A\,F\sigma\left(\alpha\,(T_f(t) + T_{abs})^4 - \varepsilon\,(T_s + T_{abs})^4\right) \qquad \text{(B5)}$$

where A is the element surface area (usually 1.0 for one-dimensional problems), h is the convective heat transfer coefficient, $T_f(t)$ is the exposure temperature, T_s is the surface current node temperature, β is a constant, F is the radiation configuration factor, σ is the Stefan-Boltzmann constant (5.669E-8 $W/m^2\text{-}K^4$ or 1.71E-9 $Btu/hr\text{-}ft^2\text{-}R^4$), α is the insulation radiative absortivity, ε is the insulation radiative emissivity, and T_{abs} is the conversion temperature to the absolute temperature scale.

FIRES-T3 allows the user to control all the parameters (such as h, β, and α) in equations B2 - B5. The parameters may be separated into three categories: material

parameters, boundary parameters, and the thermal load. The material properties $c_p(T)$, $\rho(T)$, and $\kappa(T)$) determine how a material reacts to a set of boundary conditions. The boundary condition parameters (A, h, β, F, α and ε) describe how much energy enters and leaves a material. The thermal load parameter, $T_f(t)$, describes the fire temperature-time history of the exposure.

Material properties (c_p, ρ, and κ) can be temperature dependent in FIRES-T3. In many high temperature heat transfer models, the temperature dependence of the properties is important. Two cases that illustrate the importance of the properties are materials that contain water (such as gypsum) and materials that have a radiation dominated conductivity (as with fibrous insulations). Water is usually driven off at 100°C (moisture) or around 400°C (dehydration). The heat capacity in the vicinity of such temperatures can rise an order of magnitude or greater for materials containing either form of water [B5]. The current temperature requires an integration of the heat capacity term (left side of equations B2 and B3) with respect to temperature, thus ignoring water effects can result in a higher temperature prediction. Materials that have a radiation dominated conductivity generally have a conductivity that is proportional to the instantaneous temperature to the third power [B6]. In such cases, the conductivity can easily increase two orders of magnitude over the temperature range of the model. Neglecting this phenomena may introduce substantial error in a model. Fig. B1 shows a non-dimensional heat capacity for portland cement and a non-dimensional conductivity for 16 kg/m^3 (3 lb/ft^3) Kaowool mineral fiber (from Ref. B7).

The boundary condition parameters A, h, β, F, α, and ε are all independent of the temperature (although the boundary conditions are temperature dependent). The convection parameters h and β have been experimentally determined for some conditions [B7, B8] and are at best an estimate. Since the temperatures that are encountered in fire tests commonly exceed 816°C (1500°F), the convective heat flux is of secondary importance to the radiation heat flux. The parameters for the radiation heat flux (α and ε) are documented for a wide number of materials [B6]. The exposure temperature, T_f, is specified by the user at selected time intervals.

B2.2 Verification of FIRES-T3 with Exact Solutions

FIRES-T3 was verified by comparing the program results to the exact solutions for a steady state heat transfer problem with two convection and two radiation boundaries and transient heat transfer problem exposing an infinitely long slab to a convection boundary condition. Both problems were one-dimensional.

B2.2.1 Steady State Heat Transfer

The steady state temperature distribution in a one dimensional slab with convection and radiation boundary conditions on opposite sides and constant material properties may be calculated with the following set of equations [B9]

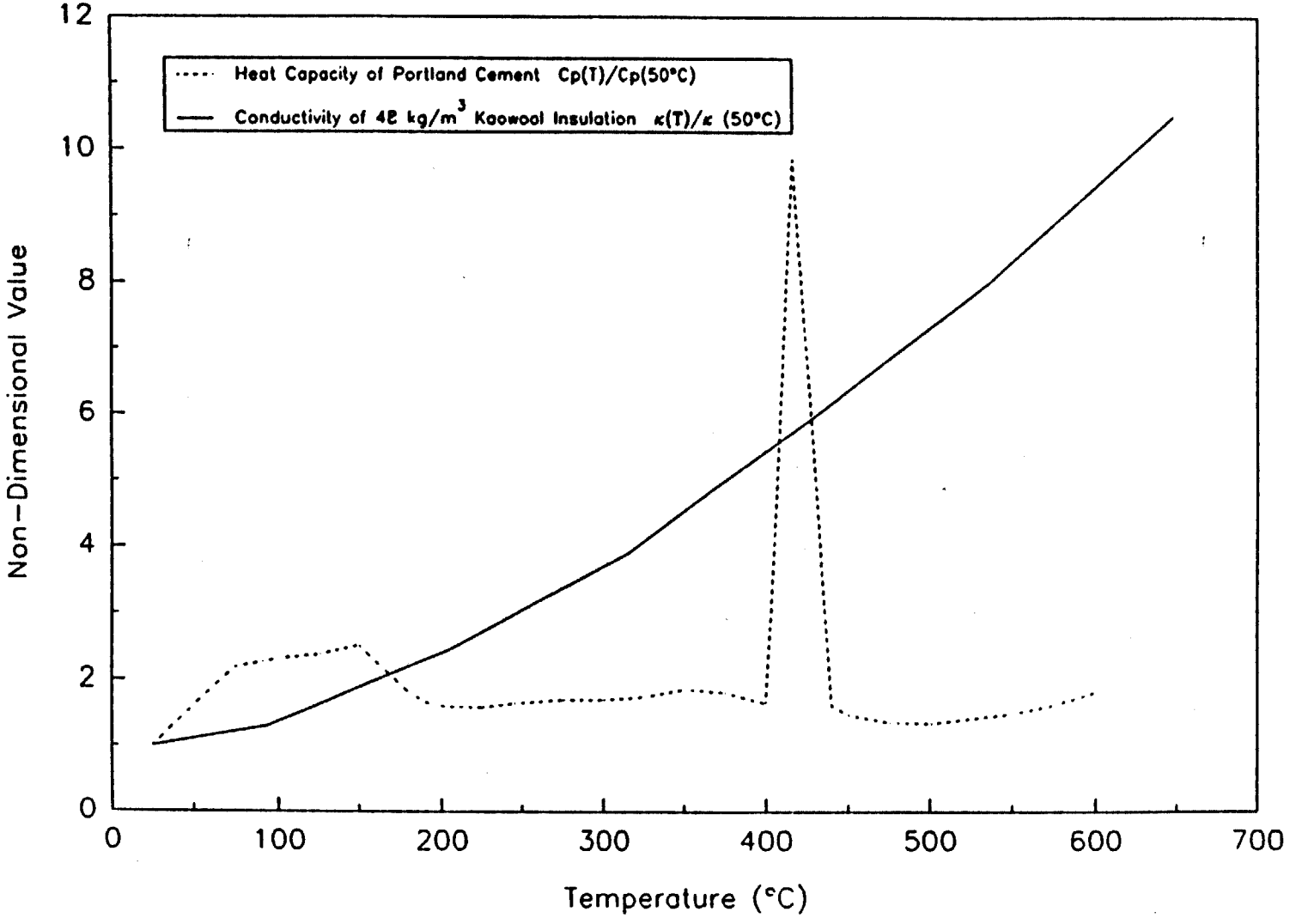

Fig. B1 - Non-dimensional heat capacity and thermal conductivity

$$Q_{in} = Q_{cond} \tag{B6}$$

$$Q_{cond} = Q_{out} \tag{B7}$$

where Q is the heat flow, Q_{in} is the heat convected and radiated into the material, Q_{cond} is the heat conducted through the slab, and Q_{out} is the heat convected and radiated out of the material (see Fig. B2). The heat flow in, through, and out of the slab can be determined using the following expressions:

$$Q_{in} = h_h A(T_h - T_1) + F_h A\sigma(\epsilon_h T_h^4 - \alpha_h T_1^4) \tag{B8}$$

$$Q_{cond} = \frac{\kappa A}{th}(T_1 - T_2) \tag{B9}$$

$$Q_{out} = h_c A(T_2 - T_c) + F_c A\sigma(\epsilon_c T_2^4 - \alpha_c T_c^4) \tag{B10}$$

where *th* is the total slab thickness and the cross sectional area, A, is constant. Here, the subscripts h,1,2, and c refer to the exposure, exposure surface, unexposed surface, and ambient, respectively. The constants that were used in equations B8-B10 to validate FIRES-T3 are listed in Table B1. The unknown quantities in equations B8-B10 are the surface temperatures, T_1 and T_2. Since there are three equations and two unknowns, the surface temperatures can be solved algebraically. Once they have been determined, the temperature field within the slab can be computed by calculating the heat flow, Q, then rearranging equation B9:

$$T(x) = T_h - \frac{Q_{cond} \cdot x}{\kappa A} \tag{B10}$$

Table B1 - Parameters for Steady State Solution

Parameter	Value	Parameter	Value
h_h	40 W/m^2-K	h_c	8 W/m^2-K
ϵ_h	0.9	ϵ_c	0.95
α_h	0.9	α_c	0.95
A	1.0 m^2	T_c	37.8°C
T_h	537.8°C	F(all)	1.0
κ	0.13 W/m-K	th	0.0254 m

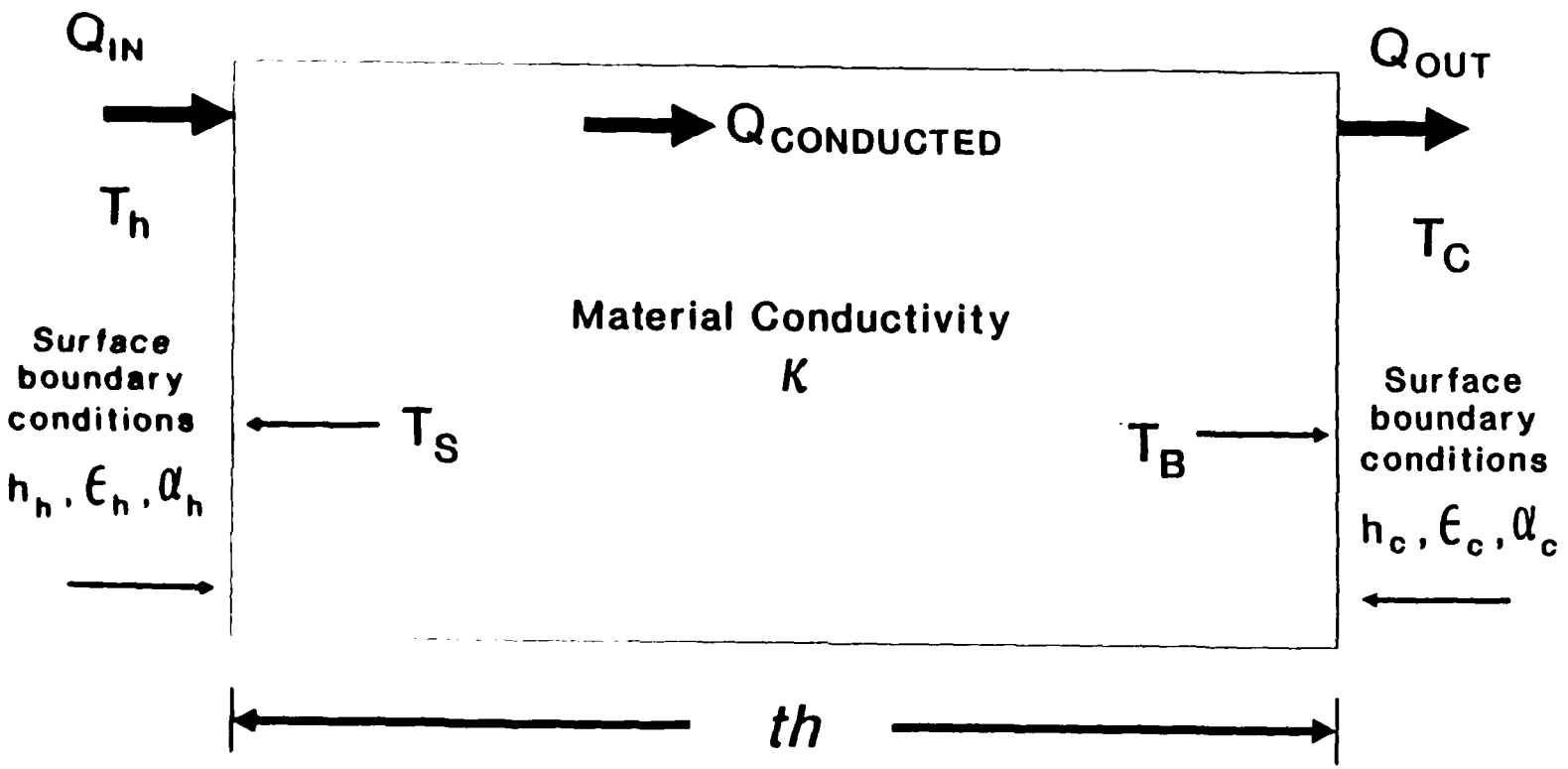

Fig. B2 - Steady state heat transfer through material with constant material properties

The problem was modeled in FIRES-T3 with 50 equidistant nodes. FIRES-T3 is a transient heat transfer program. As a result, the slab was assigned an initial temperature of 37.8°C (100°F). FIRES-T3 began to converge to a steady state solution (within 0.5°C or 1°F) after about four hours model time (20 seconds computing time). To ensure that the program solution was steady state, FIRES-T3 was run for seventeen hours model time. Table B2 compares the exact and numerical values for the hot and cold surface temperatures. The results of equations B8-B11 and FIRES-T3 have been plotted in Fig. B3. The graph indicates that there is no detectable difference between the exact and numerical methods.

Table B2 - Hot and Cold Surface Temperatures

Temperature	Exact	FIRES-T3
T_h (°C)	524.42	524.533
T_c (°C)	142.945	142.744

B2.2.2 Transient Heat Transfer

FIRES-T3 was compared to the exact solution of a transient temperature field in a one-dimensional infinitely long solid with one convection boundary. The solid is initially at a uniform temperature and then exposed on one boundary to a temperature change allowing only convective heat transfer. The temperature change is independent of time. The slab modeled in FIRES-T3 must be sufficiently thick so that no thermal energy penetrates to the other side. Table B3 summarizes the parameters used for the problem of a transient, infinite solid.

Table B3 - Parameters for Transient Problem

Parameter	Value	Parameter	Value
T_i	25.33°C	κ	0.13 W/m-C
T_h	810.930C	ρ	678 kg/m^3
h	40 W/m^2 -C	c_p	900 J/kg-C
th (FIRES-T3)	1.22 m		

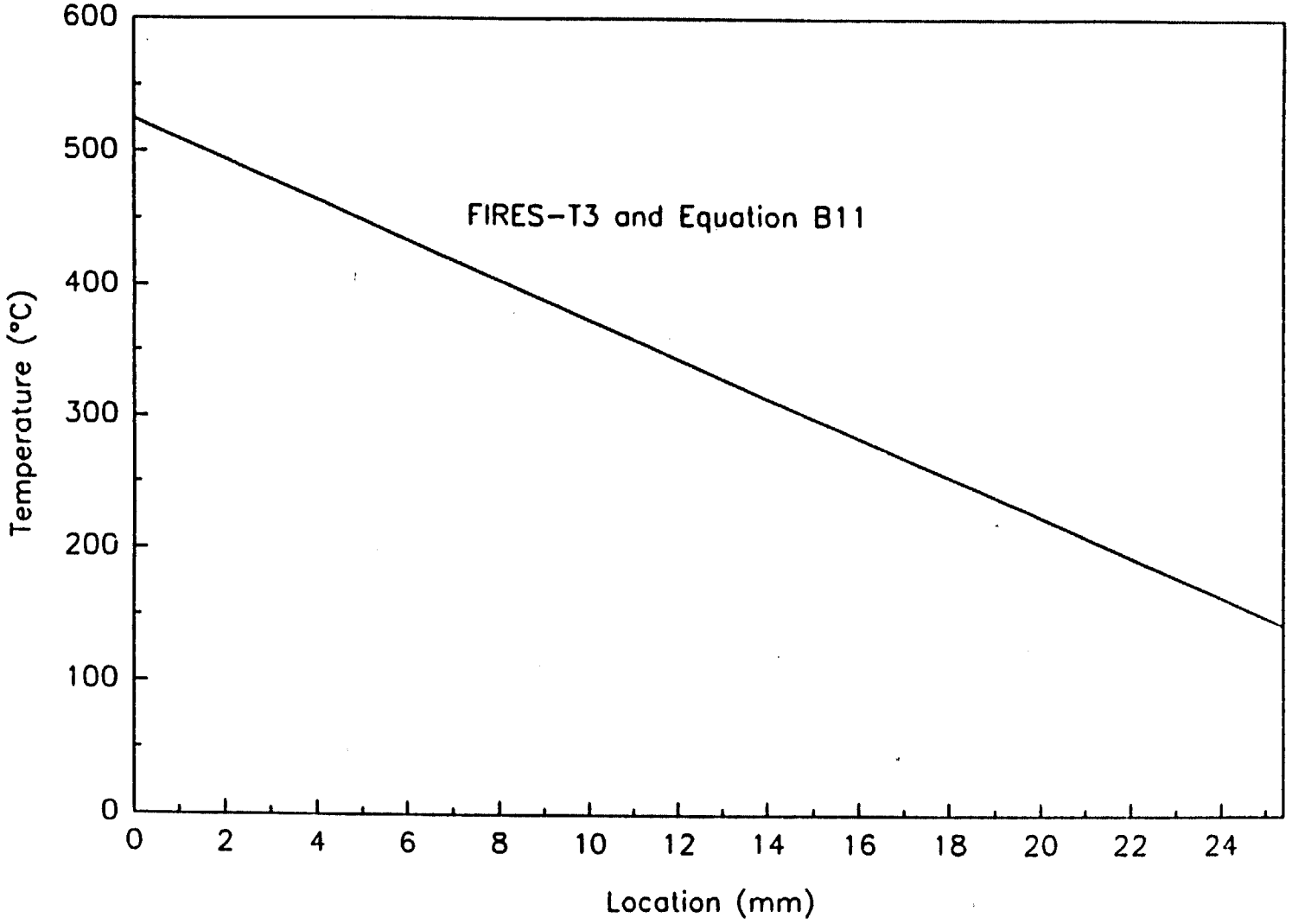

Fig. B3 - Steady state solution for two convection and two radiation boundary conditions on a one-dimensional slab

The exact solution for the transient temperature distribution in the infinite one-dimensional solid is given in Ref. [B10]:

$$\frac{T(x)-T_i}{T_h-T_i} = 1-erf\left(\frac{x}{2(\alpha t)^{0.5}}\right)-\left[\exp\left(\frac{hx}{\kappa}+\frac{h^2\alpha t}{\kappa^2}\right)\right]\left[1-erf\left(\frac{x}{2(\alpha t)^{0.5}}+\frac{h(\alpha t)^{0.5}}{\kappa}\right)\right] \quad \text{(B12)}$$

where t is time and:

$$\alpha = \frac{\kappa}{c_p\rho} \quad \text{(B13)}$$

$$erf(\xi) = \frac{2}{\pi^{1/2}}\sum_{n=1}^{\infty} = \frac{-1^n\ \xi^{2n+1}}{(2n+1)\ n!} \quad \text{(B14)}$$

ξ is an arbitrary argument to the error function (erf) between 0 and infinity.

Ninety nodes were used in FIRES-T3 to solve the transient infinite slab: 20 in the first 0.00127 m, 20 in the next 0.0381 m, 20 in the next 0.1016 m, 20 in the next 0.1524 m, and 10 in the last 0.9144 m. All the nodes were equidistant in the specified range.

A FORTRAN77 program was written to solve equation B12 at the desired times and locations in the slab. The exact solution for locations greater than 0.00127 m (0.03871 ft) could not be computed because the denominator in equation B14 grew too large.

The results of equation B12 and FIRES-T3 are shown in Figs. B4-B6 for the first 60 seconds, one to five minutes, and six to ten minutes, respectively. The graphs show that FIRES-T3 can accurately model a basic transient heat transfer problem accurately.

Fig. B7 shows the effect of improper timestep selection. The curves plotted in Fig. B4 resulted from a timestep of 0.5 second in FIRES-T3 (such that there were 20 solutions before the first ten seconds were reached). The curves in Fig. B7 resulted from a timestep of five seconds in FIRES-T3. Although the results of Fig. B7 appear to be converging to the actual solution as the total time increases, the results are not accurate for the first couple of time intervals.

B2.2.3 Validation of FIRES-T3 on Fire Test of Material with Known Properties

The modeling capability of FIRES-T3 was compared to the results of a fire test performed on a material with known temperature dependent thermal properties. A large number of tests were conducted by J. Manville Company Research and Development Center for several different insulations and insulation thicknesses [B11]. The two tests of interest used a 0.00635 m (0.02083 ft) sheet of aluminum insulated on both sides with 128 kg/m^3 (8 lb/ft^3) Kaowool. One test used 0.0381 m (0.125 ft) thick Kaowool blankets and the other used 0.0254 m (0.0833 ft) thick sheets (See Fig. B8).

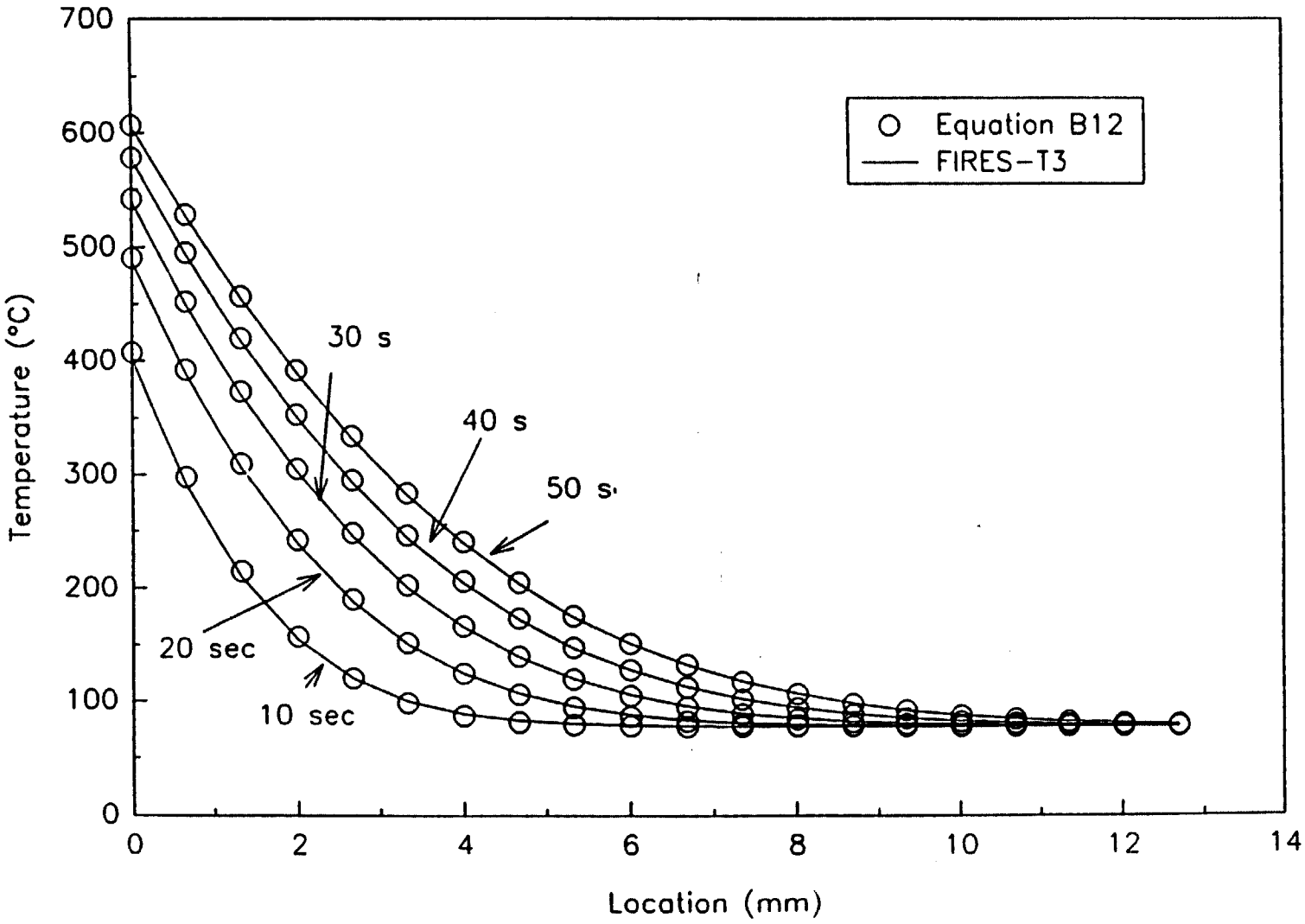

Fig. B4 - Comparison of FIRES-T3 and the exact solution for a transient infinite slab with one convection boundary condition, 0-1 minute

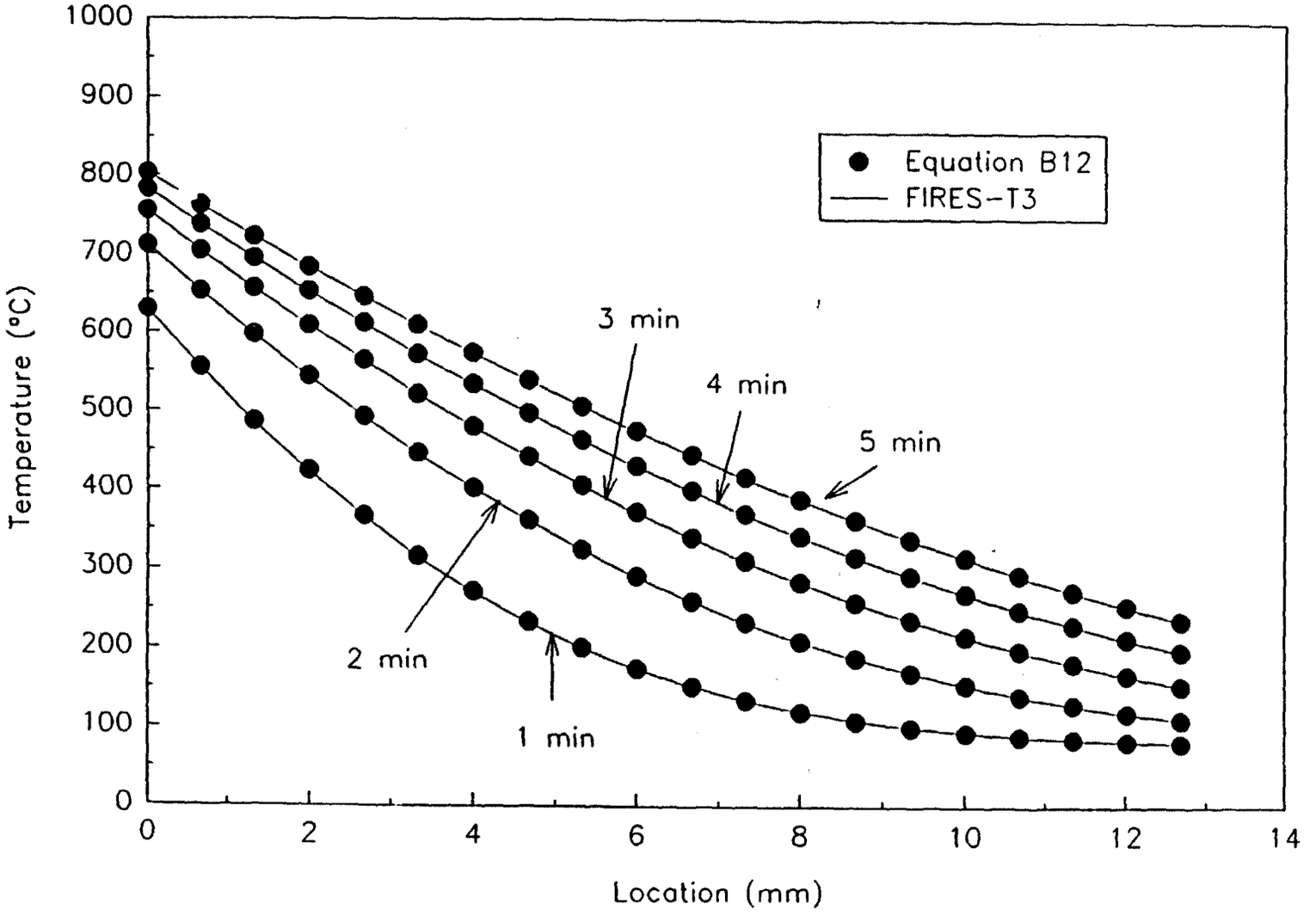

Fig. B5 - Comparison of FIRES-T3 and the exact solution for a transient infinite slab with one convection boundary condition, 1-5 minutes

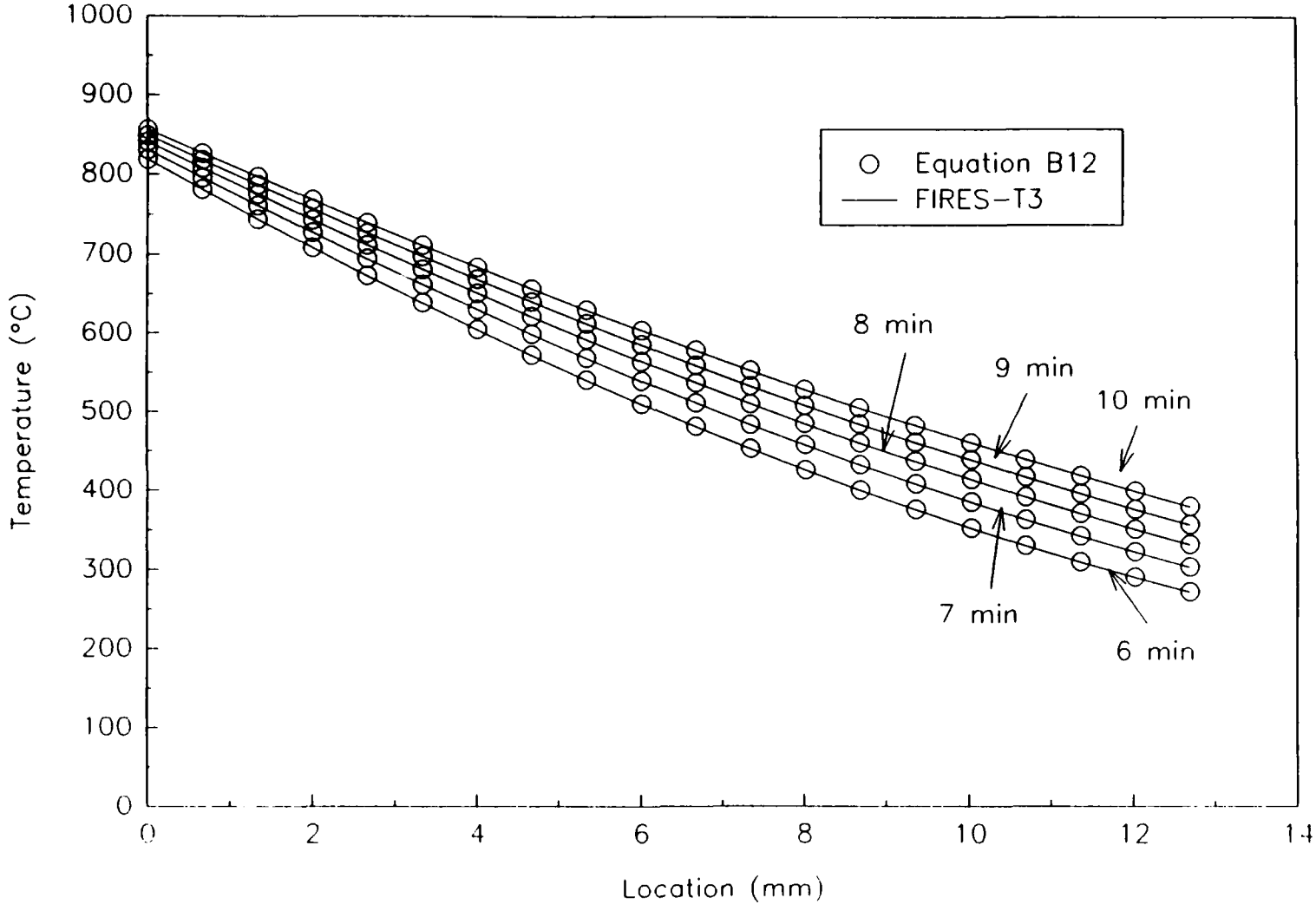

Fig. B6 - Comparison of FIRES-T3 and the exact solution for a transient infinite slab with one convection boundary condition, 5-10 minutes

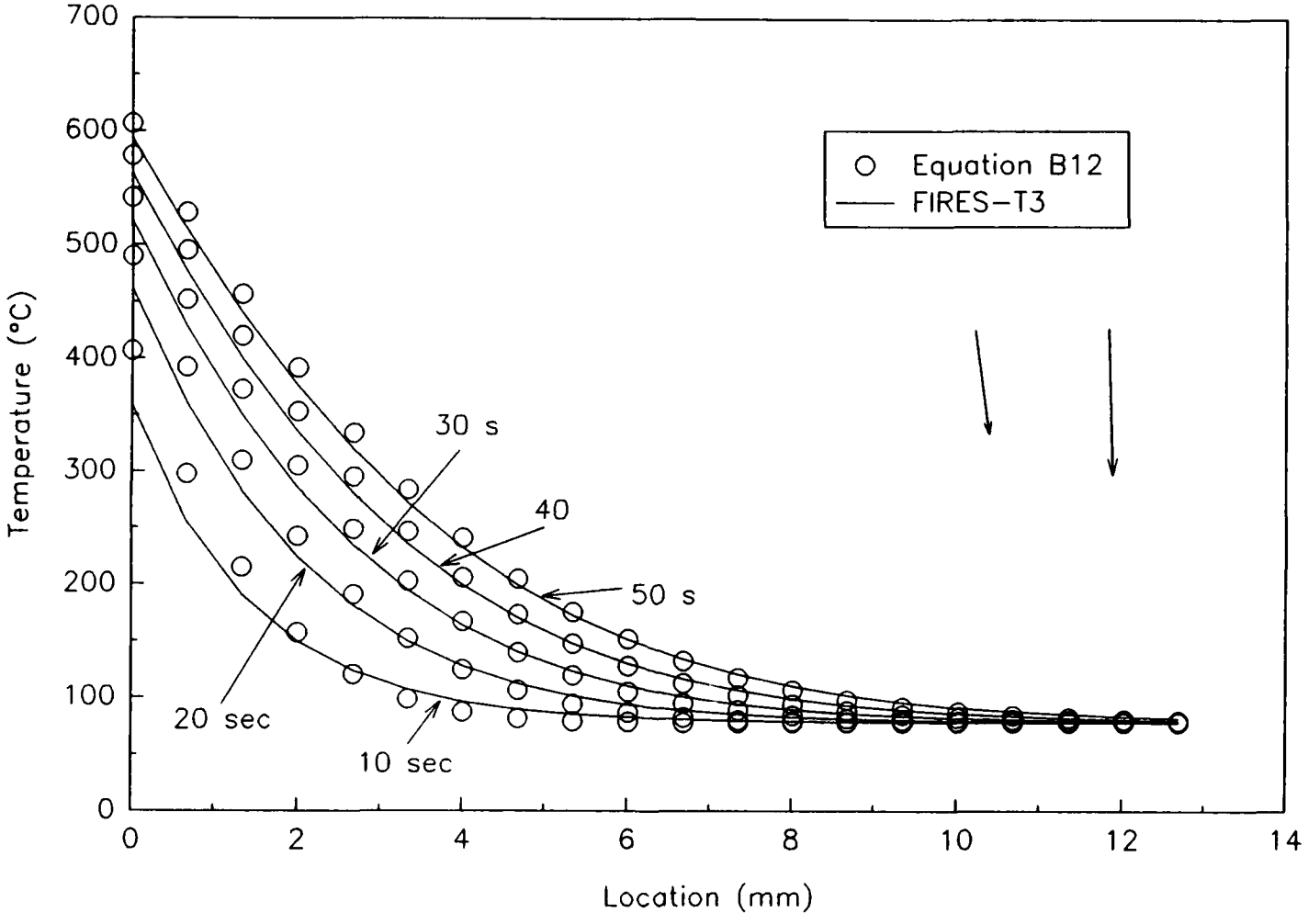

Fij. B7 - Comparison of FIRES-T3 and the exact solution for a transient infinite slab with one convection boundary condition, using 5 second time-step (too large), 0-1 minute

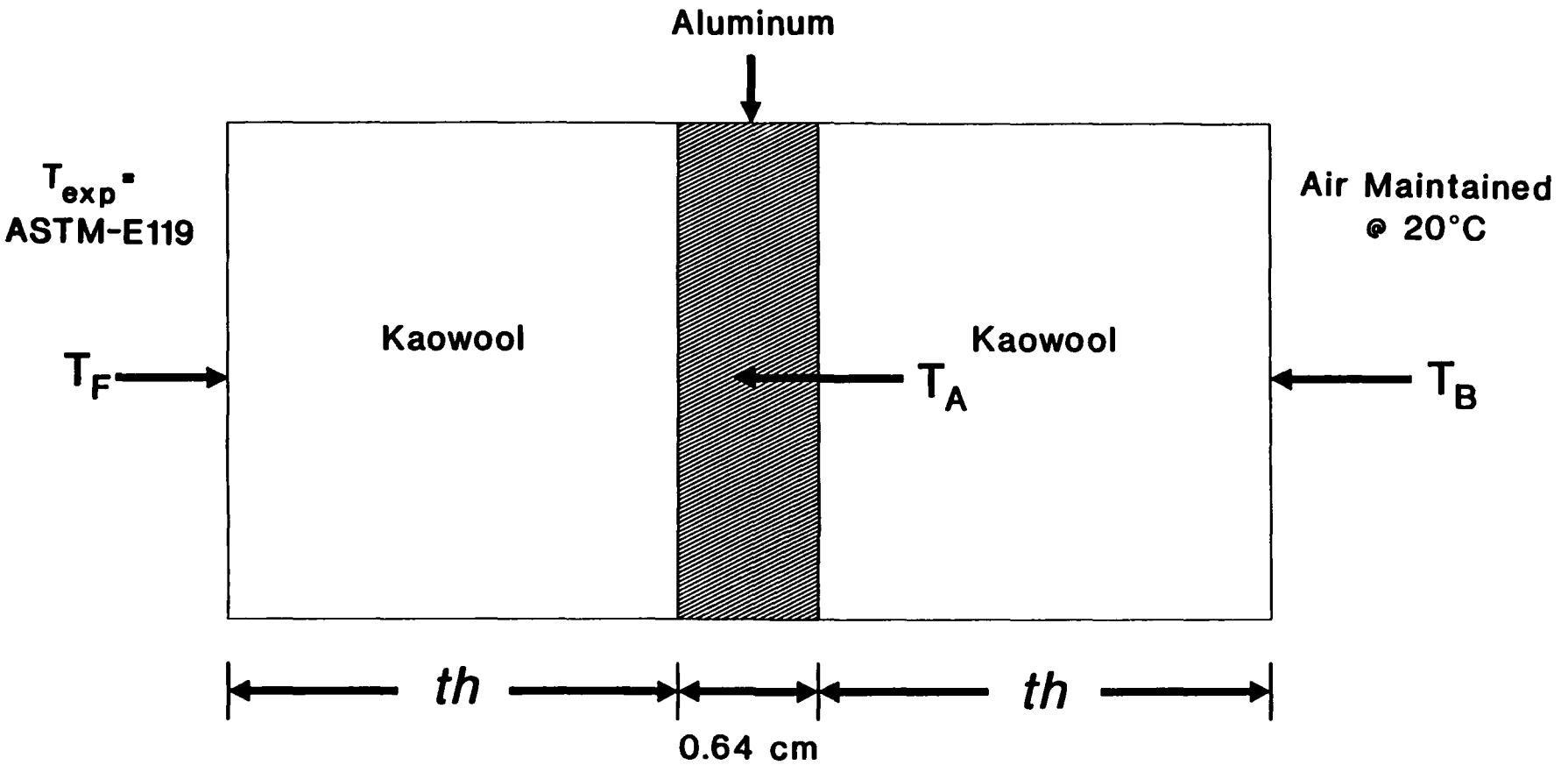

Fig. B8 - ASTM E119 fire test on 128 kg/m^3 (8 lbs/ft^3) Kaowool insulation of various thicknesses (Ref. B11)

The material properties of the Kaowool insulation have been determined by Manville using the ASTM C201, "Standard Test Method for Thermal Conductivity of Refractories." These properties are listed in the Table B4.

Table B4 - Material Properties for 128 kg/m³ Kaowool

Temperature (°C)	κ (W/m-K)	c_p (J/kg-K)
-18.0	0.0324	752.0
204.0	0.0403	919.0
427.0	0.0764	1003.0
649.0	0.1545	1044.5
760.0	0.229	1128.0
982.2	0.2638	1128.0

Ninety nodes were used in each FIRES-T3 model for the Kaowool tests: 40 in each of the front and rear layers of the Kaowool and ten through the aluminum. The front insulation layer was exposed to an approximate ASTM E119 fire curve. Since the exposure was actually slightly less than the E119 and test dependent, different curves were entered for each run. The air temperature of the unexposed side was maintained at 20°C (68°F). The input parameters that were used in FIRES-T3 are summarized in Table B5. The results, including the exposure curves are shown in Figs. B9 and B10. The radiation parameters, α and ε, were assumed to be the same as asbestos fiber, 0.93 [B6]. The convection co-efficient and exponent are consistent with the range suggested in Ref. [B7] and successfully used by Ref. [B8].

Table B5 - FIRES-T3 Input Parameters

Parameter	Value	Parameter	Value
h (W/m^2-$K^{1.25}$)	1.643	β	1.25
ε	0.93	F (radiation)	1.00
α	0.93	Δt (seconds)	1.00

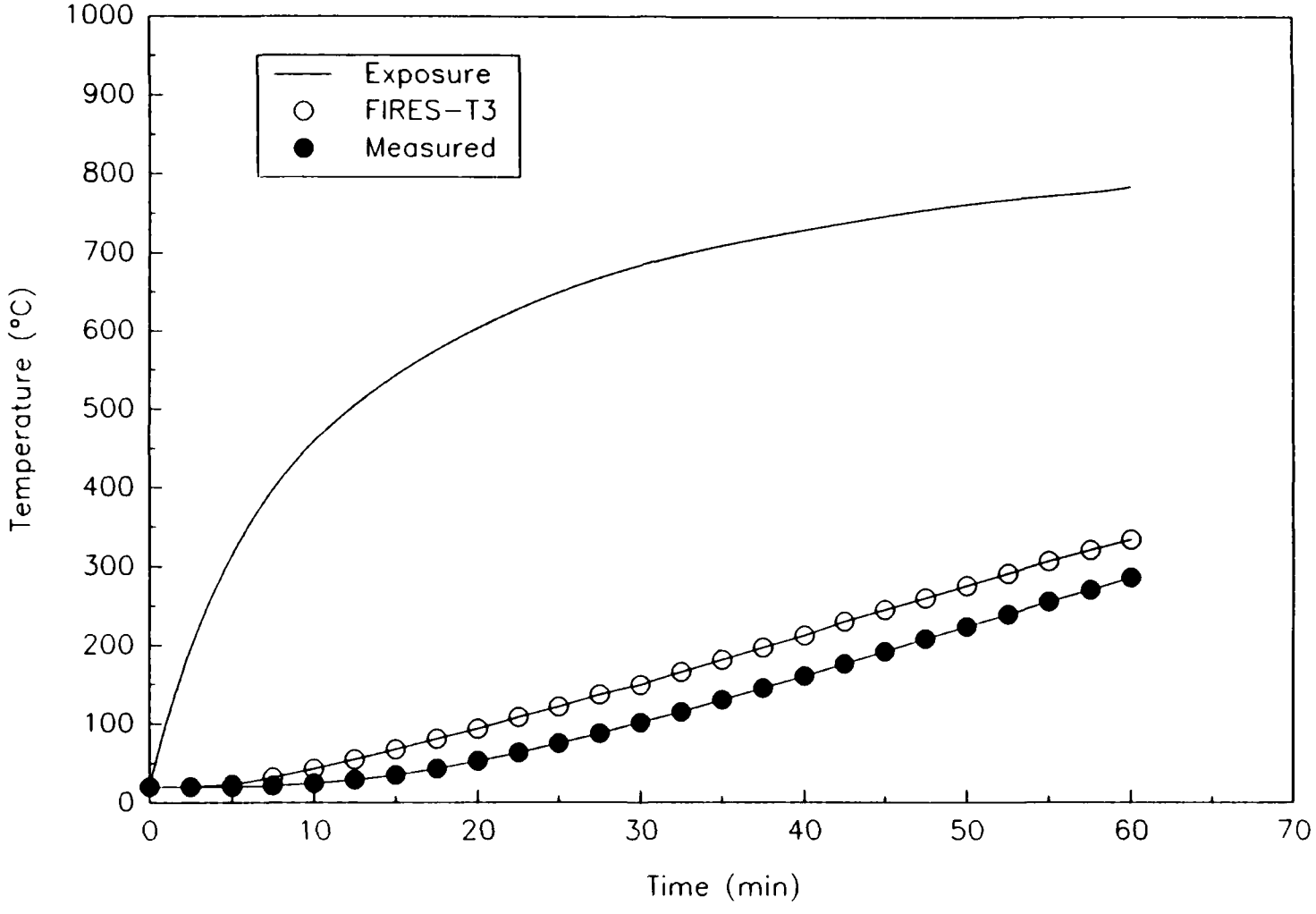

Fig. B9 - Comparison of FIRES-T3 and actual test, 2.6 cm (1 in) Kaowool

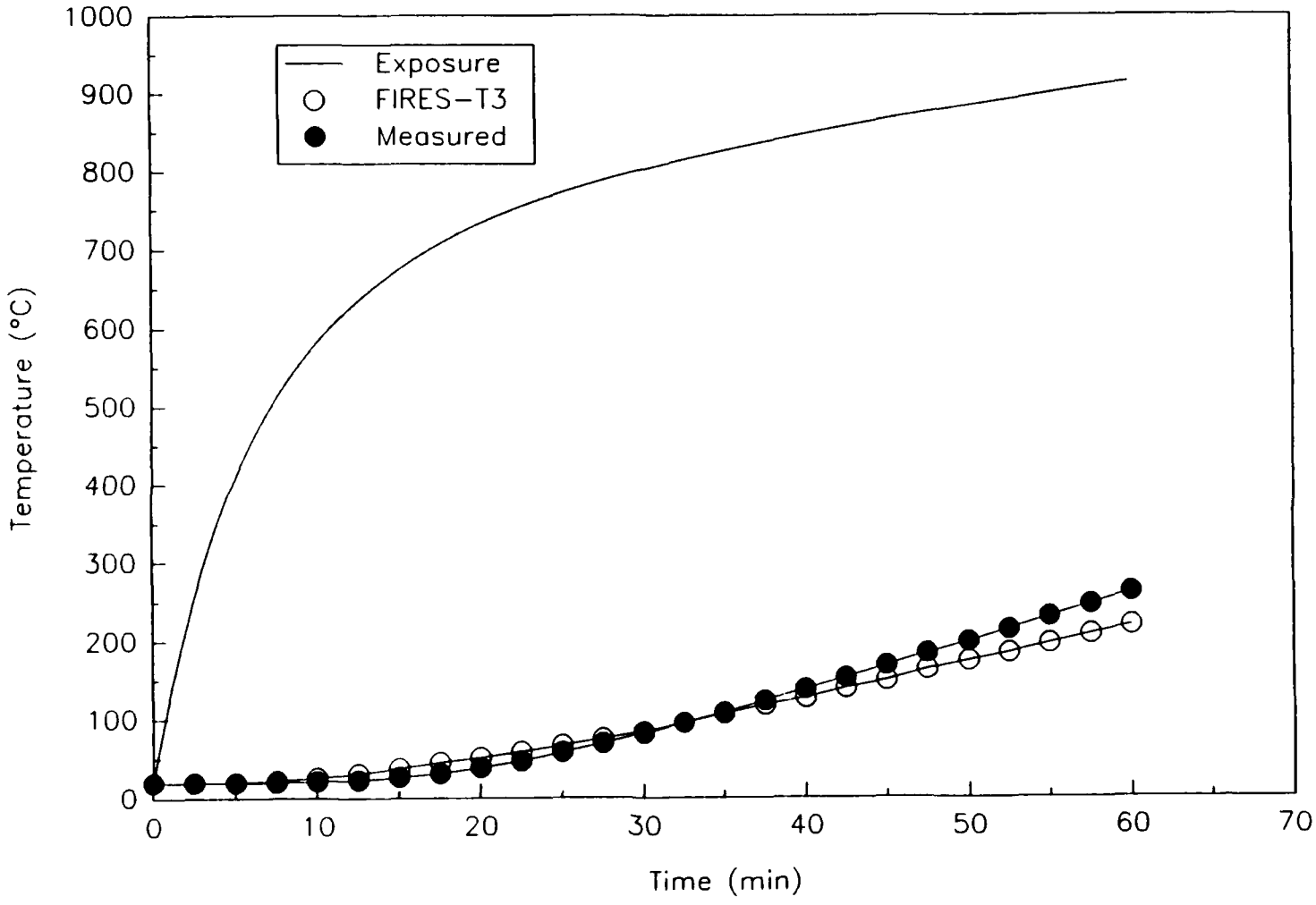

Fig. B10 - Comparison of FIRES-T3 and actual test, 3.8 cm (1.5 in) Kaowool

FIRES-T3 was able to reasonably approximate the aluminum temperature, however the modeling results were less accurate than the solutions to the simple exact problems. This may be due to the increased uncertainty in the exact boundary condition parameters, possible error in the temperature readings, material properties that have an accuracy to within 10-20 percent of the actual value [B12], and the uncertainty in the exact thickness of the insulation layers. These phenomena will be examined in a latter section of this Appendix to assess their impact on the modeling predictions of the FIRES-T3.

B3.0 HEAT TRANSFER ANALYSIS OF THE SHADWELL TESTS

The heat transfer analysis of the test data from the ex-USS SHADWELL focused on the Ins_8 - Ins_13 tests excluding Ins_11. The material and thermal properties (thickness, density, heat capacity, and conductivity) of the materials were assessed and used to model Ins_8 through Ins_13. Independent tests on the same materials were also modeled for comparison purposes.

B3.1 Materials Modeled

The standard Navy mineral wool insulation and the candidate lightweight Manville fiber insulation described in the report do not have fully documented thermal material properties. The properties were estimated on available information on fibrous insulations *and radiation heat transfer.*

Observations from the insert tests on the ex-USS SHADWELL indicated that the mineral wool may degrade at temperatures above 871-927°C (1600-1700°F). The characteristics of the decomposition are severe shrinkage, dismemberment of material, and falling away from the deck. Unfortunately, the loss of material presents serious difficulty in modeling the heat transfer due to the abrupt change in boundary conditions and random nature of the event. Further, the exact mass of insulation, location, and time that it fell off cannot be addressed because the flames and smoke obstructed the view. The Manville generally remained during the fire tests.

There were three different material thicknesses in the insert tests: one and two layers of Manville (Ins_8, Ins_9, Ins_10), and one layer of standard navy mineral wool (Ins_12, Ins_13). Each layer was nominally 2.54-cm (1-in.) thick, but actual measurements revealed that one layer of Manville was 1.59-cm (0.626-in.) thick, and one layer of the mineral wool was on average 1.91-cm (0.752-in.) thick although it ranged from 1.27-2.54 cm (0.5-1-in.).

The measured density of the mineral wool, including the facing, was reported as 83.3 kg/m^3 (5.3 lb/ft^3). The density of the mineral wool without the facing was assumed to be 64.2 kg/m^3 (4 lb/ft$^{3)}$. The heat capacity varied between 232-812 J/kg (0.1 to 0.35 Btu/lb) depending on the temperature [B5]. The conductivity curves for 96.2 and 128.3 kg/m^3 (8 and 6 lb/ft^3) mineral wool insulations were available in Refs. [B5] and [B13],

respectively. The conductivity curve for the 64.2 kg/m^3 (4.0 lb/ft^3) insulation was deduced with the following equation [B6]:

$$\kappa(T) = \sigma \frac{16}{3} \frac{T^3}{a_r} + \kappa_o \qquad \text{(B15)}$$

where a_r and κ_o are material parameters and σ is the Stefan-Boltzmann constant. The conductivity for the mineral wool was estimated by altering the constants a_r and κ_o in equation B15 until the results of Ins_12 (1 layer of mineral wool) were reproduced satisfactorily. The conductivity of the low density mineral wool was constrained to approximately the values of the higher density mineral wools at room temperature. The estimated conductivity of the 64.2 kg/m^3 (4.0 lb/ft^3) insulation is shown in Fig. B11. For comparison, the measured and computed conductivity curves for the heavier mineral wool insulations is also shown in Fig. B11. The values for a_r and κ_o are shown in Table B6 for the three mineral wool insulation densities.

Table B6 - Equation B15 Parameters for Mineral Wool

Mineral Wool	62.4 kg/m^3	96.2 kg/m^2	128.3 kg/m^3
a_r	1288	878	461
κ_o (W/m-K)	0.02019	0.0254	0.0217

The Manville insulation had a measured density of 115 kg/m^3 (7.18 lb/ft^3) including the facing material. The density was measured at approximately 56 kg/m^3 (3.5 lb/ft^3) excluding the facing material. Based on discussions with the manufacturer and from prior tests on the material [B14], the heat capacity (c_p) was estimated to be about 232 J/kg (0.1 Btu/lb) and the thermal conductivity (κ(T)) at 36.7°C (98°F) was estimated to be about 0.0274 J/m-K-s (0.19 Btu-in./ft^2-R-hr). The conductivity curve was computed using equation B15. The conductivity was constrained to 0.0274 J/m-K-s at 36.7°C. The constants in equation B15 were altered until the results of Ins_10 (1 layer of Manville) were adequately reproduced. Table B7 shows the estimated a_r and κ_o for the Manville. For comparison, the values of the 64.2 lb/ft^3 mineral wool and the deduced set for the 128 kg/m^3 Kaowool insulation are listed. Fig. B12 shows the estimated conductivity curve for the Manville as well as the actual and computed conductivity curves for Kaowool.

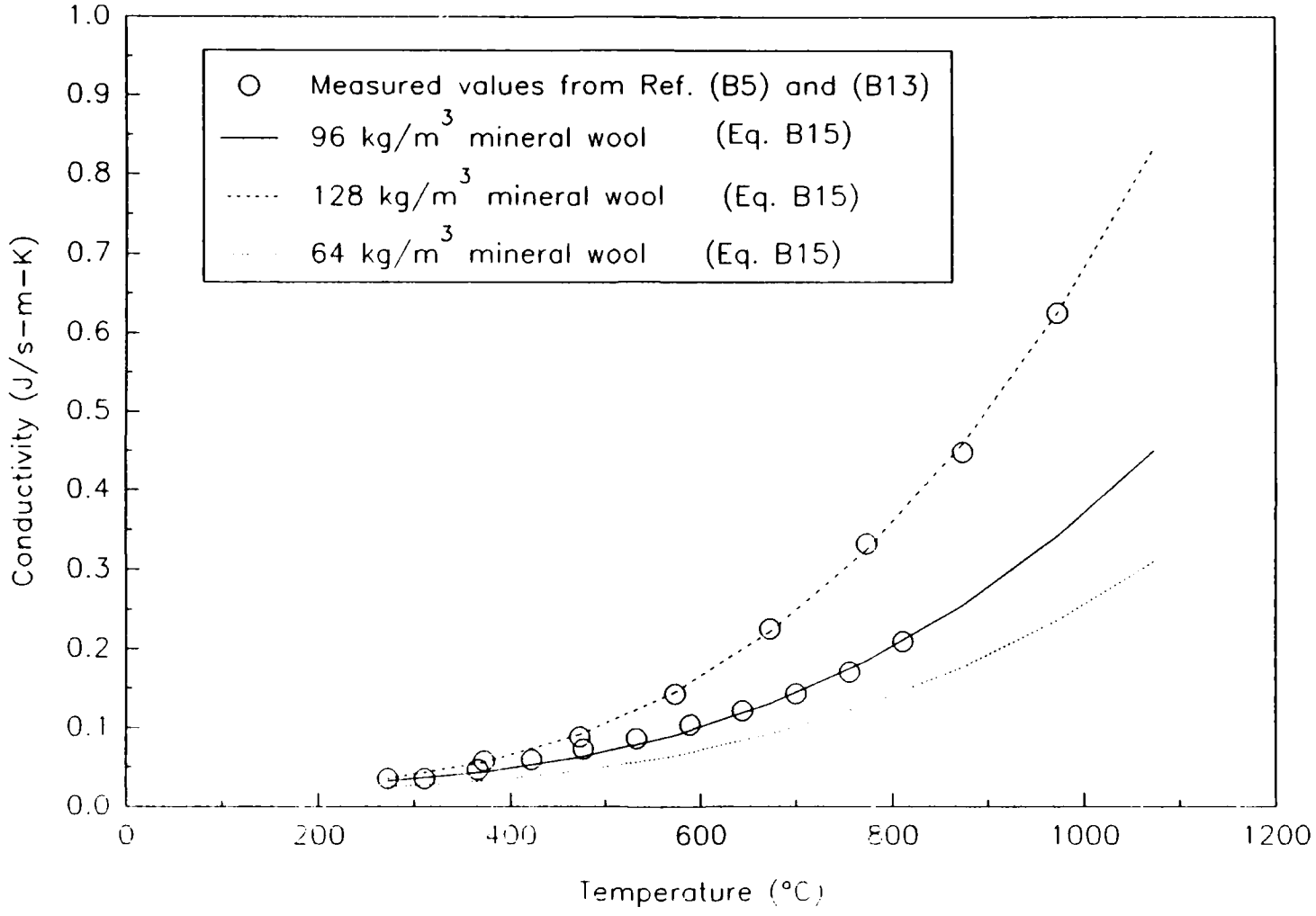

Fig. B11 - Measured and estimated thermal conductivity curves for mineral wool, 64 kg/m³ (4 lb/ft³) to 128 kg/m³ (8 lb/ft³)

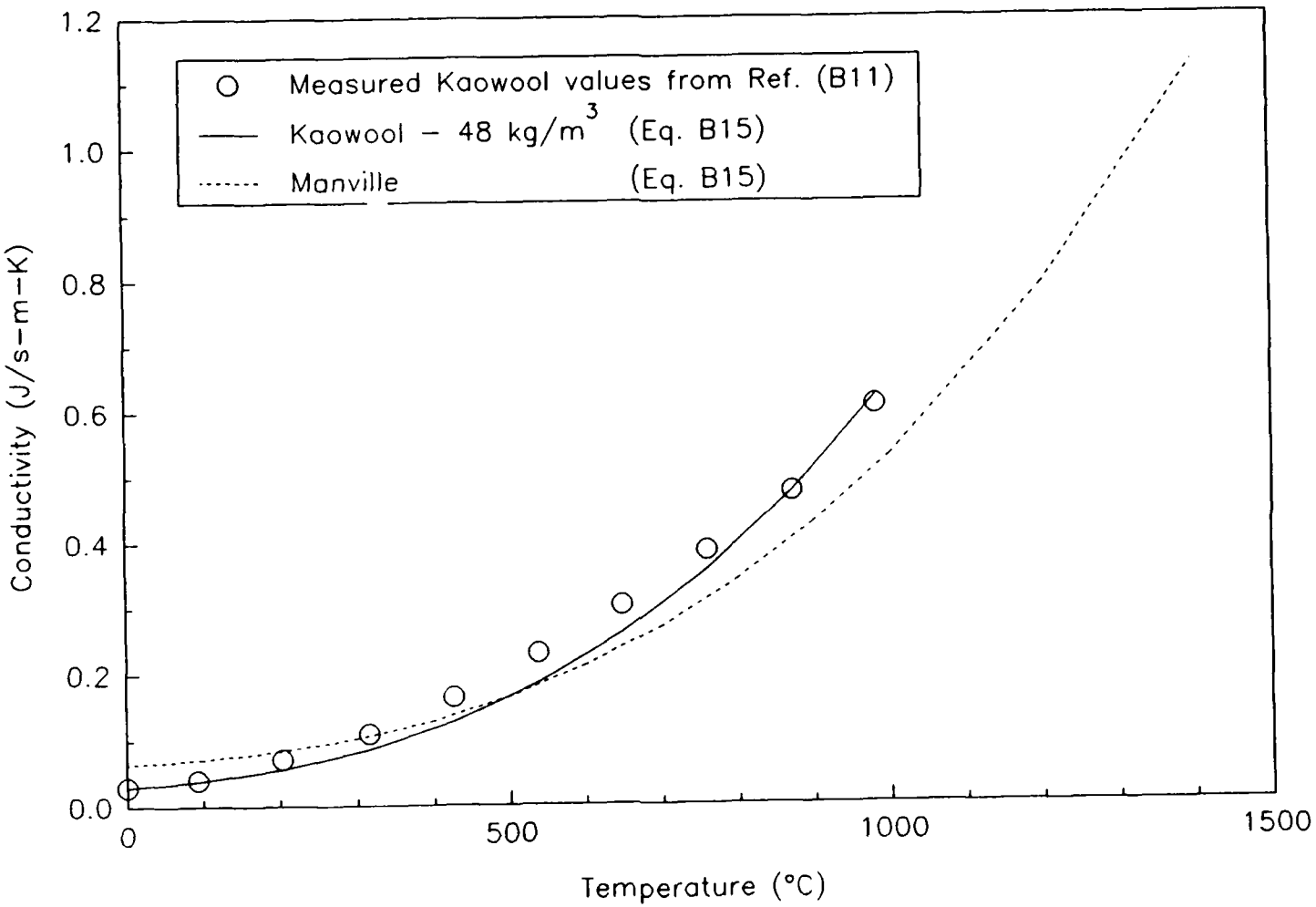

Fig. B12 - Comparison of predicted thermal conductivity of Manville to measured conductivity of Kaowool

Table B7 - Equation B15 Parameters for Insulations

Insulation	a_r	κ_o (J/s-m-K)
Manville	1326	0.05936
Mineral Wool (62.4 kg/m^3)	1288	0.02019
Kaowool (128 kg/m^3)	2318	0.02625

B3.2 Model Parameters

A total of six insulation tests from the SHADWELL were modeled with FIRES-T3. These tests are summarized in Table B8. The average fire-side exposure temperatures are shown in Fig. B13.

Table B8 - Insulation Tests Modeled in FIRES-T3

Test	Material	Nominal Thickness	Actual Thickness
Ins_8	Manville	2.54 cm (1 in.)	1.59 cm (0.625 in.)
Ins_9	Manville	5.08 cm (2 in.)	3.18 cm (1.25 in.)
Ins_10 Insert 2	Manville	2.54 cm (1 in.)	1.59 cm (0.625 in.)
Ins_10 Insert 3	Manville	5.08 cm (2 in.)	3.18 cm (1.25 in.)
Ins_12	Mineral Wool	2.54 cm (1 in.)	1.90 cm (0.75 in.)
Ins_13	Mineral Wool	2.54 cm (1 in.)	1.90 cm (0.75 in.)

The convection boundary conditions selected were consistent with the range suggested by Refs. [B7] and [B8]. The h and β values used to model the insulation tests were slightly larger than those used in the Kaowool validation model because of the greater fire temperature in the SHADWELL tests. Because the fire temperature quickly reached a high value, the convective boundary conditions were of secondary importance compared to the radiation boundary conditions. The convection boundary conditions for the fire side and the unexposed side were

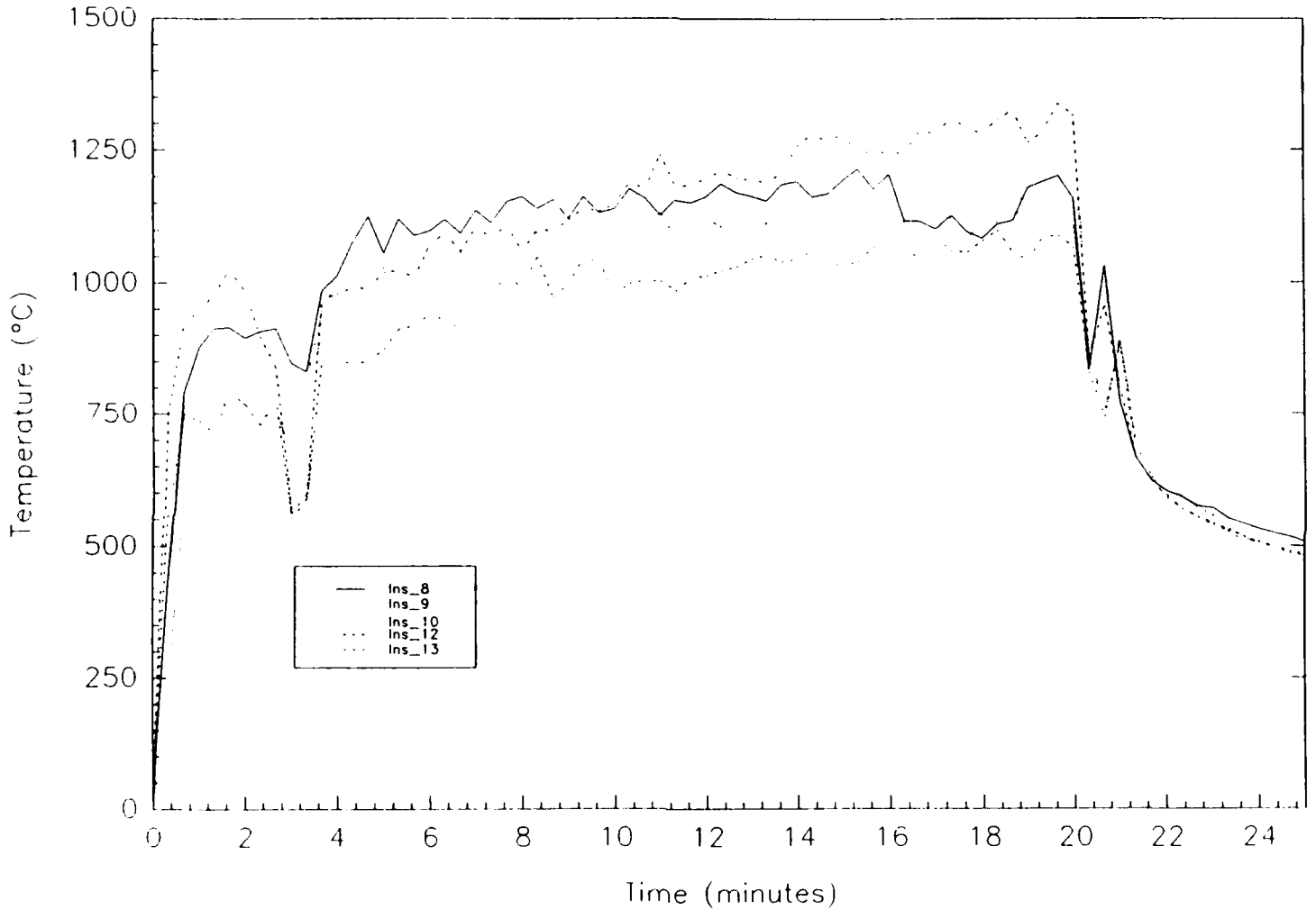

Fig. B13 - Exposure curves for Ins_8 through Ins_13, excluding Ins_11

$$\dot{Q}_{conv} = 2.07 \cdot (T_{fire} - T_{surface})^{1.33} \qquad \textit{Fire Boundary} \qquad \text{(B16)}$$

$$\dot{Q}''_{conv} = 1.97 \cdot (T_{fire} - T_{surface})^{1.25} \qquad \textit{Unexposed Boundary} \qquad \text{(B17)}$$

The radiation boundary conditions assumed the exposure temperatures had an emissivity of 1.0 (which includes the unexposed air temperature). The radiation configuration factor between the exposure temperature and the steel/insulation surface was assumed to be 1.0. Both the Manville and the mineral wool insulations were assumed to have radiative properties similar to fiberglass, viz. $\varepsilon = \alpha = 0.8$ [B6]. Steel has temperature dependent radiative properties, so an average value over the expected temperature range was used, $\varepsilon = \alpha = 0.4$ [B15].

The model was one-dimensional, ignoring edge effects. A 50-node mesh was used, 40 equidistant nodes through the insulation and 10 through the backside steel plate. The temperature gradient was not of interest in this application; thus, equally spaced nodes were suitable.

B3.3 Results

The results of the heat transfer analysis are summarized in Figs. B14-B19. A prediction of failure (232°C (450°F)) within one or two minutes is considered good. Table B-7 compares the predicted and actual times for the steel to reach 232°C (450°F).

The Manville failure times were underestimated by about 1 minute for the single layer tests and overestimated by about 1.5 minutes for the two layer tests. Failure times in both of the mineral wool tests were slightly under-predicted. Table B9 indicates that even with assumed conductivity curves and convection boundary conditions, the predictions are fairly close for the temperature and time range of interest.

B3.4 Application of Derived Material Properties and Assumed Convection Boundary Conditions to E119 Fire Tests

For comparative purposes, modeling was performed on several tests using the same insulations VTEC laboratories conducted two fire tests on the mineral wool insulation and one fire test on the Manville insulation [B16]. The exposure temperature was approximately the ASTM E119 fire curve, but slightly different for each test. The test samples were 91 cm by 91 cm (3 ft by 3 ft) in area and of various thicknesses. They were affixed to a 0.32 cm (1/8 in.) thick carbon steel plate. One mineral wool test and the Manville test used 0.0254 m (0.0833 ft) thick insulations and the other mineral wool test used 0.0508 m (0.1667 ft) thick insulation. The actual thickness was assumed to be the reported thickness.

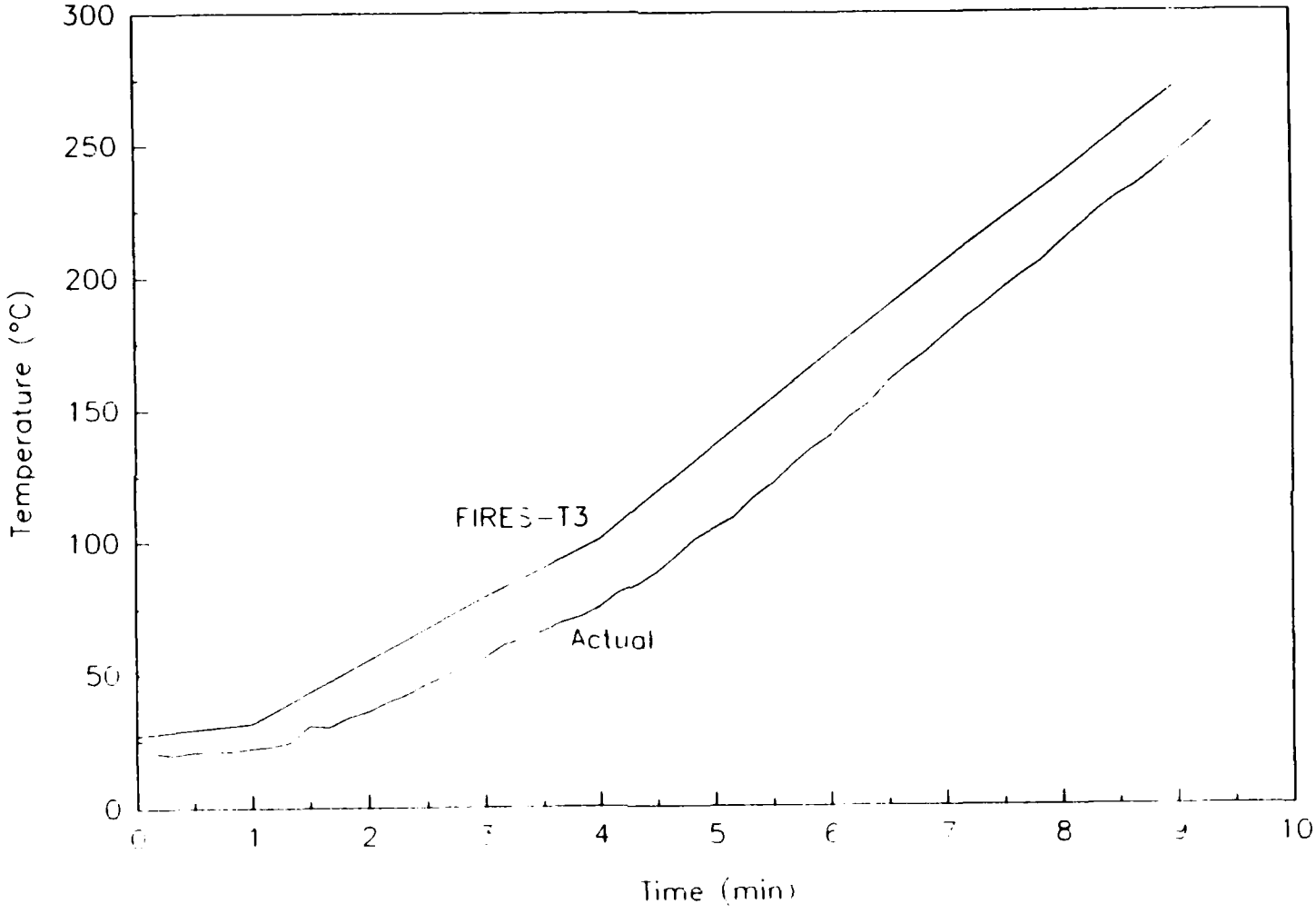

Fig. B14 - Predicted vs. actual steel insert temperatures, 1.6 cm (0.63 in) Manville insulation from Ins_8

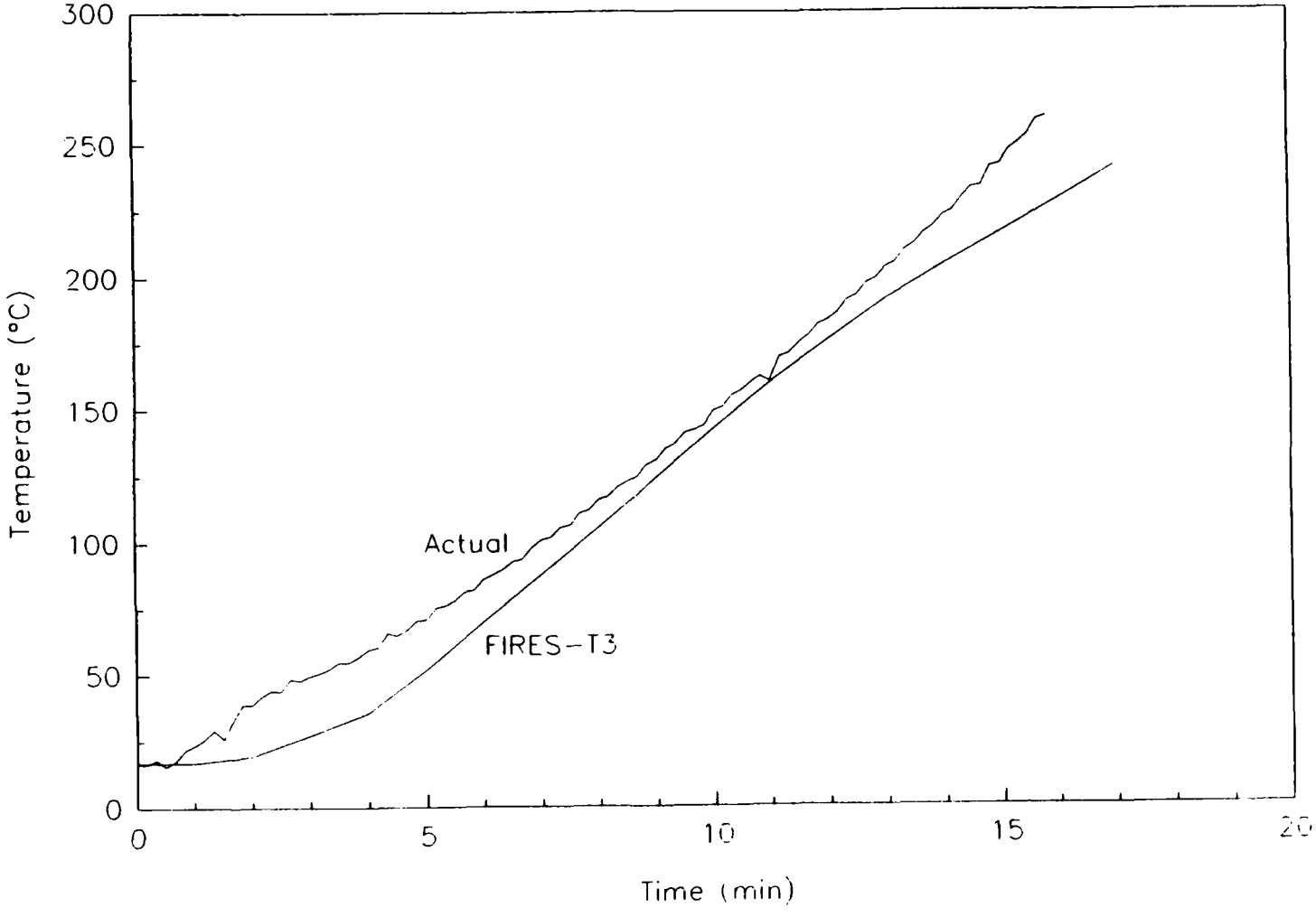

Fig. B15 - Predicted vs. actual steel insert temperatures, 3.2 cm (1.3 in) Manville insulation from Ins_9

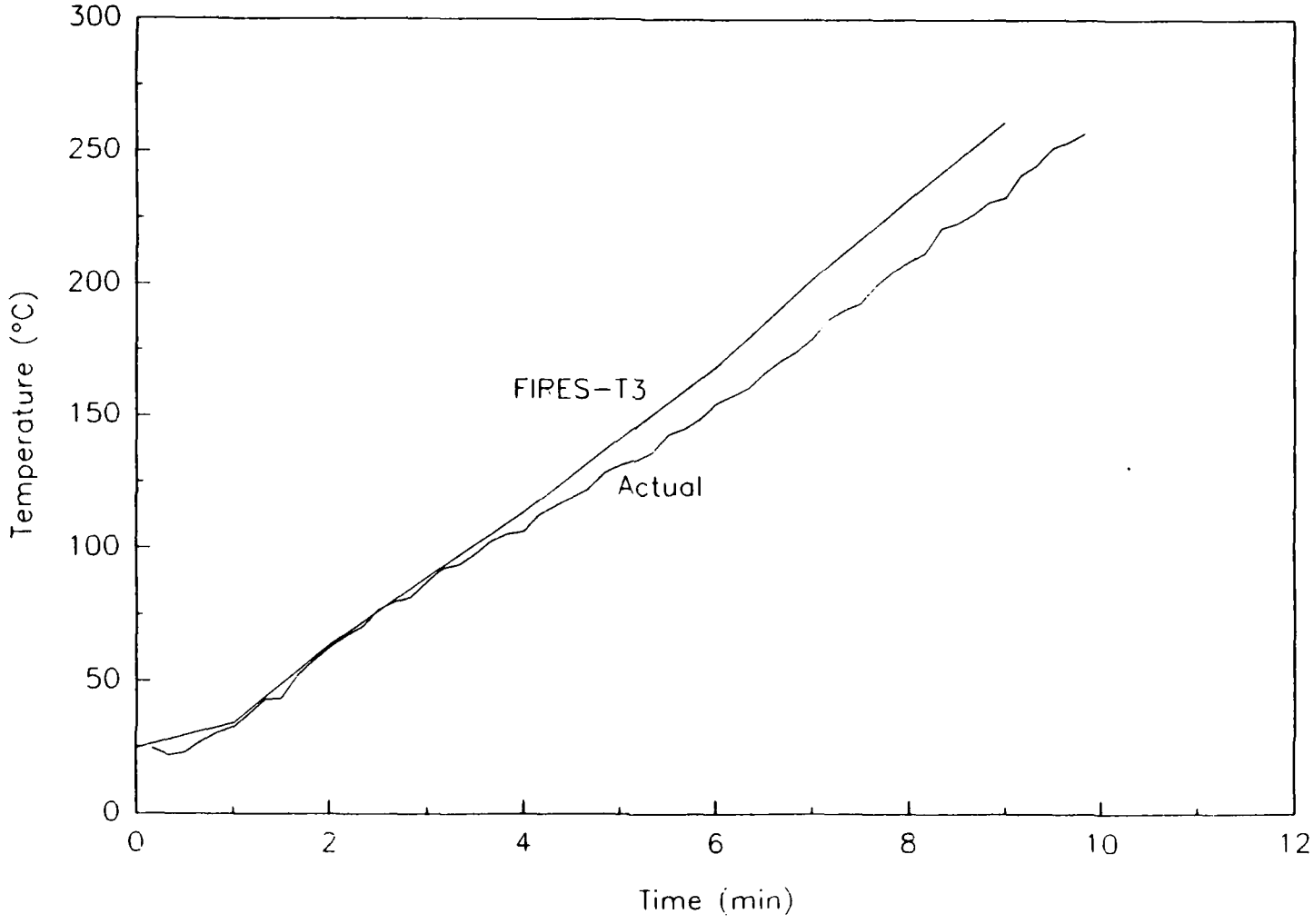

Fig. B16 - Predicted vs. actual steel insert temperatures, 1.6 cm (0.63 in) Manville insulation from Ins_10

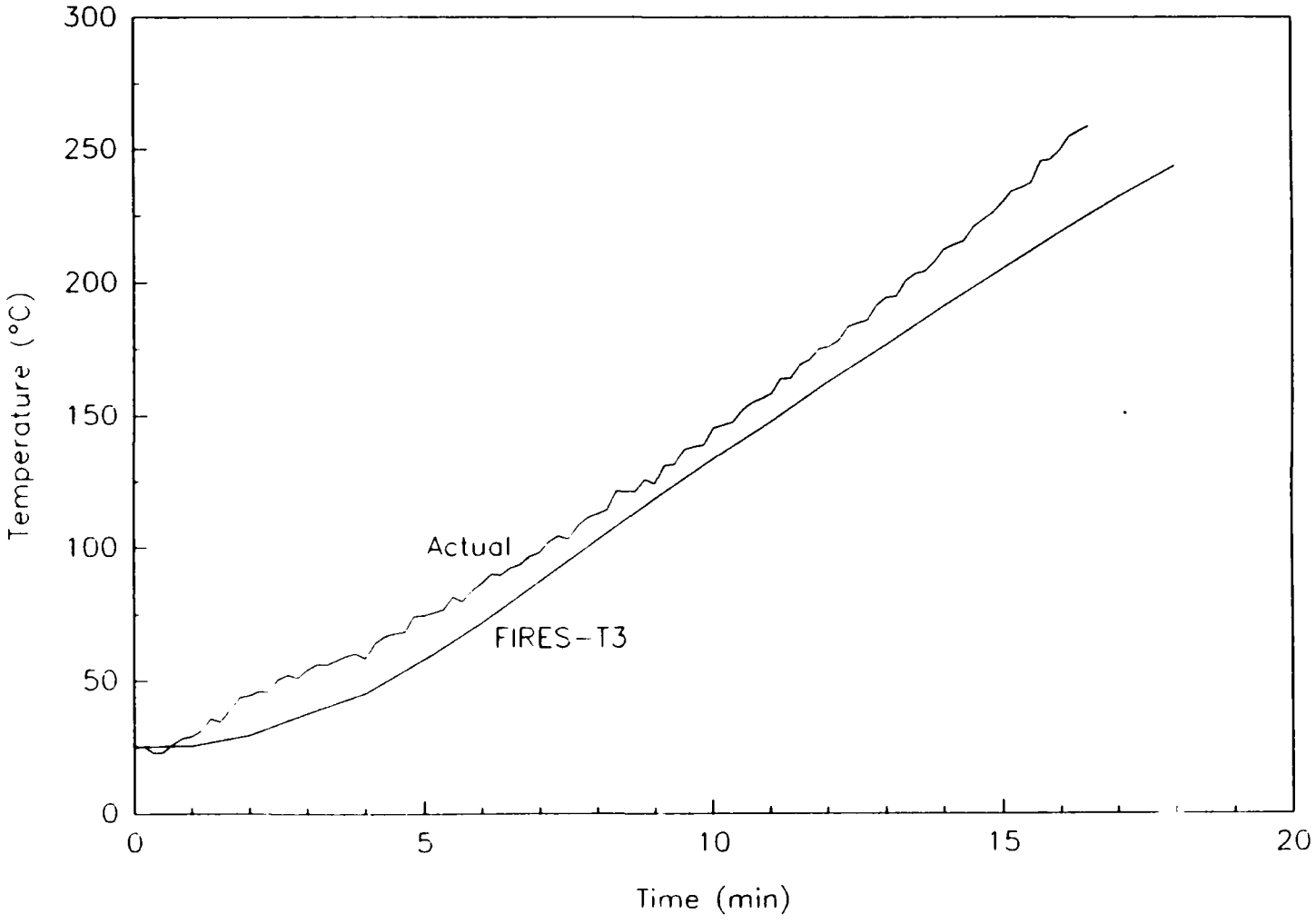

Fig. B17 - Predicted vs. actual steel insert temperatures, 3.2 cm (1.3 in) Manville insulation from Ins_10

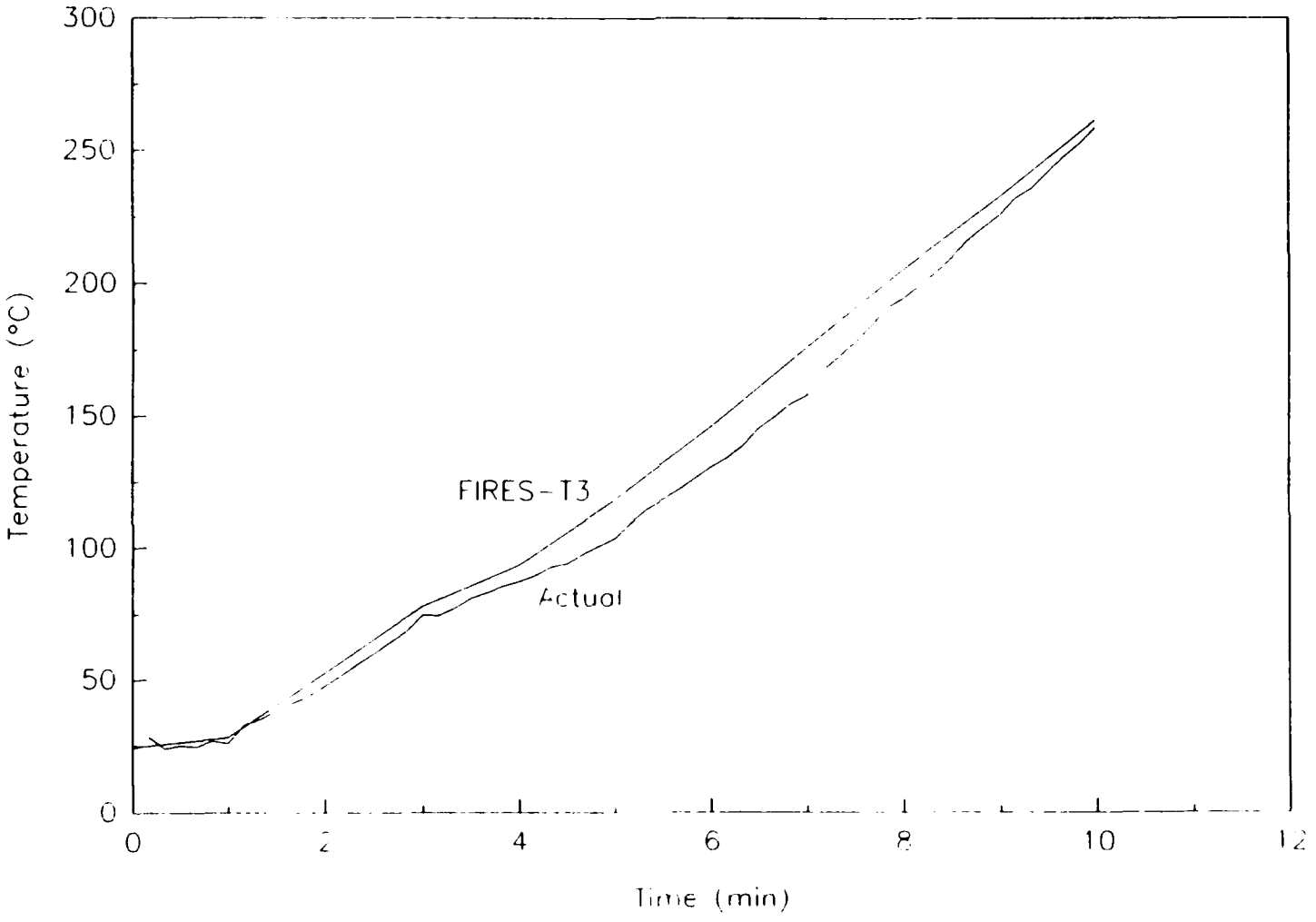

Fig. B18 - Predicted vs. actual steel insert temperatures, 1.9 cm (0.75 in) mineral wool insulation from Ins_12

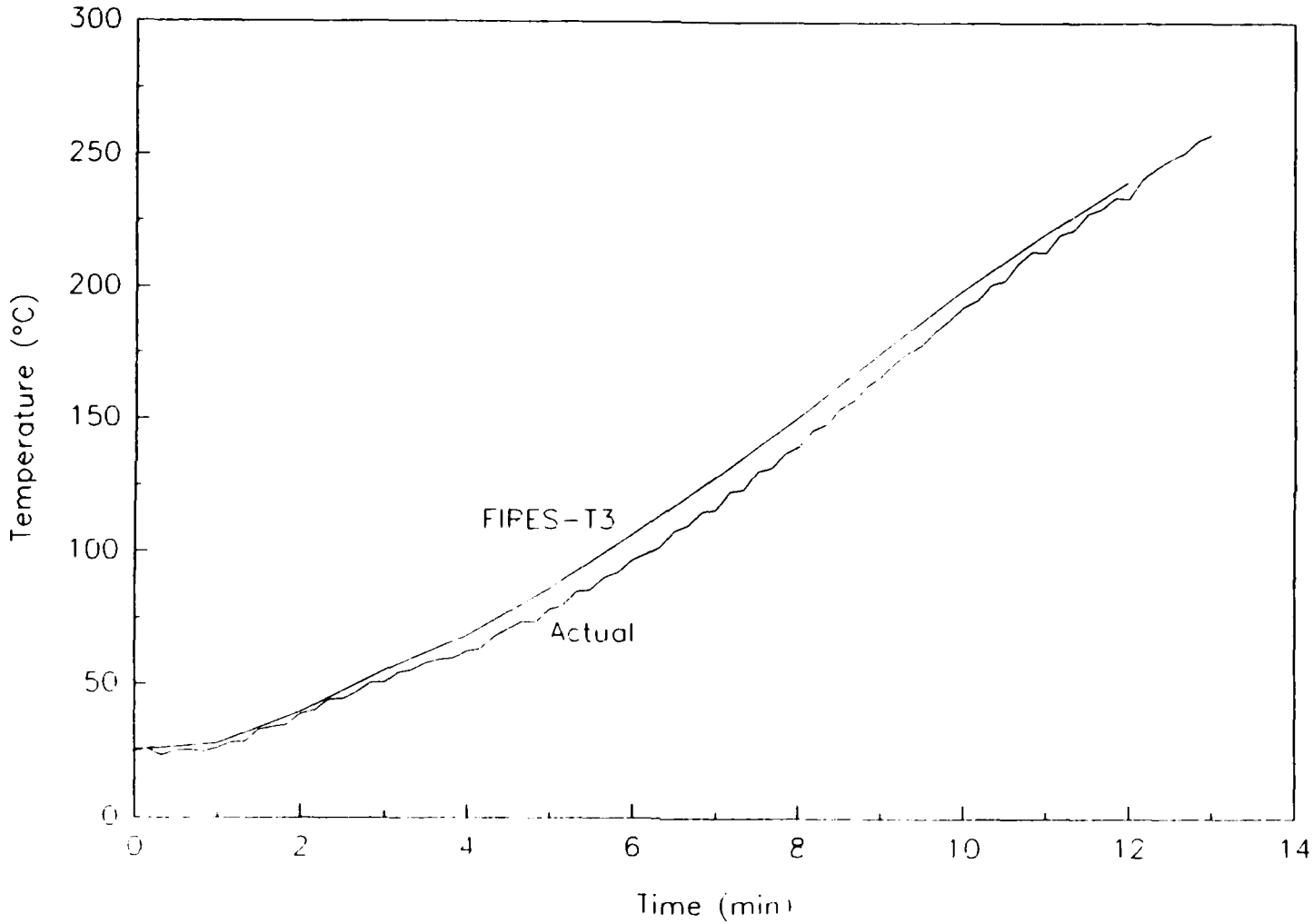

Fig. B19 - Predicted vs. actual steel insert temperatures, 1.9 cm (0.75 in) mineral wool insulation from Ins_13

Table B9 - Actual and Predicted Failure Times

Test	Actual time (minutes)	Predicted time (minutes)	% difference between actual and predicted
Ins_8 (1 layer Manville)	8.7	7.8	-10.3
Ins_9 (2 layers Manville)	14.6	16.1	10.3
Ins_10 (1 layer Manville))	9.0	8.0	-11.1
Ins_10 (2 layers Manville)	15.1	16.2	7.3
Ins_12 (mineral wool)	9.2	9.0	-2.2
Ins_13 (mineral wool)	11.7	11.5	-1.7

The temperature of the fire exposure (furnace temperature) at the front face of the insulation (three thermocouples), the unexposed air temperature (one thermocouple) and the backside steel temperature (six thermocouples) were recorded at VTEC. The temperatures were reported at two minute intervals. The exposure temperatures and the steel temperatures used in this appendix are averages, which exclude highly erratic data.

The convection boundaries used were identical to those imposed for the Kaowool modeling for the exposed and unexposed boundaries:

$$Q''_{conv} = 1.64 \cdot (T_{fire} - T_{surf})^{1.25} \qquad \text{(B18)}$$

The radiation boundary conditions were the same as those used in the SHADWELL models. The material property data was assumed to be the same as the mineral wool and Manville materials used in the SHADWELL tests.

The results of the three VTEC tests and the predictions of FIRES-T3 for the backside steel temperatures are compared in Figs. B20-22. Table B10 compares the actual and predicated times to reach a steel temperature of 232°C (450°F).

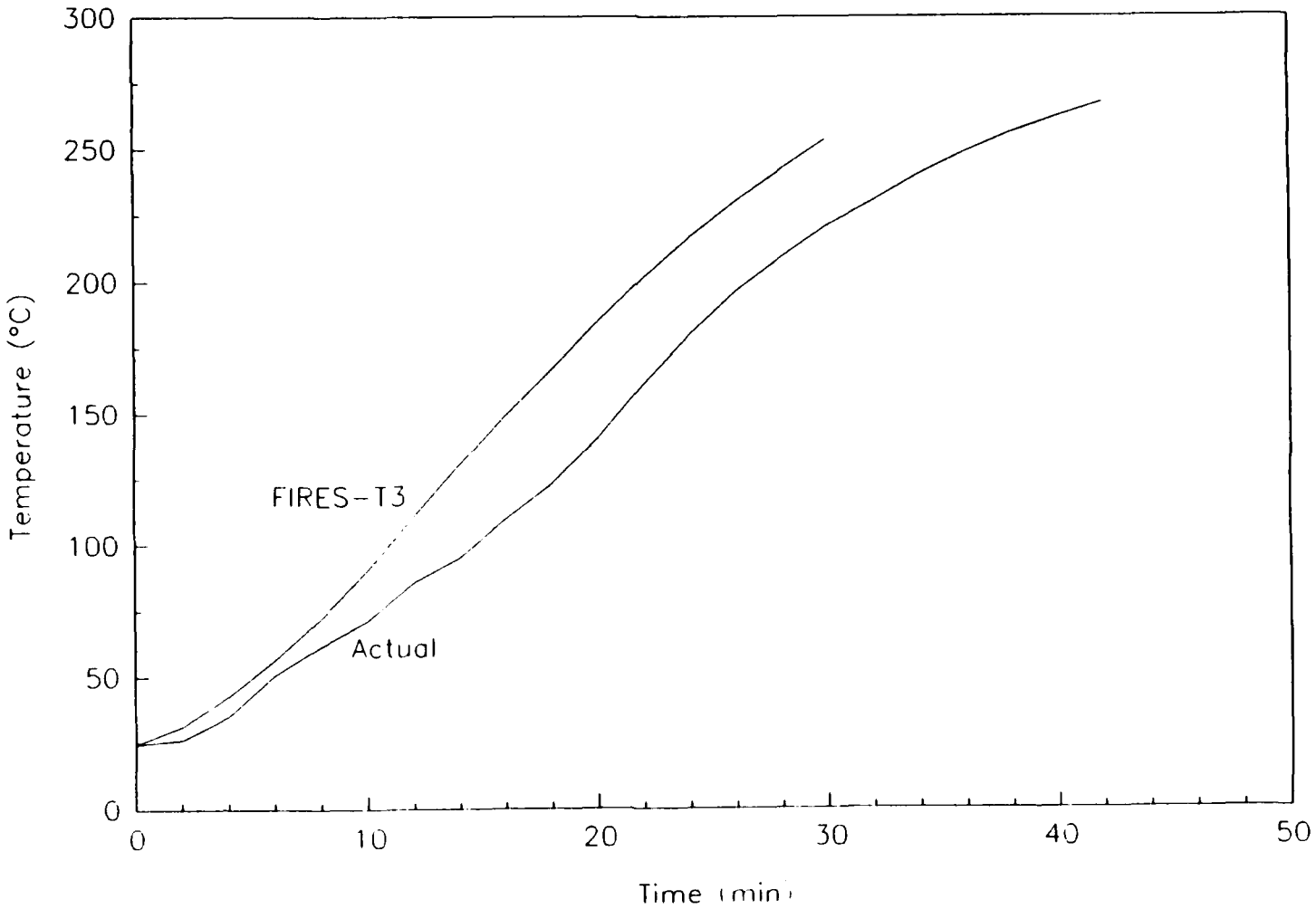

Fig. B20 - Predicted vs. actual steel insert temperatures, 2.5 cm (1 in) mineral wool insulation (Ref. B16)

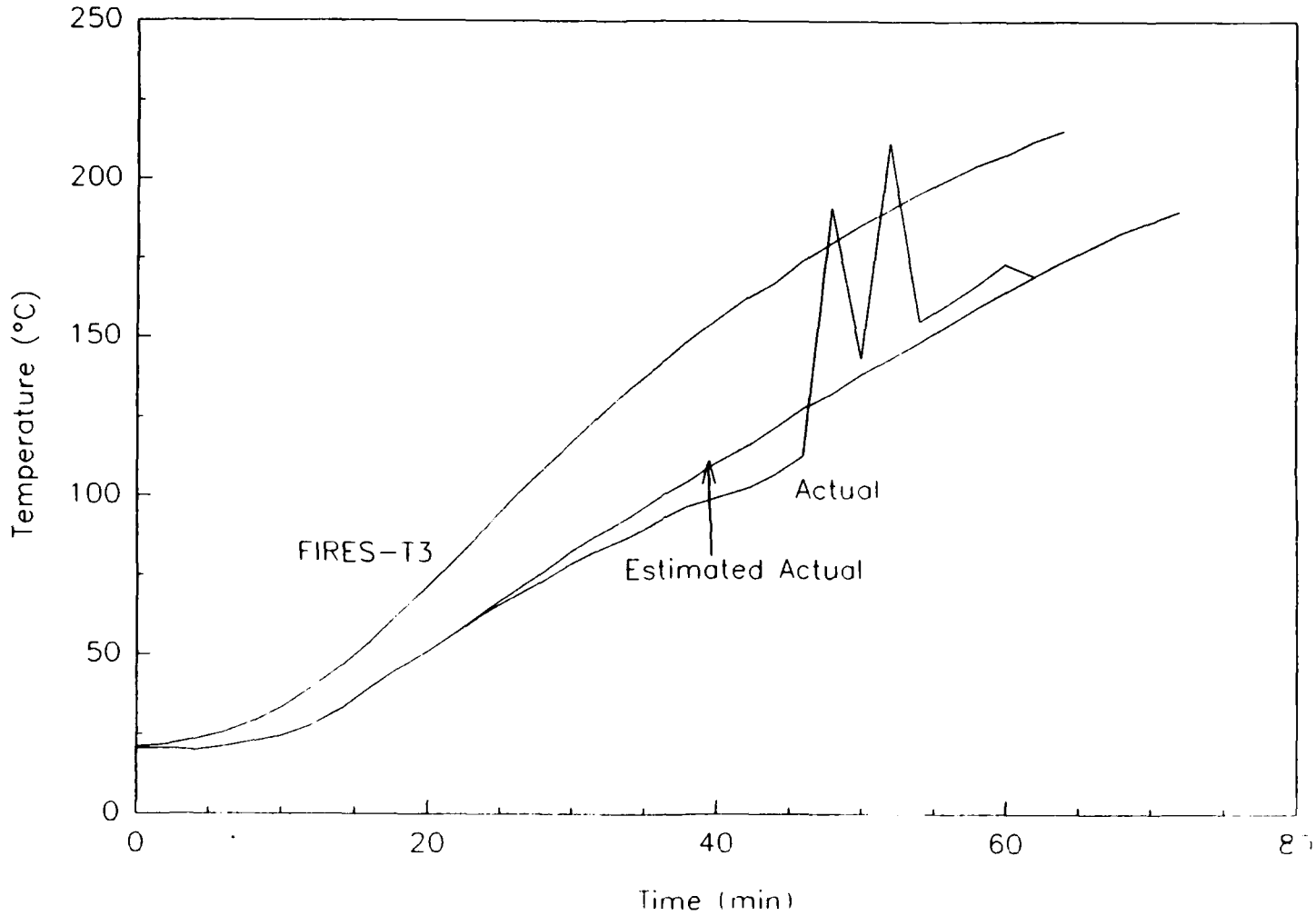

Fig. B21 - Predicted vs. actual steel insert temperatures, 5.1 cm (2 in) mineral wool insulation (Ref. B16)

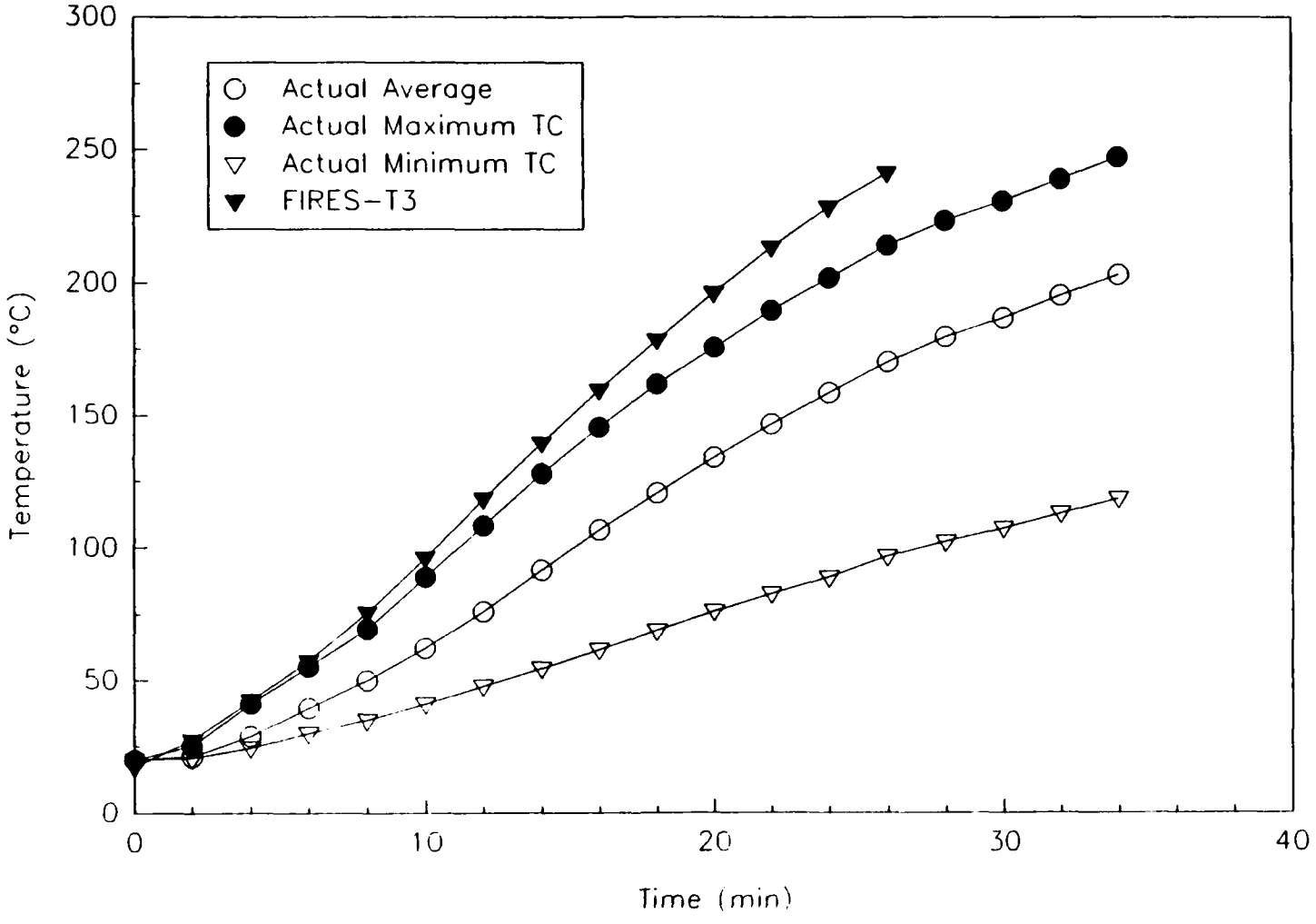

Fig. B22 - Predicted vs. actual steel insert temperatures, 2.5 cm (1 in) Manville insulation (Ref. B16)

Table B10 - Actual and Predicted Failure Times

Test	Actual time to 232°C (minutes)	Predicted time to 232°C (minutes)	% difference between actual and predicted
2.54 cm mineral wool	31.5	25	-20.6
5.08 cm mineral wool	77	64	-16.9
1.91 cm Manville	34	24	-29.4

FIRES-T3 under-predicted the steel temperatures for the VTEC tests in all the cases by about 20 percent. The consistency in the relative magnitude of the failure predictions indicates a systematic error with the modeling parameters used in FIRES-T3. An explanation of the under-predicted values may be attributed to one or more of the following: the thermal properties of the VTEC materials may have been different than those used on the SHADWELL; the reported nominal thicknesses may not have been the actual thicknesses; the emissivity of the furnace may not have been unity; and possible errors in the thermocouple readings taken during the tests. For example, the nominal thickness of the mineral wool and Manville materials tested in the SHADWELL were substantially different (see section B3.1). Attempts to model the SHADWELL data with the nominal thickness resulted in significantly different steel temperature predictions.

Fig. B23 shows the individual thermocouple readings for the steel temperature for the VTEC 1.91 cm Manville test. Even when the erratic thermocouple are ignored, there is over a ten minute difference in the time to reach 232°C (450°F) in the steel. The difference suggests that there is a highly irregular temperature distribution in the steel plate. Such irregularities may be caused by any number of local insulation disturbances, such as damage during installation or localized compression. Such conditions are impossible to model without further information. Further, since the extent of the localized conditions were unknown, the average temperature distribution may not be indicative of ideal material conditions. Thus, the predictions of FIRES-T3 fall within the uncertainty of the local conditions of the insulation. Localized deviations in the exposure temperatures was not considered a factor because all of the VTEC thermocouples for each test were within 5°C (9°F) of each other.

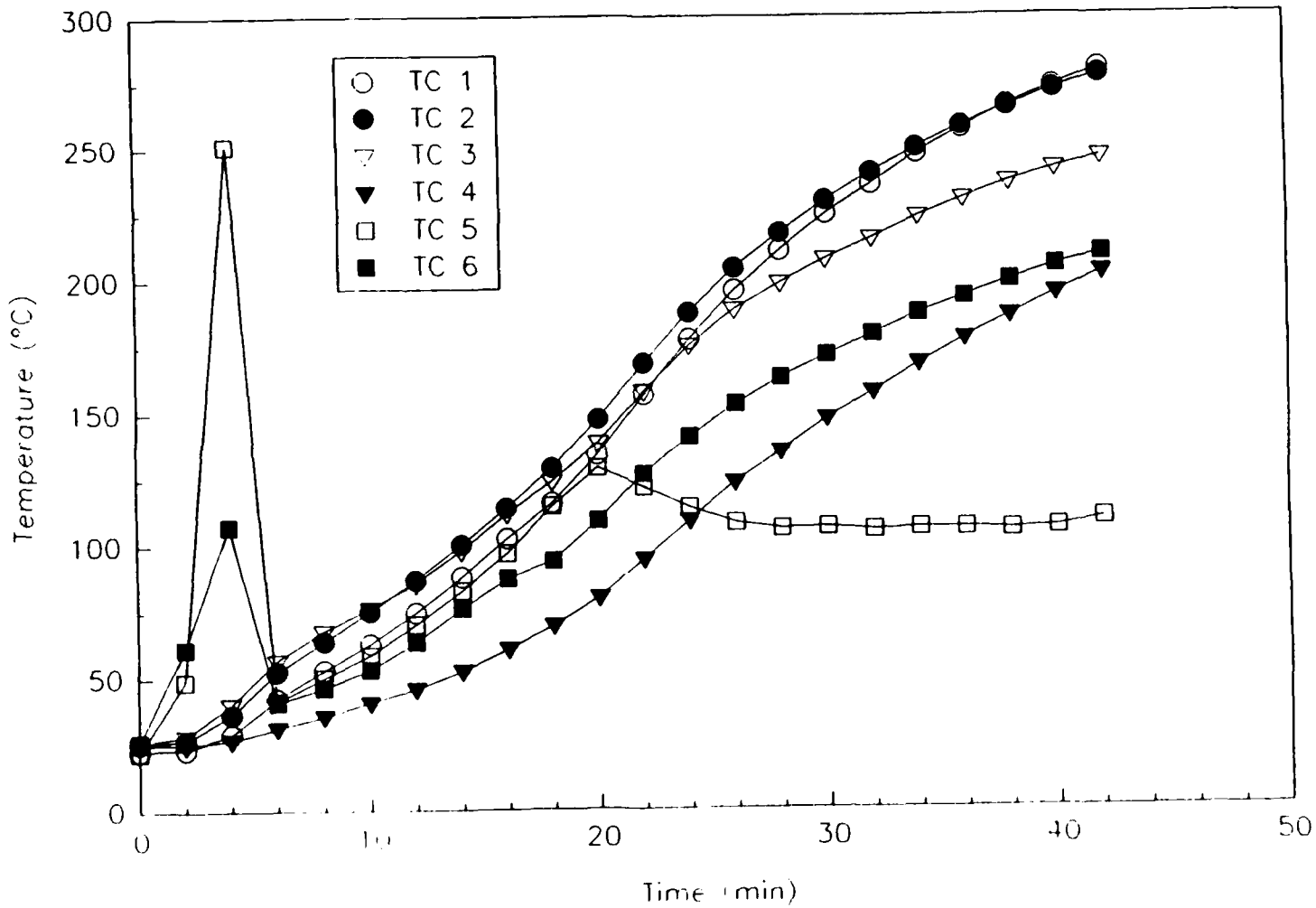

Fig. B23 - Individual thermocouple recordings for steel temperature, 2.5 cm (1 in) Manville insulation (Ref. B16)

B4.0 SENSITIVITY ANALYSIS

A sensitivity analysis was performed to determine the effects of eleven variable parameters in FIRES-T3. The variable parameters were actual insulation thickness, insulation conductivity, insulation density, insulation heat capacity, steel thickness, exposure radiation boundary conditions, exposure convection parameters, fire exposure temperature, mesh size/node density, the convergence criteria, and material loss during test. All of these parameters may cause large variations in the model solution depending on the amount of uncertainty in the parameter. The material properties of the steel are well known; thus, they were not varied. The sensitivity analysis was performed for the SHADWELL fire test conditions. Consequently, the results were only applicable to tests with similar configurations and materials and may change for other types of heat transfer analyses. Except for the variable being considered, all parameters are held constant using the values described in section B3.2.

Ins_8 with one layer of Manville was the only SHADWELL test used to observe the effects of varying the parameters. The results of a similar analysis on the other tests are expected to be analogous.

B4.1 Effect of the Material Thickness

The nominal thickness of one layer of the Manville insulation was 2.54 cm (1 in.) and the actual thickness was measured at 1.59 cm (0.625 in.). FIRES-T3 was run for the following thickness variations of the Manville: 1.27, 1.59, and 2.54 cm (0.5, 0.625, and 1 in.) respectively. The results of the variation in the thickness on the backside steel temperature are shown in Fig. B24. There is a substantial difference in the temperature predictions that arise from only changing the thickness. At ten minutes, the temperature of the steel ranges from 352°C (665°F) to 212°C (414°F). The actual temperature of this test (Ins_8) at ten minutes was 280°C (536°F).

B4.2 Evaluation of the Effect of the Insulation Thermal Conductivity

The thermal conductivity deduced for the Manville insulation was shown in Fig. B12. The values from Fig. B12 were altered by factors of 0.75 and 1.25. Conductivity was also evaluated as a constant "mean" conductivity, averaged over the range of possible temperatures (room temperature to 1100°C). This mean is the conductivity at 815°C (1500°F). The steel temperature curves that result from the conductivity variations are shown in Fig. B25.

Fig. B25 indicates that even small variations in the conductivity curve can substantially alter the predicted steel temperatures. The predicted steel temperature at ten minutes ranged from 247°C (476°F) to 384°C (724°F). Accurate conductivity data for an insulation is an important parameter for the model.

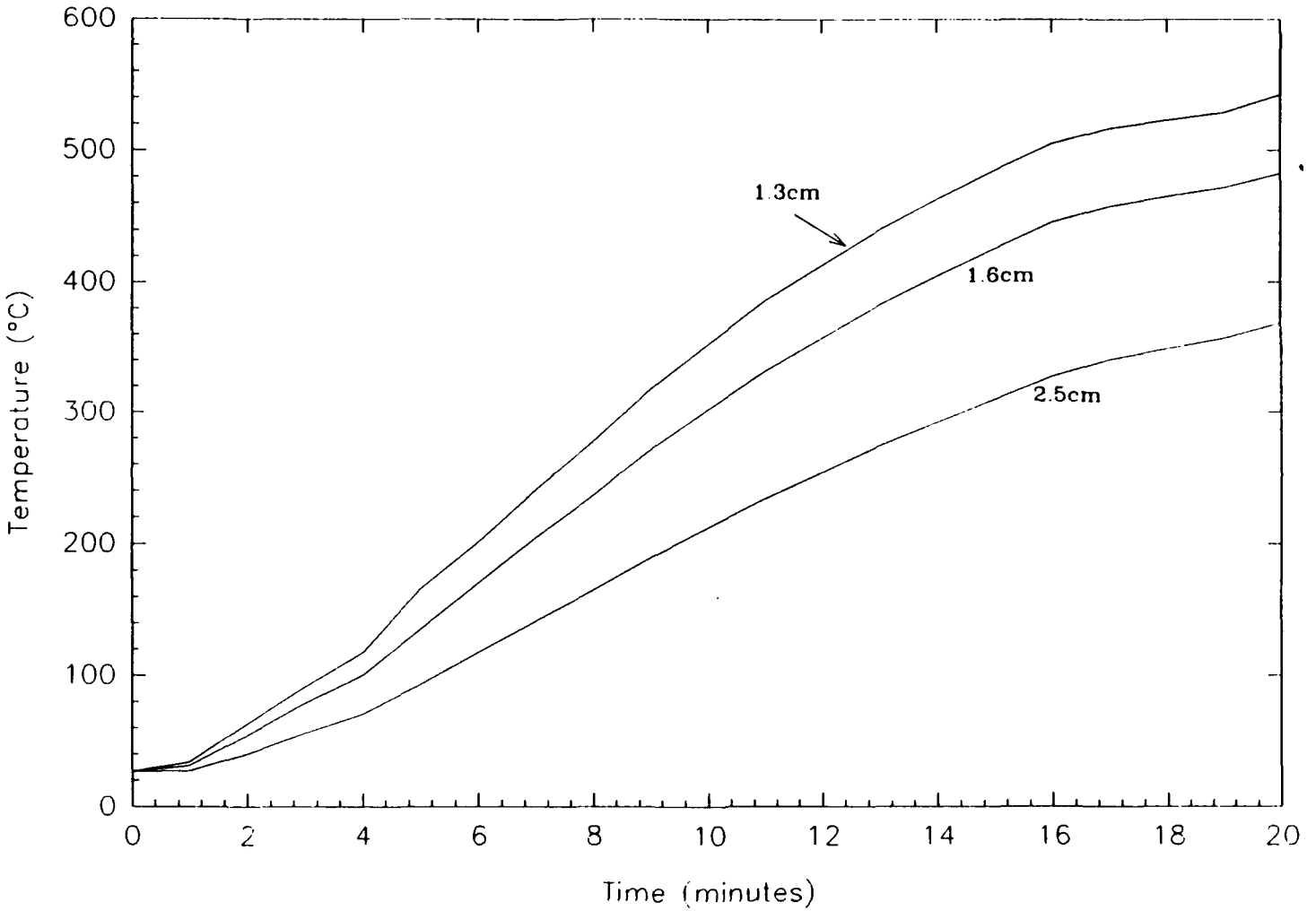

Fig. B24 - Effect of insulation thickness on steel insert temperature predictions

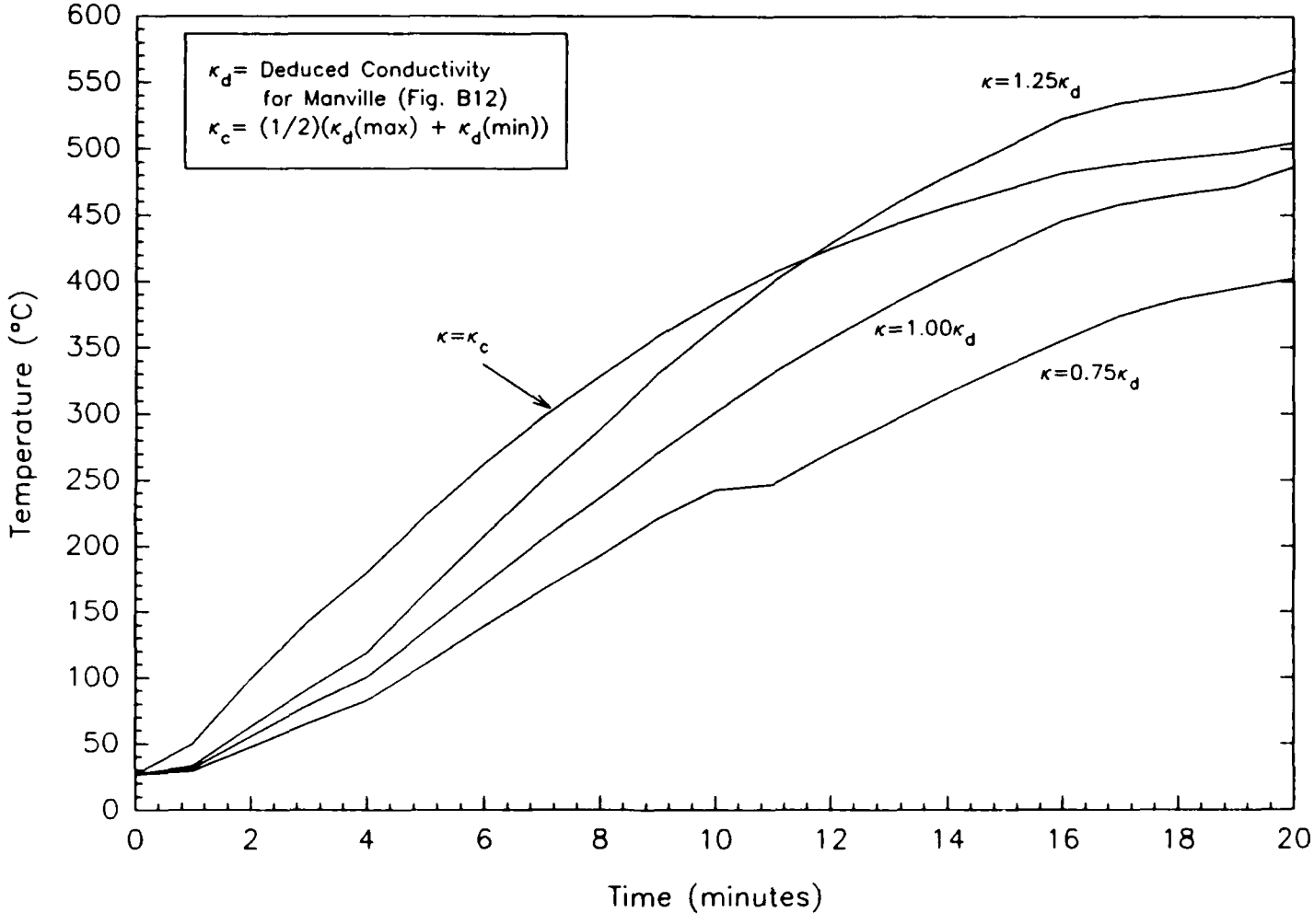

Fig. B25 - Effect of insulation thermal conductivity on steel insert temperature predictions

B4.3 Effect of the Insulation Density on the Temperature Predictions

The actual density of the Manville insulations tested on the SHADWELL was 16 kg/m^3 (3.52 lb/ft^3) without the facing material. The density impact was evaluated by altering the actual density by 50 percent (for a range of 8 kg/m^3 (1.76 lb/ft^3) to 24 kg/m^3 (5.28 lb/ft^3)). The results are shown in Fig. B26. The impact of the insulator density is not significant. A measured density within 50 percent of the actual value is well within the expected range that may occur due to experimental error. The relative significance of the density may increase as the thickness of a material decreases. For very thin sheets of insulation, a sensitivity analysis should be performed to determine the required precision of the density value. One layer of Manville insulation was the thinnest insulation tested on the SHADWELL, which was thick enough so that density was not a significant factor in the thermal analyses of these tests.

B4.4 Evaluation of the Impact of the Material Heat Capacity

Closely related to the density in a heat transfer analysis is the heat capacity (see eqs. B2 and B3). It is the integral of the product of the density and heat capacity with respect to temperature that determines the quantity of energy stored in a given material for a given temperature increase. Thus, alterations in the heat capacity should produce the same results as comparable alterations in the density.

The heat capacity was varied by ± 50 percent. Another variation included a sharp increase in the heat capacity at 100°C (212°F) to simulate moisture content. The results are shown in Fig. B27. The heat capacity had the same impact as the density. As with the density, the material thickness may increase the effect of the heat capacity. The reaction at 100°C (212°F) did not significantly alter the results.

B4.5 Evaluation of the Impact of the Steel Thickness

The steel thickness was varied by ± 33 percent. The actual steel thickness was 4.764 mm (0.1875 in.) and the variation ranged from 3.176 mm to 6.352 mm (0.125 to 0.25 in.). The results are shown in Fig. B28. The actual steel thickness has a significant influence on the backside steel temperature. The thickness is important because steel has a high product of the density and heat capacity. Steel is also an excellent heat conductor causing it to be essentially at a uniform temperature at all times for the steel thicknesses under consideration. FIRES-T3 predicted a steel temperature variation that never exceeded 0.4°C (0.7°F), which confirmed that the steel is approximately at a uniform temperature. Consequently, the amount of energy stored per unit volume and unit temperature rise is high and the steel acts as a significant heat sink.

B4.6 Evaluation of the Impact of the Radiation Boundary Condition Parameters

The user specified radiation parameters are the radiation configuration factor, insulation surface emissivity, and the surface absorbtivity. The radiation configuration

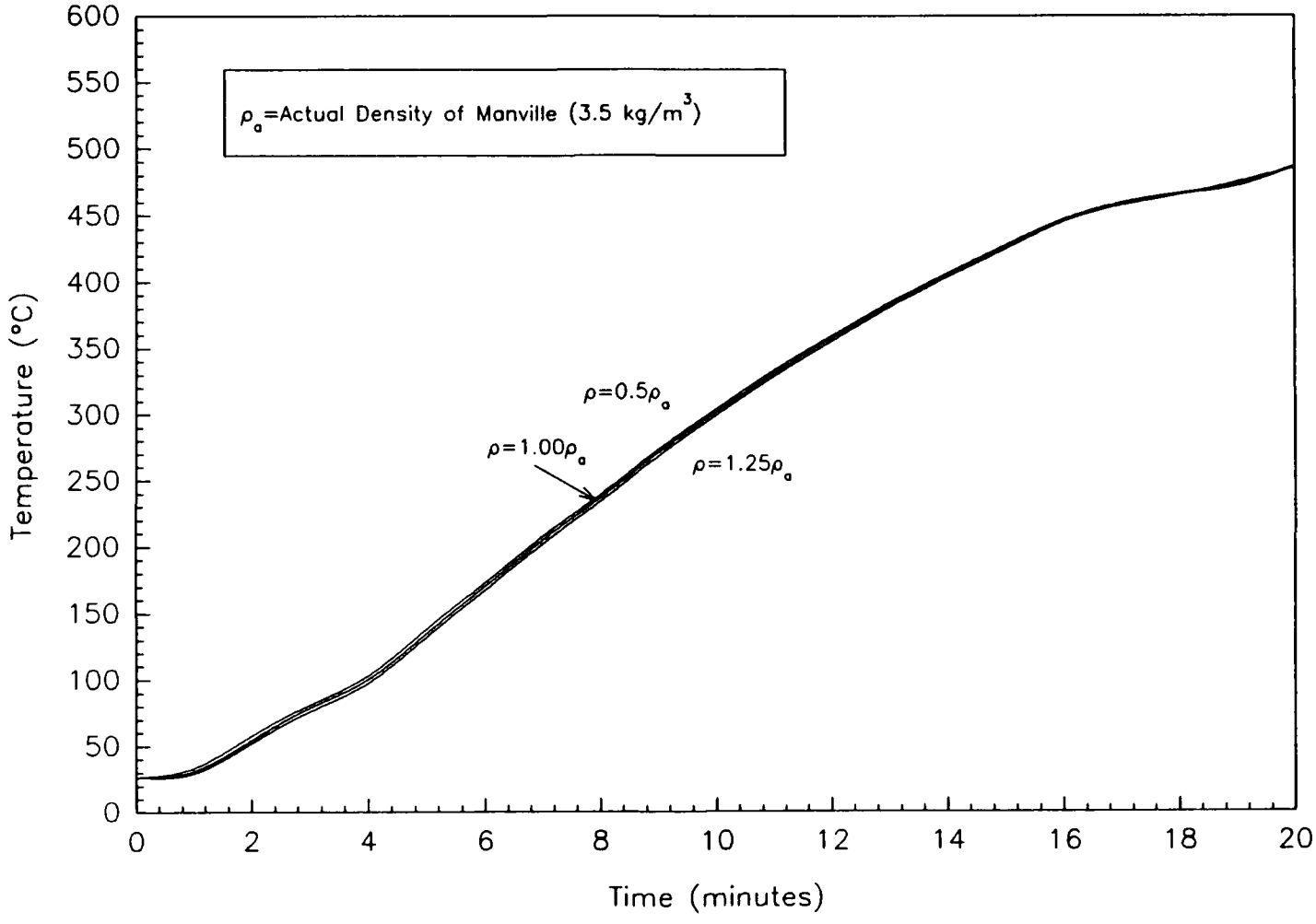

Fig. B26 - Effect of insulation density on steel insert temperature prediction

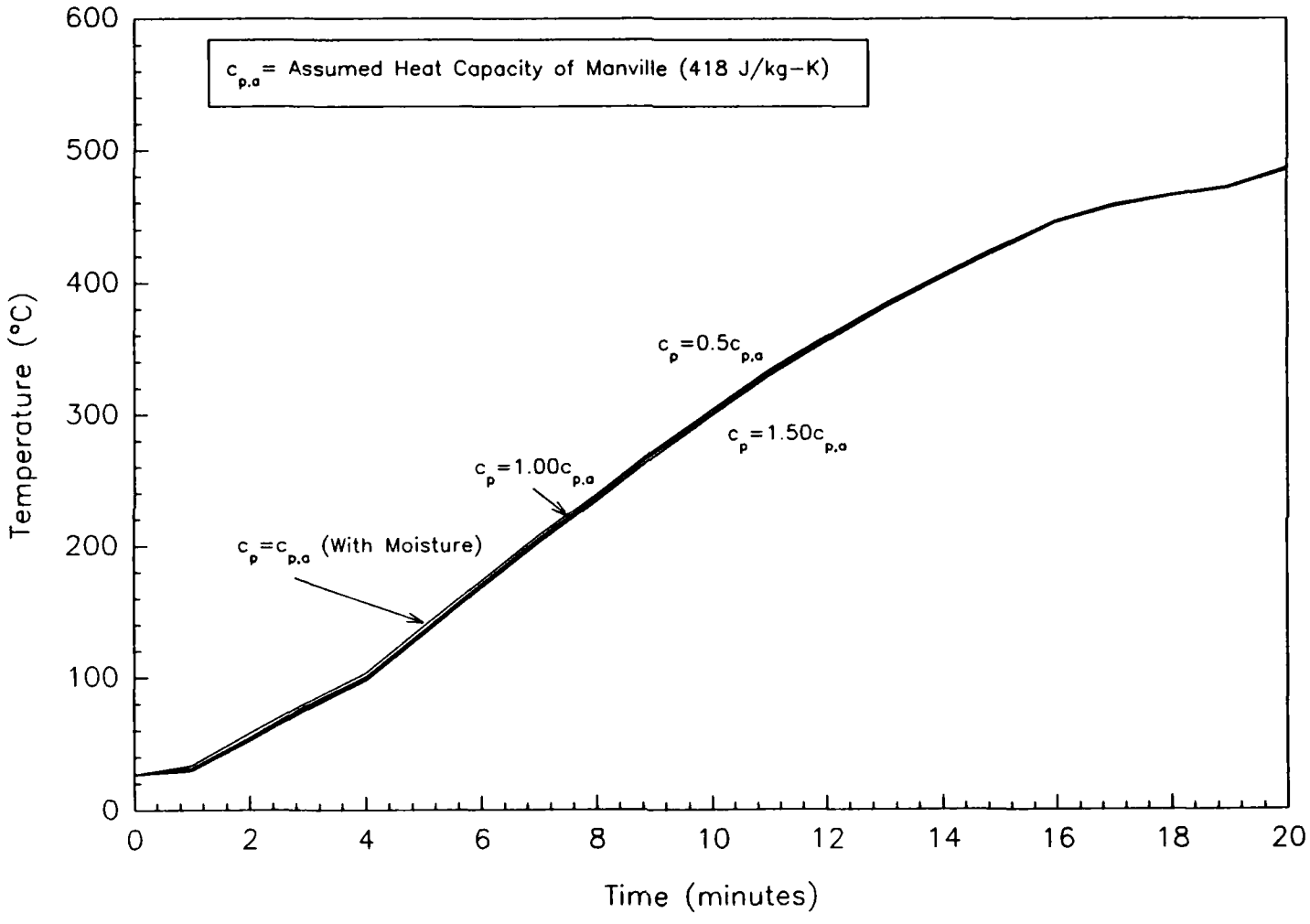

Fig. B27 - Effect of insulation heat capacity on steel insert temperature prediction

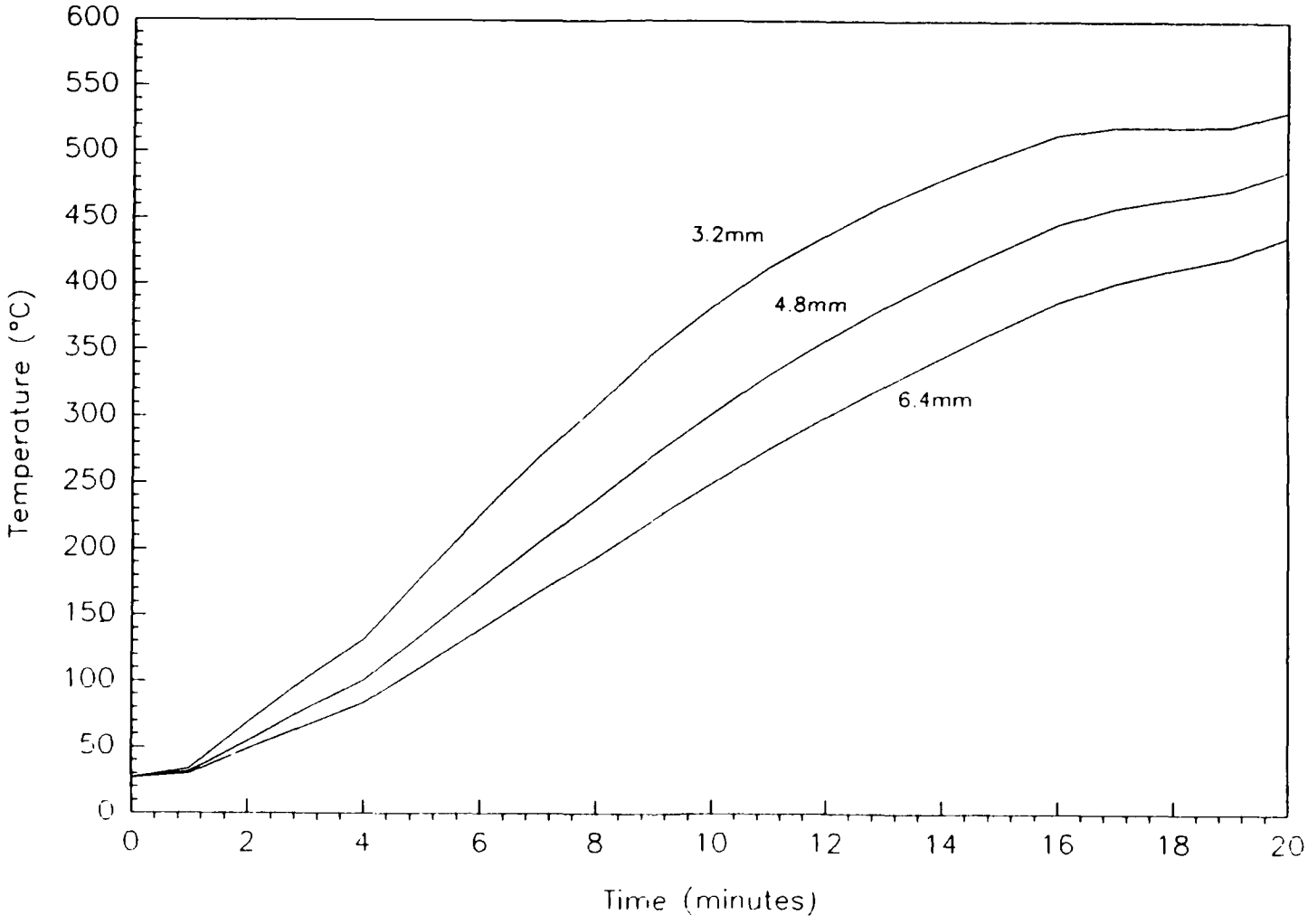

Fig. B28 - Effect of steel thickness on steel insert temperature prediction

factor in the SHADWELL tests was 1.0 due to flame impingement. The surface emissivity and absorbtivity, usually considered equivalent (Kirchoff's Identity, see Ref B6), were assumed to be 0.8, a typical value for fiberglass. The emissivity can be temperature dependent, especially if soot is deposited on the surface during the test (Refs. B6 and B15). FIRES-T3 does not permit temperature dependent emissivities and absorbtivities; thus, it requires an estimation. In this evaluation, the emissivity and absorbtivity are varied between 0.5 and 0.95. Because the emissivity and absorbtivity are equal, an equivalent change in the radiation configuration factor will have the same effect (see eq. B5)

The results of altering the radiative properties are shown in Fig. B29. The impact of the radiation properties of the insulation is not significant for the range of emissivity and absorbtivity between 0.5 and 0.95. The emissivity and absorbtivity of the insulation is likely to be at least 0.8, further reducing the expected uncertainty due to these parameters. The impact of altering the steel radiative properties is comparable and similar results would be expected.

B4.7 Effect of the Convective Parameters

The convection parameter, β in eq. B4, was altered in four ways. The heat transfer coefficient, h_c, was not altered because the convection equation is dominated by the exponent. The exponent varied between 1.0 and 1.4. For a temperature difference of 27.8°C (50°F), a β value of 1.4 would have an equivalent convection heat transfer coefficient five times greater than a β value of 1.0. The results of FIRES-T3 indicated that there was never more than a 0.6°C (1.1°F) temperature difference between any of the steel temperature predictions.

B4.8 Effect of Actual Temperature Exposure

The impact of the actual exposure temperature was investigated by using exposures from different insulation tests that were more and less intense than Ins_8 exposure. Specifically, the exposures from Ins_12 (hotter) and Ins_9 (cooler) were used as input fire exposures (Fig. B13).

The results shown in Fig. B30 indicate that the correct exposure curve is an important factor. The exposures were not substantially different, but the steel temperatures at ten minutes ranged from 260°C (500°F) to 302°C (575°F). The practical application for these tests is to select appropriate thermocouple measurements. This was addressed in these tests by installing thermocouples directly under each insert.

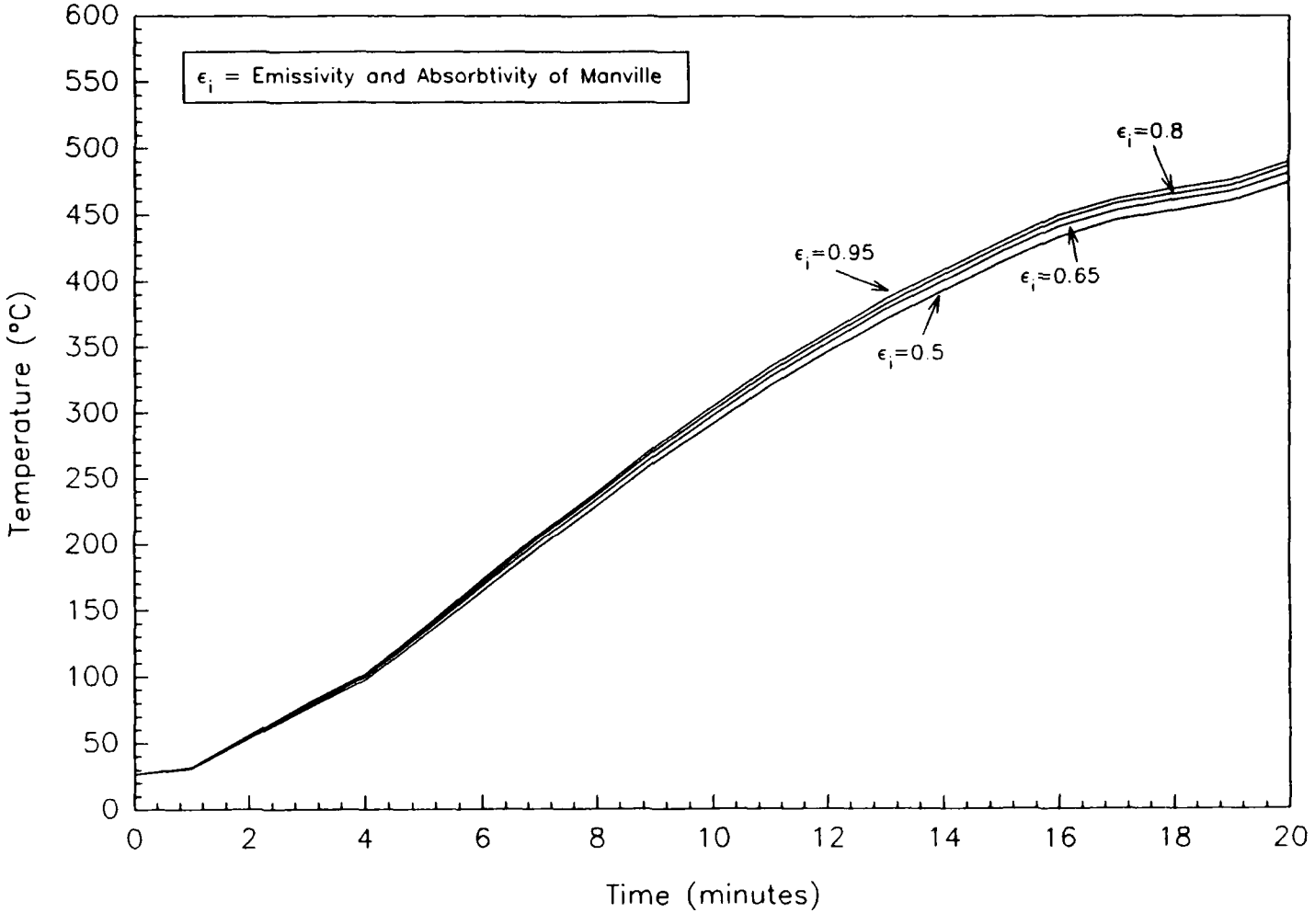

Fig. B29 - Effect of insulation radiation parameters on steel insert temperature prediction

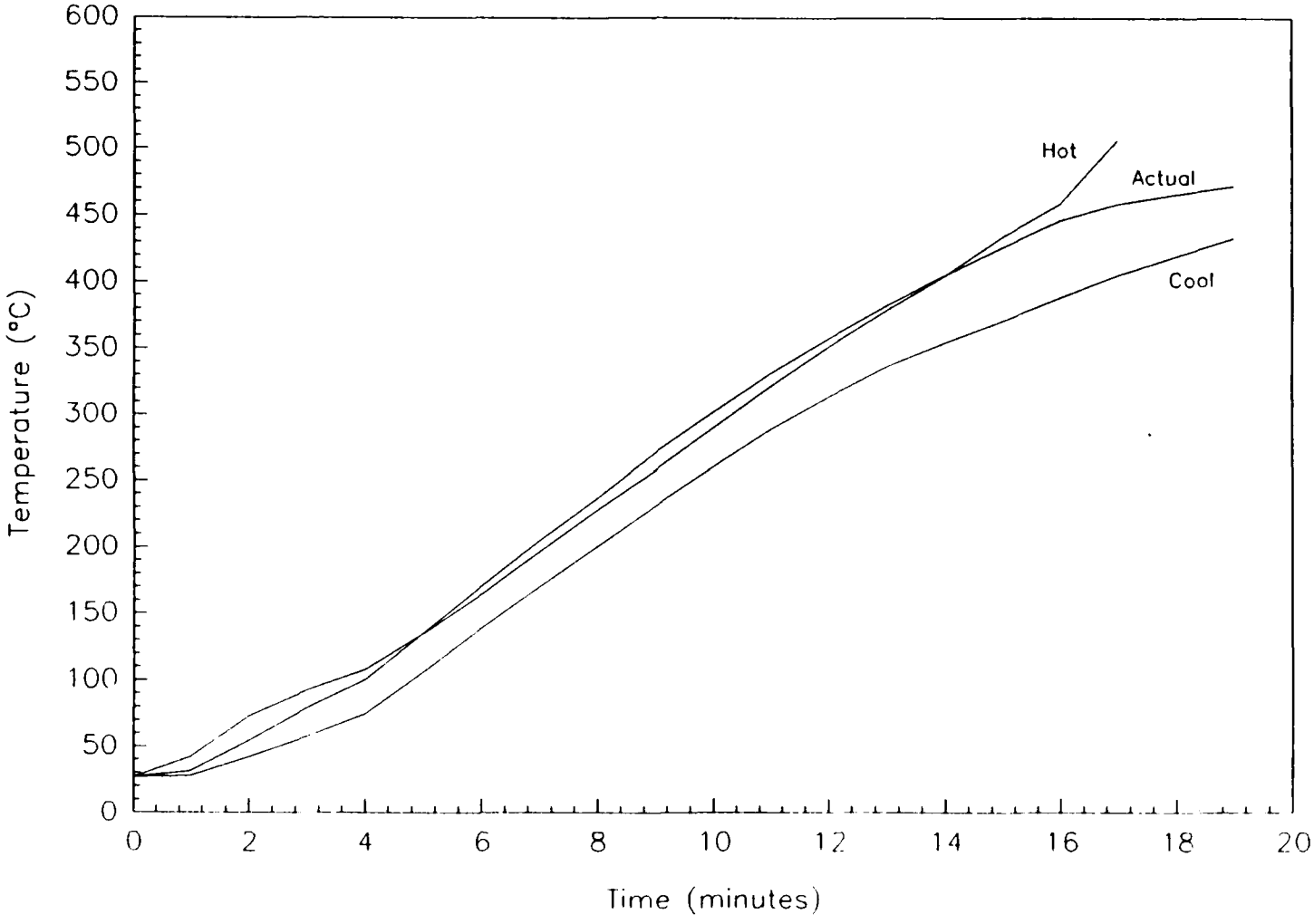

Fig. B30 - Effect of exposure curve on steel insert temperature prediction

B4.9 Mesh

The basic mesh for all the SHADWELL models was 40 equally spaced nodes in the insulation and 10 equally spaced nodes in the steel. The node selection in the steel was assumed adequate because FIRES-T3 predicted a nearly uniform steel temperature, as expected. The mesh was consequently only altered in the insulation. The mesh size was reduced so that 3,5,10,and 20 and the original 40 nodes were used through the insulation.

The effects of the mesh density are shown in Fig. B31. The additional refinement in the steel temperature predictions is indistinguishable for insulation mesh sizes greater than 10 nodes. The selection of mesh density is a matter of refining the mesh until further node additions do not change the temperature predictions significantly.

B4.10 Timestep and Iteration Error

The timestep and the maximum iteration error are user-specified in FIRES-T3. The timestep is a time increment over which FIRES-T3 seeks a solution to the heat transfer equations. Whenever a timestep is specified, the boundary conditions may be updated (the exposure temperatures). The iteration error is the maximum ratio allowed for the temperature difference between two iterations and the average temperature for the two iterations. The iteration error and the timestep are related to the total error per timestep by the maximum number of iterations per timestep.

It was briefly shown in Section B2.1 (See Fig. B7) that the timestep makes a difference when the desired solution is close to the timestep. Although the inaccuracy was not significant, it was noticeable. The inaccuracy was eliminated by selecting a more refined timestep.

The SHADWELL models used a timestep of 10 seconds. In this section, the timestep is varied from 10 seconds to 40 seconds. The results are shown in Fig. 32. The timestep does not have a large effect in the SHADWELL models, especially near the end of the model run, for the values chosen. A timestep greater than 40 seconds would be impractical because the refinement in the exposure curve is lost. Like the mesh density, a suitable timestep can be determined by reducing the timestep until the variation in the solution is less than a specified value.

The iteration error was varied to address the impact of improper selection. The ratio used in the SHADWELL models was 0.0002 for the boundary conditions and 0.002 for the entire system (used for non-linear material properties). In this section, the boundary condition ratio was altered. Similar results would be anticipated for the system iteration error ratio.

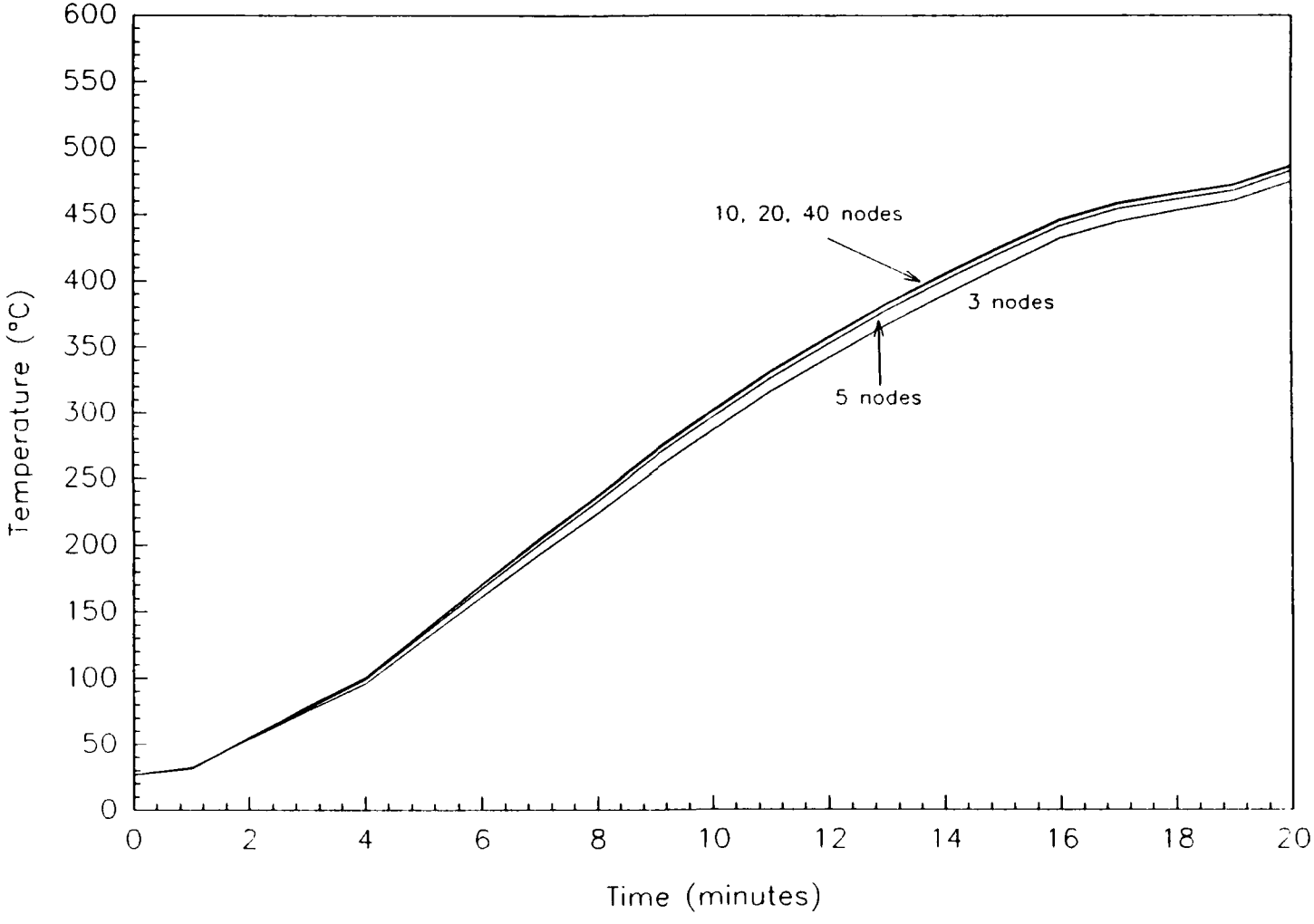

Fig. B31 - Effect of insulation mesh density on steel insert temperature prediction

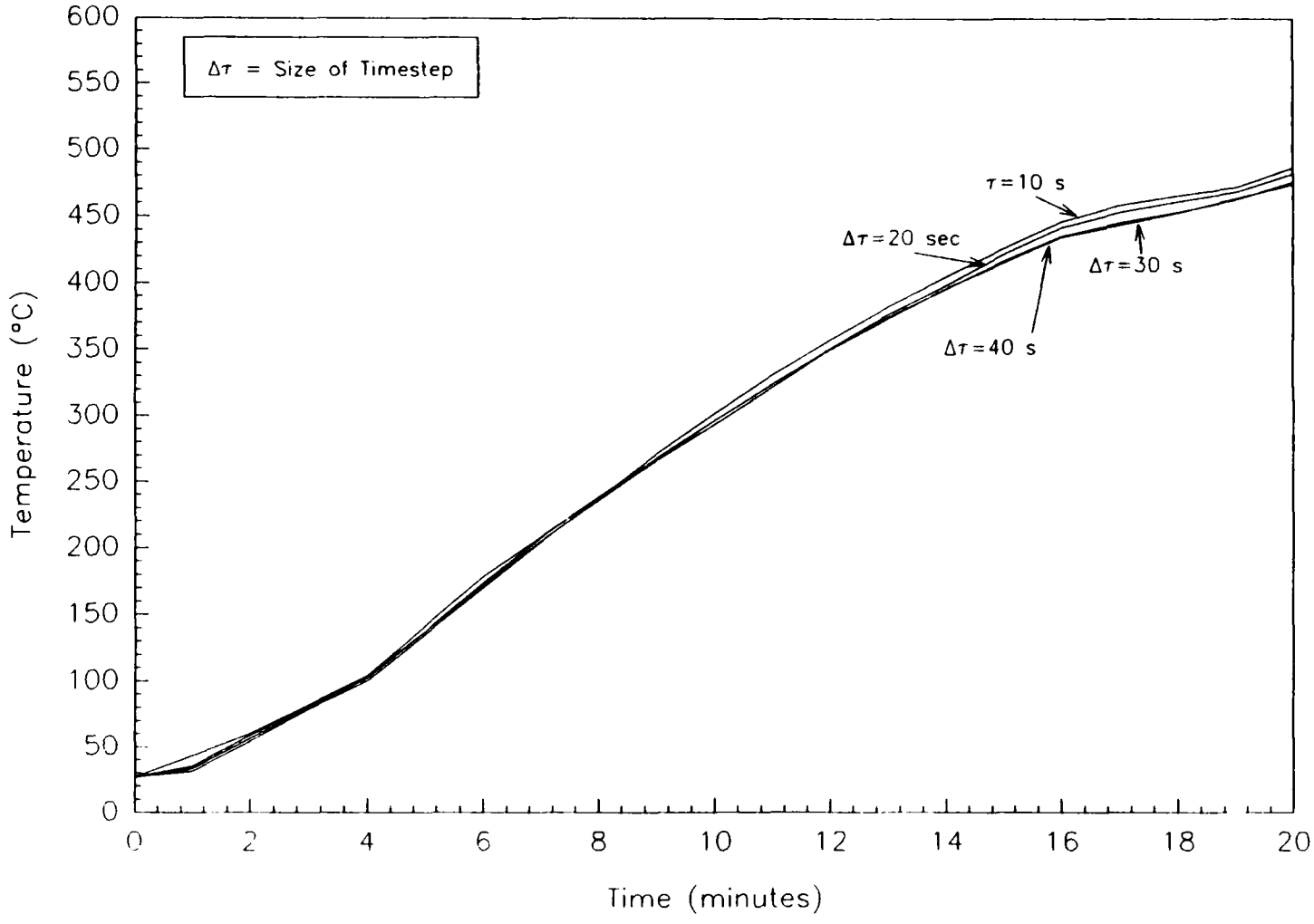

Fig. B32 - Effect of the timestep on steel insert temperature prediction

Three different ratios were evaluated: 0.2, 0.02, and 0.002. The effects are plotted in Fig. B33. The error ratio had little effect on the temperature predictions for the range used. Like the mesh density and the timestep selection, a suitable iteration error can be determined by refining it until the solution remains constant to an acceptable degree.

The combined effects of the error ratio, mesh density, and timestep may yield significant error if they are all improperly selected. Thus, it is worthwhile in such an analysis to ensure each component is properly refined.

B4.11 Effect of Material Loss During Test

Material loss during a test (as observed in some mineral wool tests) was simulated by using the temperature distribution in the insulation at an assumed time of material separation as the initial condition in a new model. One half of the insulation was assumed to fall away at 2, 4, and 6 minutes into the test. The insulation thickness in the new model was reduced by one-half and the temperature distribution in remaining material was used as the initial condition. The results are shown in Fig. B34. At the instant the material is lost, FIRES-T3 predicts that the rate of temperature rise on the backside of the steel insert increases sharply.

None of the backside steel insert temperatures from the actual data had a temperature curve that resembled the ones shown in Fig. B34. Since at the conclusion of some tests material was observed to have fallen off, one of the following may have occurred:

1. none of the thermocouples in the tests were over a spot where material fell off in the time interval of interest;

2. two dimensional effects may have been important, i.e., there may have been lateral heat transfer in the exposed steel which diffused the heat to the cooler, protected steel; and

3. the material fell away gradually, i.e., eroded instead of dropping off in clumps.

The effect of material falling away is an important factor in a heat transfer analysis. Due to the random nature of the variables involved (one versus two dimensional, time, amount), this is perhaps the most difficult aspect of the heat transfer analysis to model.

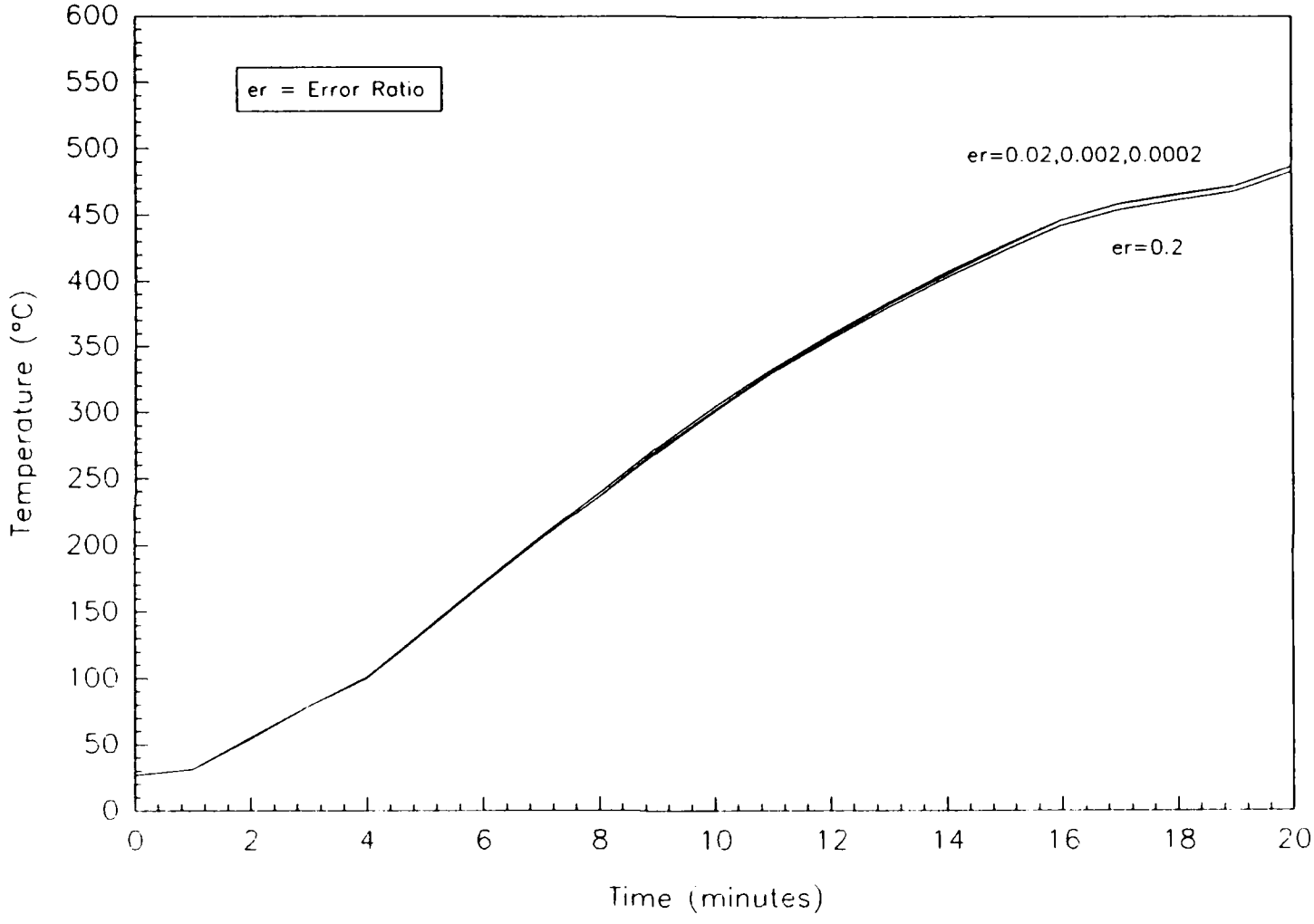

Fig. B33 - Effect of the error ratio on steel insert temperature prediction

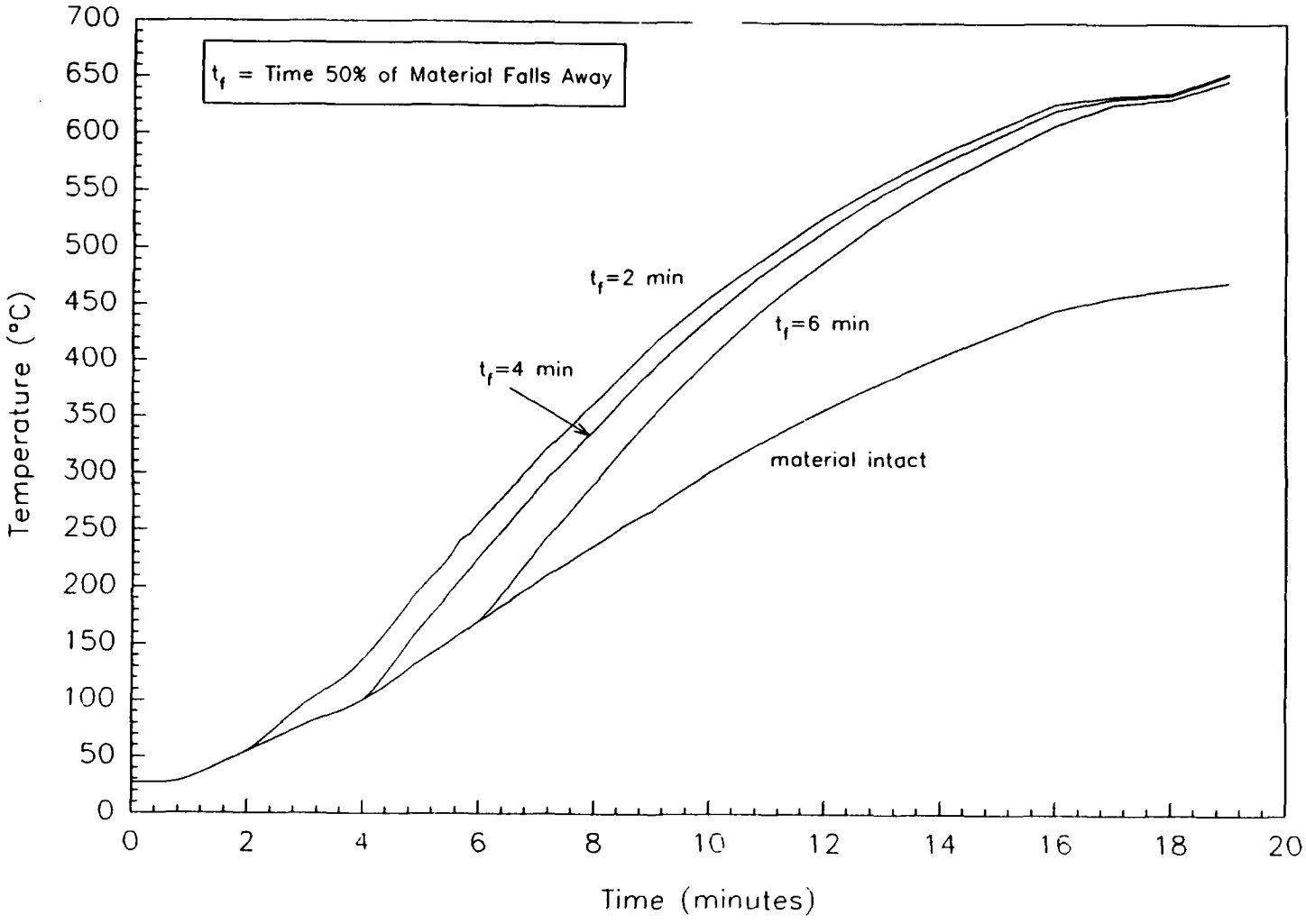

Fig. B34 - Effect of random material loss on steel insert temperature prediction

B4.12 Conclusions of SHADWELL Insulation Test Modeling

Several conclusions may be drawn from the validation of FIRES-T3, the modeling of the Shadwell tests, and the sensitivity analysis.

1. FIRES-T3 is capable of accurately modeling one-dimensional heat transfer problems. It solves the one dimensional heat transfer equations (equations B2 and B3) correctly with the finite element method. The overall results of the program are affected by a combination of the boundary conditions and the material properties, both of which must be carefully assessed by the user.

2. The Kaowool verification tests indicated that the accuracy of FIRES-T3 when applied to fire tests was in the range of ± 14 percent. The only true unknowns in the Kaowool test were the nominal versus actual thickness and the convection boundary conditions. Secondary errors may have resulted from the exposure temperature estimate. Since the furnace is never at a completely uniform temperature, local cool and hot spots may cause deviances in the predictions.

3. FIRES-T3 successfully modeled the SHADWELL insulation tests Ins_8 through Ins_13, excluding Ins_11. This is likely a result of the conductivity curve that was extracted from actual test data for each material. It is suspected that the conductivity curve may have been compensating for other unknown factors such as variable material thicknesses, actual steel thickness, boundary conditions and varying exposure temperatures.

4. FIRES-T3 was not able to model the VTEC tests with the same degree of accuracy as the SHADWELL tests. This is possibly a result of the derived conductivity curves from the Shadwell tests that were compensating for conditions not present in the VTEC tests.

5. The sensitivity analysis revealed that there were four primary user-specified parameters that have the greatest impact on the temperature predictions of FIRES-T3. These were the actual insulation thickness, the material thermal conductivity, the thickness of the steel deck, and the actual exposure temperatures. All three of the fire tests modeled (Kaowool, Shadwell, and VTEC) required the assumption of at least one of these parameters.

6. A heat transfer analysis may be useful in addressing the impact of material defects such as installation damage or compression during installation. These variables are likely to occur but it is not practical to test each and every situation.

B5.0 EVALUATION OF THE IMPACT OF HEATING RICER 2 ON THE FAILURE TIME OF THE STEEL DECK ABOVE THE INSERTS

The objective of this section was to evaluate the impact of the temperature of RICER 2 on the temperature and failure times of the steel inserts (steel temperature greater than 232°C or 450°F) as recorded by the backside thermocouples. After Ins_2, the deck between Berthing 1 and RICER 2 was not completely insulated. Instead, insert panels were used that only protected a small percentage of the steel (steel inserts), leaving the greater part of the bare steel deck exposed directly to fire. As a result, a significant temperature rise occurred in RICER 2 during the course of a test. This section addresses the situation in a general manner in order to determine if the temperature in RICER 2 was significantly effecting the steel insert temperature, i.e., was the backside air heating causing premature "failure" in terms of the unexposed side temperature data.

B5.1 Approach

A relation between the RICER 2 compartment temperature and the exposure temperature was established. Actual exposure curves from Ins_8 through Ins_13 were selected to represent the extreme exposure cases. Using the fire model FIRES-T3, the impact of the exposures and the corresponding RICER 2 compartment temperatures on the temperature of the steel insert was evaluated for various thicknesses of insulation. The results were compared to the steel temperatures that would occur if RICER 2 remained at 26.7°C (80°F). The thermal properties of the Manville insulation were used for the insulation evaluation. The results would be analogous for the mineral wool insulation properties.

B5.2 Correlation Between the RICER 2 Temperature and the Exposure Temperature

Because of the constant surface area of the steel deck, the air temperature of RICER 2 was a function of the exposure temperature of the fire in Berthing 2. This can be observed in Fig. B35 from Ins_12 and Ins_13. The exposure temperatures are the average of two thermocouples measuring the exposure at the insert face. The corresponding RICER 2 compartment temperatures are the average of the temperatures recorded by the lowest thermocouple on each of the two thermocouple trees.

Fig. B13 shows the average exposure curves for Ins_8 through Ins_13, excluding Ins_11. The exposures for Ins_12 and Ins_13 were approximately the hottest and coolest fires among the six exposures. For this analysis, the Ins_12 exposure and the corresponding RICER 2 temperatures were assumed to be the most representative "hot" fire and the Ins_13 exposure the most representative "cool" fire for the SHADWELL test conditions.

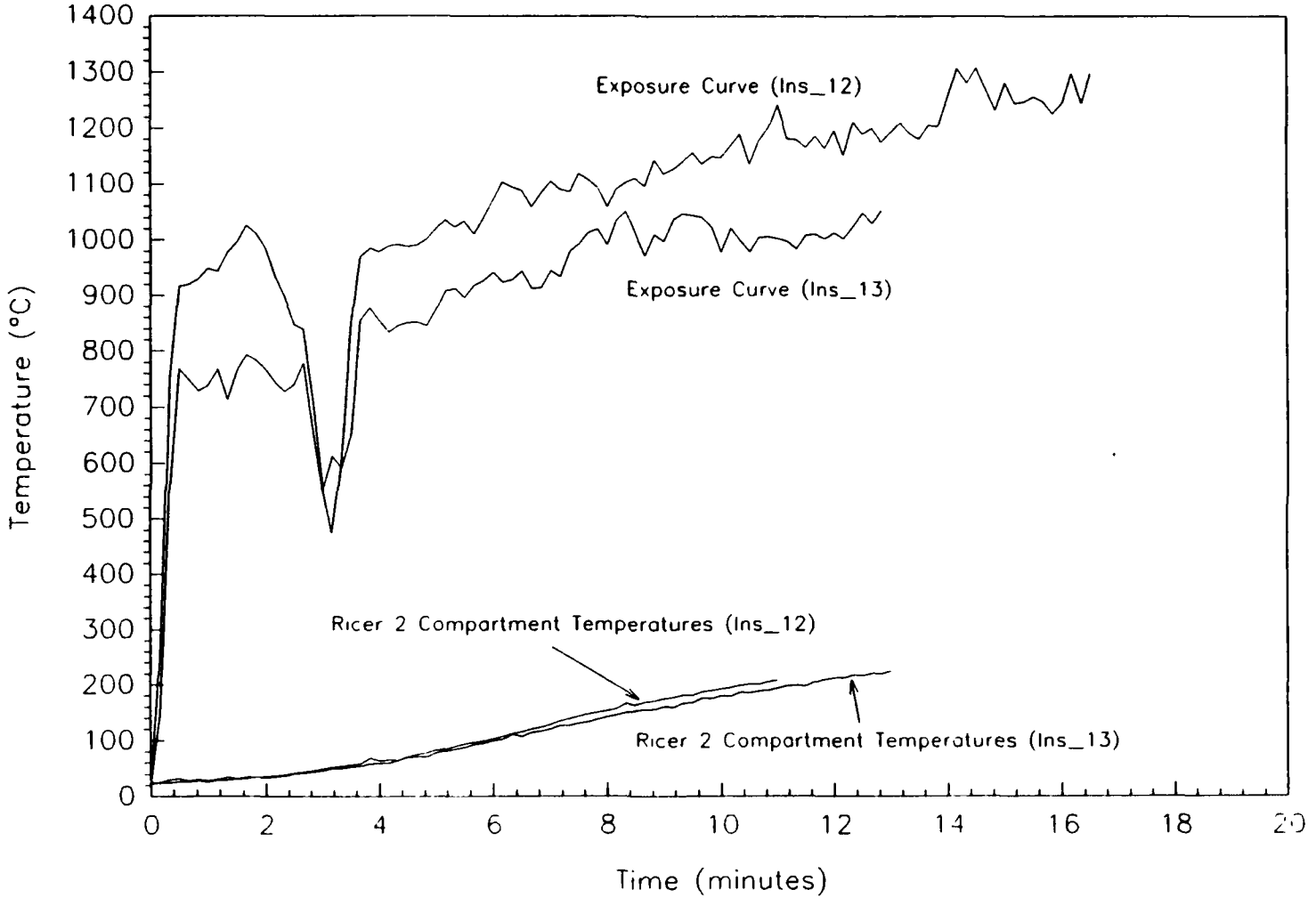

Fig. B35 - Comparison of exposure curves and RICER 2 compartment air temperatures

B5.3 The Effect of the RICER 2 Compartment Temperatures Resulting from the Hot and Cool Fires on the Unexposed Side of the Steel Inserts

There are three possible steel insert and RICER 2 temperature combinations. They are the following:

1. The steel temperature is greater than the RICER 2 air temperature above the insert;

2. The steel insert temperature is equal to the RICER 2 air temperature; and

3. The steel temperature is less than the RICER 2 air temperature.

The first case may occur when RICER 2 is kept at room temperature (26.7°C or 80°F). The steel insert temperature may also be greater than the compartment temperature for relatively cool fire exposures (and consequently cooler RICER 2 temperatures) and for thermally thin insulations. The second case represents adiabatic conditions. There is no heat transfer between the steel and the compartment in this condition. The adiabatic case is the boundary between the first and third cases and is used for comparison. The third case is most likely to occur when there is thermally thick insulation protecting the steel inserts concurrent with rapid temperature rise in RICER 2.

B5.3.1 RICER 2 Compartment Temperature Effects on a Steel Insert with a Temperature Greater Than RICER 2

Using FIRES-T3, one layer (1.6 cm or 0.63 in.) of the Manville insulation was exposed to the cool fire. The model was arranged so that the backside steel was exposed to the corresponding RICER 2 air temperatures. In other words, the boundary condition in the model was set to the RICER 2 air temperature. Fig. B36 shows the predicted backside steel temperature that resulted from the exposure and accompanying RICER 2 compartment temperatures. Additionally, Fig. B36 shows the predicted backside steel insert temperatures that resulted when the RICER 2 air was held at room temperature (26.7°C or 80°F) and when there was no heat transfer between the steel and RICER 2 (adiabatic). The steel insert temperature lies between the adiabatic curve and the room temperature curve. The RICER 2 temperature effect, as shown in Fig. B36, is small in this situation, on the order of a 1 minute decrease in predicted failure time as a result of the heating of RICER 2.

The temperature in the RICER 2 compartment would be less than the steel under the following conditions:

1. RICER 2 was maintained at room temperature;

2. The exposure was cool so that RICER 2 heated slowly; or

3. The insulation was thermally thin, so that the steel insert heated rapidly.

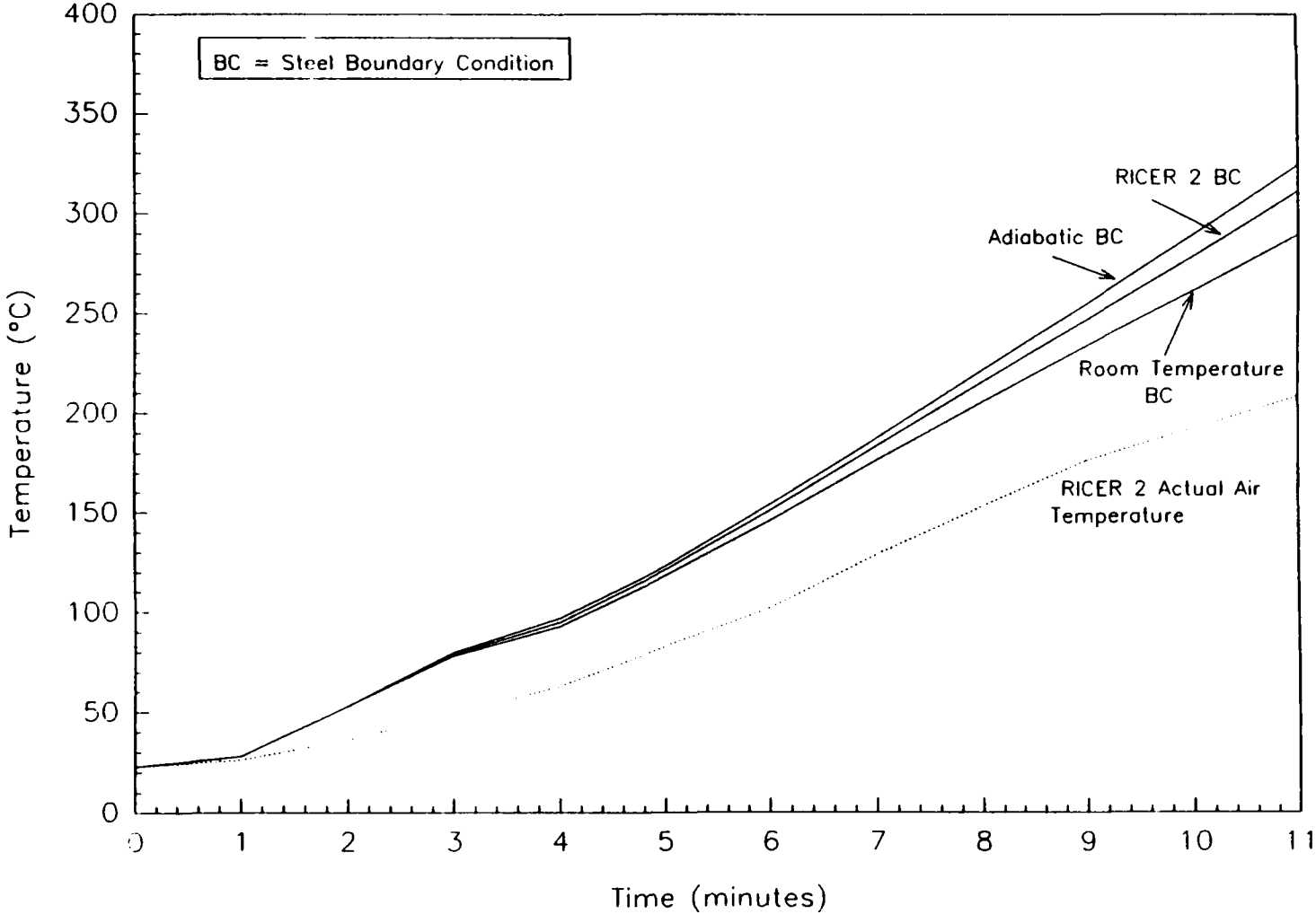

Fig. B36 - Steel insert temperature predictions for 1.6 cm (0.6 in) Manville insulation exposed to cool fire and with various boundary conditions on the steel

The last two conditions (and combinations of them) may be evaluated on an individual basis with suitable heat transfer programs to determine if the steel insert temperature is expected to be greater than the surrounding air temperatures. If the air temperatures of RICER 2 are expected to be less than the anticipated steel temperatures, the effect of RICER 2 on the steel temperature can be considered of secondary importance.

B5.3.2 RICER 2 Compartment Temperature Effects on a Steel Insert with a Temperature Lower Than RICER 2

The hot exposure curve and the corresponding RICER 2 temperature were used in FIRES-T3 to predict the effect of a compartment temperature in RICER 2 which is greater than the steel insert temperature. The thickness of the insulation was varied to demonstrate the effect of greater thermal penetration thicknesses. Three insulation thicknesses were used: 1.6 cm (0.63 in.), 3.2 cm (1.3 in.), and 4.8 cm (1.9 in.). Each insulation thickness was exposed to the Ins_12 exposure temperatures and the corresponding RICER 2 compartment temperatures. The thermal material properties of Manville were used for the model insulation.

Figs. B37, B38, and B39 show the predictions for the three thicknesses of Manville insulation. The predicted steel insert temperatures that result from adiabatic and room temperature boundary conditions in RICER 2 are also shown. One layer of the Manville insulation exposed to the hot fire was thermally thin and resulted in steel insert temperatures greater than the RICER 2 compartment temperatures (Fig. B37). Two or more layers of the Manville insulation exposed to the hot fire resulted in the steel insert temperatures less than the RICER 2 compartment temperatures (Figs. B38 and B39). Consequently, there would be heat flow from RICER 2 into the steel. Equivalent insulation thicknesses and cooler exposure fires may result in RICER 2 compartment temperatures greater than the steel insert temperatures as well. The effect of the thicker insulations is most pronounced with the simulated three layers of Manville, where failure was predicted to occur at about 13.5 minutes. If RICER 2 were kept at room temperature (26.7°C or 80°F), failure of the same insulation configuration was predicted to occur at about 18.5 minutes. Table B11 summarizes the differences in predicted failure times for the various simulated insulation thicknesses and boundary conditions.

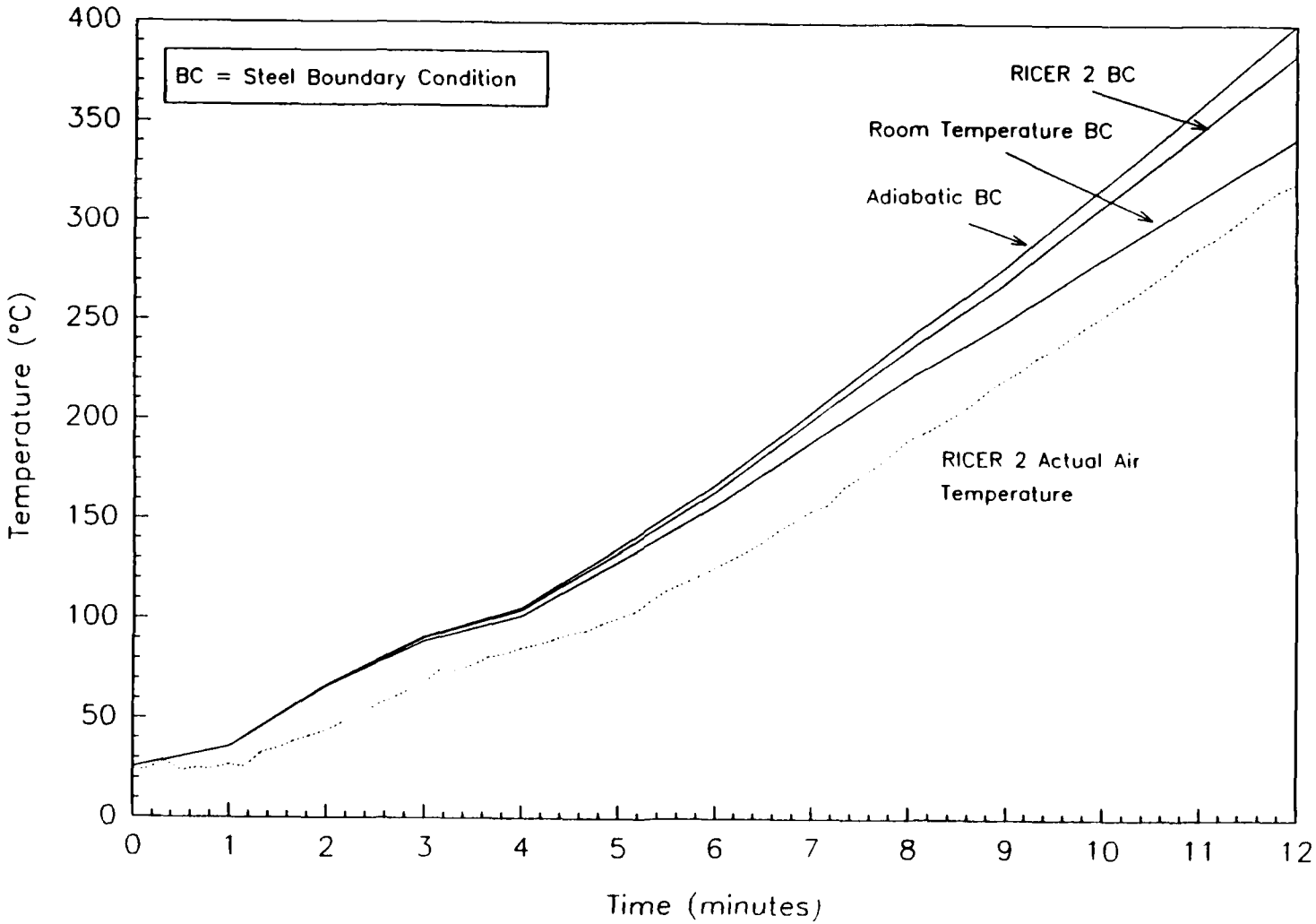

Fig. B37 - Steel insert temperature predictions for 1.6 cm (0.6 in) Manville insulation exposed to hot fire and with various boundary conditions on the steel

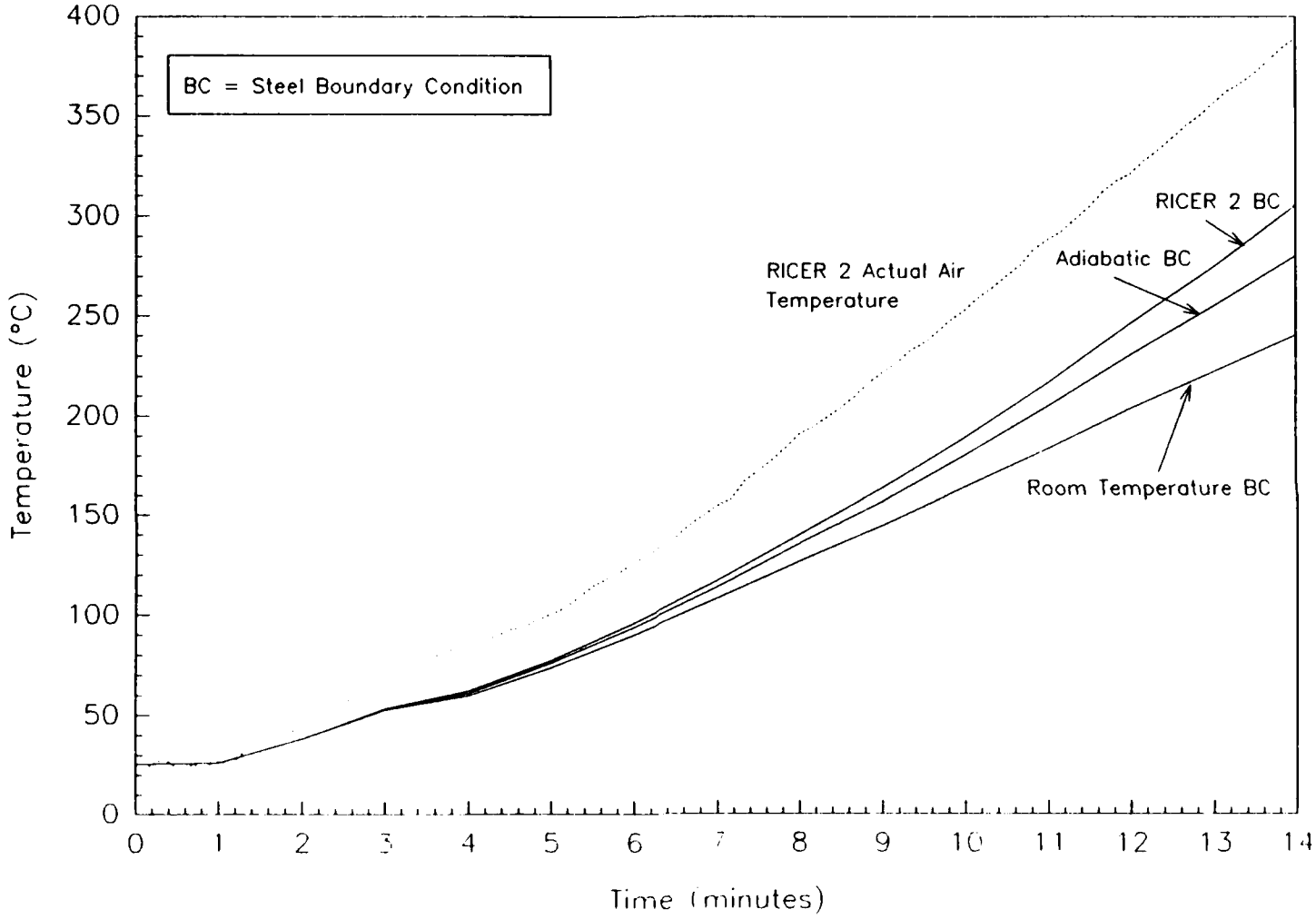

Fig. B38 - Steel insert temperature predictions for 3.2 cm (1.3 in) Manville insulation exposed to hot fire and with various boundary conditions on the steel

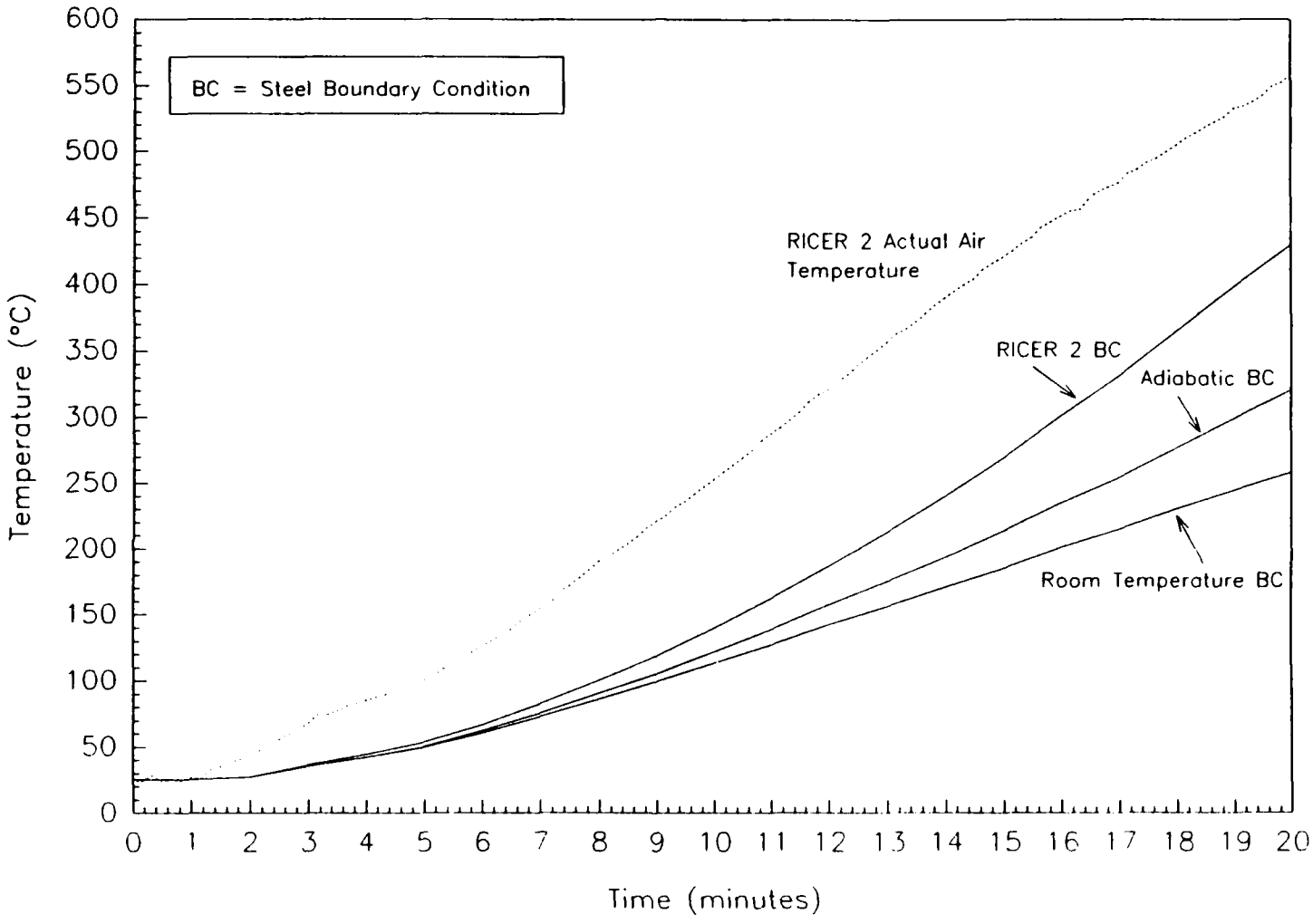

Fig. B39 - Steel insert temperature predictions for 4.8 cm (1.9 in) Manville insulation exposed to hot fire and with various boundary conditions on the steel

Table B11 - Failure times for Manville Insulation Thicknesses

Insulation thickness (cm)	Steel Failure Time (minutes)	
	RICER 2 - heated	RICER 2 - room temperature
1.6	7.7	8.1
3.2	12	14
4.8	13.5	18.5

Table B11 shows that the impact of hot RICER 2 compartment temperatures becomes significant for Manville insulation thicknesses greater than 3.2 cm (1.3 in.). The impact of a specific insulation thickness should be individually analyzed with both the hot curve and cool curve to assess the impact RICER 2 air temperatures may have on the steel insert. In situations where the entire deck is insulated, the temperature of RICER 2 is not expected to remain at room temperature, but somewhere in between the steel temperature and room temperature at any given time.

B5.4 Summary of the Impact of RICER 2 Heating on the Steel Temperature

This section demonstrated the impact of RICER 2 compartment temperature effects on the steel insert temperatures for various insulation thicknesses. It was shown that if the steel temperature is greater than the compartment temperature, the effect is secondary. If the steel temperature is less than the compartment temperature, the effect becomes increasingly significant as the insulation thickness (and the resulting thermal penetration thickness) increases. A set of extreme (high and low) exposure curves could be used to identify insulation configurations that are sensitive to the increase in air temperature of RICER 2. A possible application of FIRES-T3 or another heat transfer program could be to screen the tests beforehand to determine if such an effect is important. Alternatively, the RICER 2 air temperature could be reduced using mechanical blowers during tests with insulation inserts.

B6.0 REFERENCES

B1. Iding, R.H., Nizamuddin, Z., and Bressler, B., "FIRES-T3–A Computer Program for the FIre REsponse of Structures–Thermal Three-Dimensional Version," Department of Civil Engineering, University of California, Berkeley, CA, October 1977.

B2. Jeanes, D.C., "Predicting Temperature Rise in Fire Protected Structural Steel Beams," SFPE Technology Report 84-1, Society of Fire Protection Engineers, Boston, MA, 1984.

B3. Bresler. B., and Iding, R.H., "Evaluation of Fireproofing Requirements for Raymond-Kaiser Engineers Building, Oakland, CA," Wiss, Janney, Elstner and Associates, Inc., WJE Job No. 820908, February 25, 1983.

B4. Atreya, A., "Convection Heat Transfer," *SFPE Handbook of Fire Protection Engineering*, National Fire Protection Association, Quincy, MA, 1988.

B5. Harmathy, T.Z., "Properties of Building Materials at Elevated Temperatures," DBR Paper No. 1080 of the Division of Building Research, National Research Council of Canada, Ottawa, March 1983.

B6. Siegel, R., and Howell, J.R., *Thermal Radiation Heat Transfer*, Second Edition, Hemisphere Publishing Corporation, Washington, DC 1981.

B7. Emmons, H.W., and Mitler, H.E., "Documentation for CFC V, the Fifth Harvard Computer Fire Code," Division of Applied Sciences, Harvard University, Cambridge, MA, October 1981.

B8. Iding, R.H., and Bresler, B., "Effect of Fire Exposure on Steel Frame Buildings, Final Report, Volume I," Wiss, Janey, Elstner and Associates, Inc., WJE Job No. 78124, Emeryville, CA, March 1982.

B9. Holman, J.P., *Heat Transfer*, 7th ed., McGraw-Hill, 1990.

B10. Schneider, P.J., "Conduction Heat Transfer," Addison-Wesley Publishing Company, Inc., Reading, MA, 1955.

B11. Wulliman, R.S., "Evaluation of Insulation Materials and Combinations for Bulkhead Fire Protection," prepared for Naval Research Laboratory, Manville Service Corporation, Denver, CO, 20 January 1982.

B12. American Society for Testing and Materials, "C 201 - 86, Standard Test Method for Thermal Conductivity of Refractories," American Society for Testing and Materials, Philadelphia, PA, 1992.

B13. Johns-Manville Research and Development Center, Manufacturer's Specifications, 6PCF, Mineral Wool Insulation.

B14. Rollhauser, C., of DTRC supplied data from VTEC Labs Insulation Value Tests, transmitted to Hughes Associates, Inc., January 13, 1992.

B15. Elich, J.J., and Hamerinck, A.F., "Thermal Radiation Properties of Galvanized Steel and its Importance in Enclosure Fire Scenarios," *Fire Safety Journal*, **16**, 1990, pp. 469-482.

B16. Integrated Systems Analysts, Inc., "Fire Resistance Testing of Lightweight Insulation," VTEC 100-228-5, Arlington, VA, January 16, 1991.